2018

Tetratricopeptide 39C (TTC39C) Is Upregulated During Skeletal Muscle Atrophy and is Necessary for Muscle Cell Differentiation

Caleb Hayes
University of North Florida, n01054826@unf.edu

TETRATRICOPEPTIDE 39C (TTC39C) IS UPREGULATED DURING SKELETAL MUSCLE ATROPHY AND IS NECESSARY FOR MUSCLE CELL DIFFERENTIATION

By

Caleb Stevenson Hayes

A thesis submitted to the Department of Biology

in partial fulfillment of the requirements for the degree of

Master of Science in Biology

University of North Florida

April 2018

CERTIFICATE OF APPROVAL

The thesis of Caleb Stevenson Hayes "Tetratricopeptide 39c (Ttc39c) is upregulated during skeletal muscle atrophy and is necessary for muscle cell differentiation" is approved by:

Date

_____ _____

Dr. David Waddell, Ph.D
Committee Chair

_____ _____

Dr. Doria Bowers, Ph.D.

_____ _____

Dr. John Hatle, Ph.D.

Accepted for the Department:

_____ _____

Dr. Cliff Ross, Ph.D.
Department Chair

Accepted for the College of Arts and Sciences:

_____ _____

Dr. George Rainbolt, Ph.D.
Dean

Accepted for the University:

_____ _____

Dr. John Kantner, Ph.D.
Dean of the Graduate School

Table of Contents

List of Figures

List of Tables

Abstract

Ttc39c has been identified as a novel gene in skeletal muscle that is upregulated in response to neurogenic atrophy in mice. Quantitative PCR and Western blot analysis confirmed that Ttc39c is expressed in both proliferating and differentiated muscle cells. Furthermore, comparison of Ttc39c expression in undifferentiated and differentiated C_2C_{12} cells demonstrated that Ttc39c levels peak in early differentiation, but decreases as cells become fully differentiated myotubes. The transcriptional regulation of Ttc39c was examined by cloning promoter fragments of the gene and fusing it with the SEAP reporter gene. The Ttc39c reporter gene constructs were transfected into muscle cells and confirmed to have significant transcriptional activity in cultured muscle cells and were also found to be transcriptionally repressed in response to ectopic expression of myogenic regulatory factors (MRF). Furthermore, conserved E-box elements in the proximal promoter region were identified, mutated, and analyzed for their role in the transcriptional regulation of Ttc39c expression. Mutation of the conserved E-box sequences reduced the activity of the Ttc39c reporter gene, suggesting that these elements are potentially necessary for full Ttc39c expression. To determine the sub-cellular location of Ttc39c in muscle cells, the Ttc39c cDNA was fused with the green fluorescent protein (GFP), expressed in muscle cells, and visualized by confocal microscopy revealing that Tct39c is localized to the cytoplasm of proliferating myoblasts and differentiating myotubes. Furthermore, Ttc39c appears to localize to the microtubule network and differentiating muscle cells developed elongated primary cilia in response to Ttc39c ectopic expression. Additionally, Ttc39c overexpression resulted in impaired muscle cell differentiation, attenuated Hedgehog and MAP Kinase signaling, and increased expression of IFT144, a component of the intraflagellar transport complex A involved in retrograde movement in primary cilia. Interestingly, Ttc39c knockdown also resulted in abrogated muscle cell differentiation and impaired Hedgehog and MAP Kinase signaling, but did not affect IFT144 expression levels. These results suggest that muscle cell differentiation is sensitive to aberrant Ttc39c expression, that Ttc39c is necessary for proper muscle cell differentiation, and that Ttc39c may participate in retrograde transport of the primary cilia of developing muscle cells.

Chapter 1: Background of Skeletal Muscle Atrophy, MuRF1, and Cell Signaling During Myogenesis

Skeletal Muscle and Skeletal Muscle Atrophy

Skeletal muscle is a dynamic tissue that, in humans, contains 50-75% of all body protein, conducts 30-50% of whole-body protein turnover, and comprises around 40% of total body weight (Frontera and Ochala, 2014; Crist, 2016). The dynamic nature of skeletal muscle is exemplified by its ability to interpret a physiological response based off the reception and integration of external cues. The many important functions of skeletal muscle include generating force and power, posture maintenance, the production of heat for maintaining a physiologically appropriate core body temperature, and acting as storage for amino acids and carbohydrates (Frontera and Ochala, 2014; Crist, 2016). Skeletal muscle tissue mass is regulated based on an individual's physiological needs, either by increasing in mass via protein synthesis (hypertrophy) or decreasing in mass via protein degradation (atrophy). Muscle mass is maintained by a balance between these two processes (McKinnell and Rudnicki, 2004). Skeletal muscle atrophy occurs when protein degradation outpaces protein synthesis, leading to the partial or complete wasting of skeletal muscle (McKinnell and Rudnicki, 2004; Bodine and Baehr, 2014). This process occurs for a number of reasons, including aging (sarcopenia), cancer, disuse, corticosteroid treatment, and denervation (Bodine, et al., 2001; Bonaldo and Sandri, 2013; Waddell et al., 2008). Increasing our understanding of this condition by studying the molecular and genetic mechanisms of skeletal muscle atrophy is important and may eventually provide new insights into alleviating or preventing the damaging effects of pathological muscle wasting.

Ubiquitin Proteasome System and E3 Ubiquitin Ligases

The Ubiquitin Proteasome System (UPS) is the primary pathway by which protein is degraded during skeletal muscle atrophy. This pathway functions via E3 ubiquitin ligases, which ubiquitinate (tag) proteins for degradation by the 26S proteasome, which does so by hydrolyzing the peptide bonds of tagged proteins (Figure 1) (McNaught, et al., 2001; Ardley and Robinson, 2005; Bodine and Baehr, 2014).

Ubiquitination of proteins is accomplished by E3 ubiquitin ligases that covalently link a small ubiquitin protein to lysine residues on the target polypeptide. The ubiquitination modification requires three different proteins: the E1, E2, and E3 proteins. The E1 protein, called the ubiquitin activating enzyme, hydrolyzes an ATP molecule and adds adenylate to the ubiquitin molecule (McNaught, et al., 2001; Ardley and Robinson, 2005; Bodine and Baehr, 2014). The E2 protein, called the ubiquitin conjugating enzyme, then transfers the adenylated ubiquitin to one of its cysteine residues (McNaught, et al., 2001; Bodine and Baehr, 2014). Finally, the E3 ubiquitin ligase covalently attaches the ubiquitin to the target protein (McNaught, et al., 2001; Bodine and Baehr, 2014). While all three of the proteins work together to tag proteins for degradation, the E3 is most important as it provides specificity by binding a unique subset of targets that will be ubiquitinated for degradation via the UPS (Ardley and Robinson, 2005; Bodine and Baehr, 2014).

MuRF1 and MAFbx

Two E3 ubiquitin ligases that have been identified as being upregulated in response to virtually all atrophy-inducing conditions are Muscle-RING Finger 1 (MuRF1) and Muscle Atrophy F-box (MAFbx) (Bodine, et al., 2001). In the study conducted by Bodine et al., rats subjected to

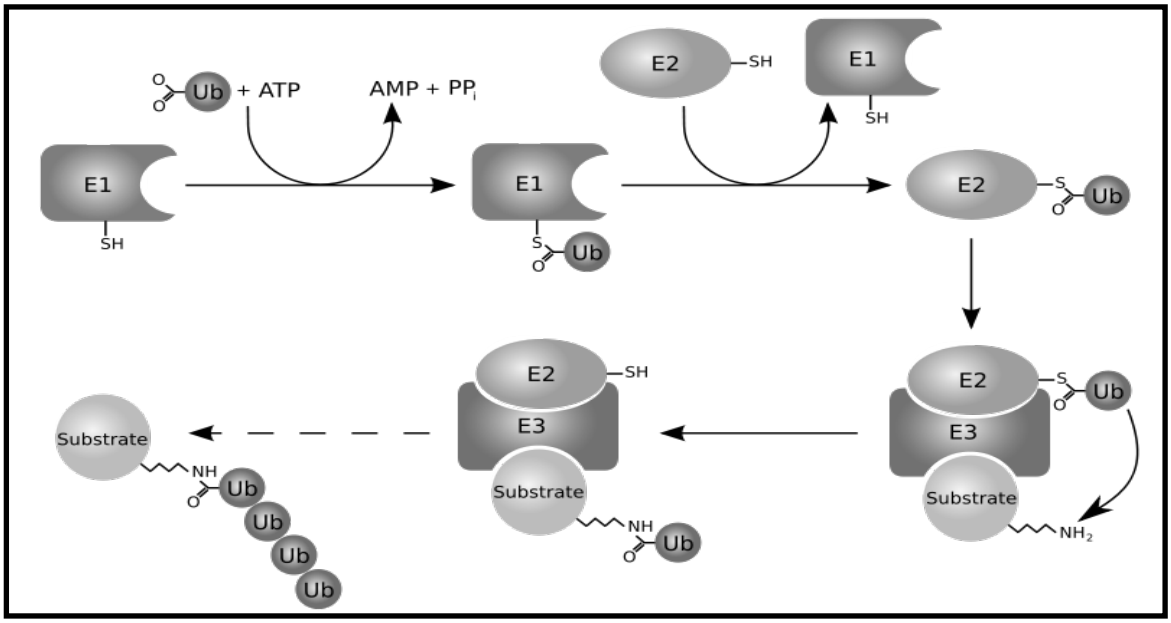

Figure 1. A schematic of the Ubiquitin Proteasome System. The ubiquitin activating enzyme (E1), the ubiquitin conjugating enzyme (E2), and the ubiquitin ligase (E3) work in concert to ubiquitinate proteins for degradation via the 26S proteasome (Adapted from Dodd, 2011).

immobilization, denervation, and handlimb suspension had their medial gastrocnemius muscle isolated and analyzed to identify genes that were differentially expressed under these atrophy-inducing conditions. Of the many genes identified, only MuRF1 and MAFbx were shown to be upregulated in response to all three conditions (Fig. 2). Additionally, mice with MuRF1 or MAFbx knocked out exhibited atrophy resistance when compared to wild-type mice. It is clear that MuRF1 and MAFbx are key regulators in skeletal muscle atrophy, but the exact molecular mechanisms are not well understood and only a small number of potential targets have been identified to date, such as myosin-binding protein C (MyBP-C), myosin light chains 1 and 2 (MyLC1 and MyLC2), and myosin heavy chain (MyHC) (Bodine and Baehr, 2014). A lack of clear protein targets of MuRF1 and MAFbx has led to additional questions about their role in the muscle atrophy cascade and calls into question the widely accepted role that these proteins are believed to play in muscle wasting.

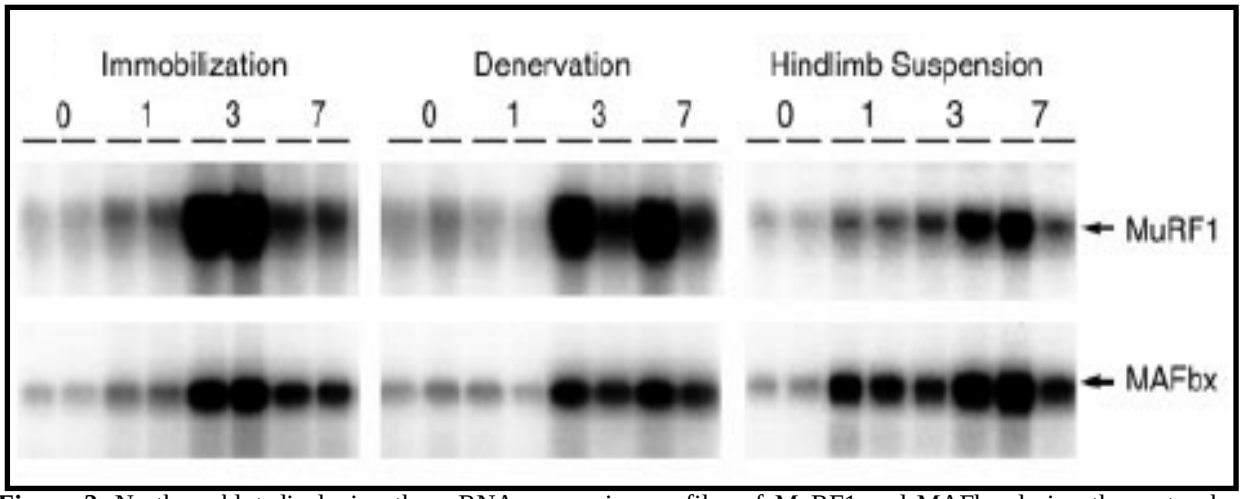

Figure 2. Northern blot displaying the mRNA expression profiles of MuRF1 and MAFbx during three atrophy-inducing conditions: immobilization, denervation, and hindlimb suspension. Increased expression of both genes is observed at day 1 and reaches maximum expression at day 3. (Bodine, et al., 2001).

MuRF1 as a transcriptional regulator

MuRF1 has been hypothesized to function as an E3 ubiquitin ligase based on its three functional domains, although few targets have been identified (Bodine and Baehr, 2014). The RING domain is a zinc finger protein domain that contains cysteine and histidine residues that interact with zinc ions. The RING domain is believed to be required for E3 enzyme activity and is predicted to perform the catalytic ligase activity of MuRF1 (Furlow et al., 2013; Bodine and Baehr, 2014). The two other domains are the B-box and B-box c-terminal (Bbc) domains, which may aid in the binding of DNA and/or other proteins by forming additional zinc finger structures (Mrosek et al., 2008). Furthermore, MuRF1 has an acidic c-terminus that currently has no known function, although it is hypothesized that acidic carboxyl termini may aid in the subcellular localization of proteins (McElhinny, et al., 2002; Hohlfeld et al., 2006).

A study published in 2013 by Furlow et al. suggested that the role of MuRF1 in skeletal muscle atrophy is likely more complex than initially believed. Two populations of 4 to 6 month old female mice consisting of either wild-type (WT) and MuRF1 knock-out (KO) littermates were compared under control and atrophy conditions. The KO mice were created by inserting a β-galactosidase-encoding LacZ cassette in the MuRF1 gene (Furlow et al., 2013). The design of the MuRF1 knockout mouse preserved the endogenous promoter, which results in β-galactosidase being expressed as a reporter MuRF1 locus activity in the MuRF1-null animals. This system allowed researchers to quantitatively assess when the MuRF1 endogenous promoter was active even though there was no functional MuRF1 being produced in the KO animals. Following denervation, the gastrocnemius muscle was isolated, and a genome-wide microarray was performed to identify differences in gene expression in response to neurogenic atrophy at two different time points: 3 days and 14 days post-denervation (Furlow et al., 2013). In the WT mice, MuRF1 expression increased at day 3, but returned to baseline levels by day 14. In the MuRF1-KO mice, however, β-galactosidase levels were elevated at day 3 and remained elevated at day 14 (Fig. 3; Furlow et al., 2013). This suggests that MuRF1 may negatively regulate its own expression.

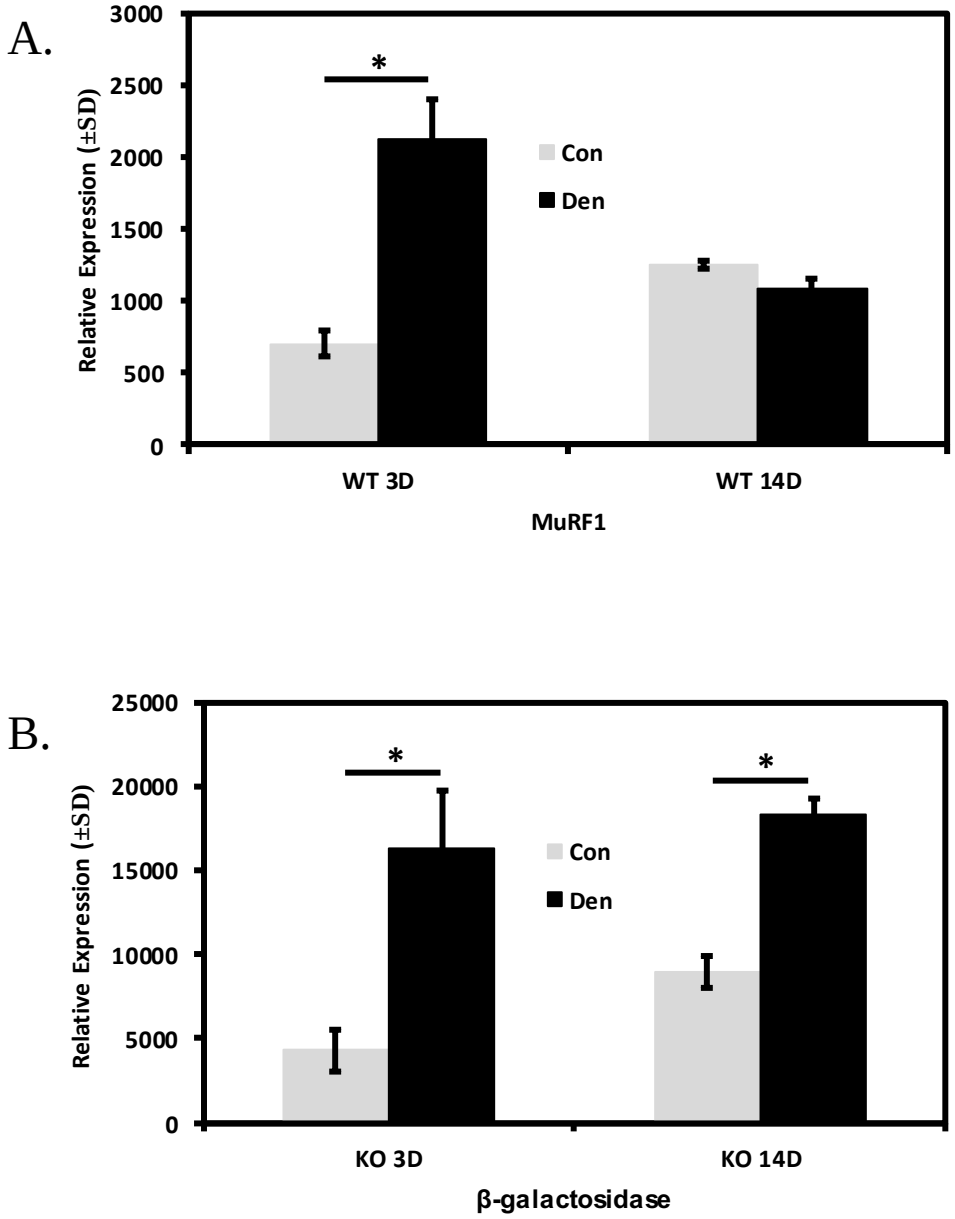

Figure 3. Transcriptional activity of the MuRF1 locus in WT and MuRF1 KO mice postdenervation. **(A)** Denervated WT mice showed an increase in MuRF1 gene expression at day 3 (3D), but a return to baseline at day 14 (14D) post-denervation. **(B)** Denervated KO mouse showed at increase in β-galactosidase expression, which is under the control of the MuRF1 promoter, at day 3 and expression remained elevated at day 14 post-denervation (Furlow, et al., 2013).

Furthermore, MAFbx expression was also found to be affected by MuRF1 expression levels as well. In WT mice, MAFbx expression was increased by day 3, but returned to baseline by day 14, while in MuRF1 KO mice MAFbx expression remained elevated at both day 3 and day 14 post-denervation (Fig, 4; Furlow et al., 2013). This suggests that MuRF1 may also negatively affect the expression of MAFbx.

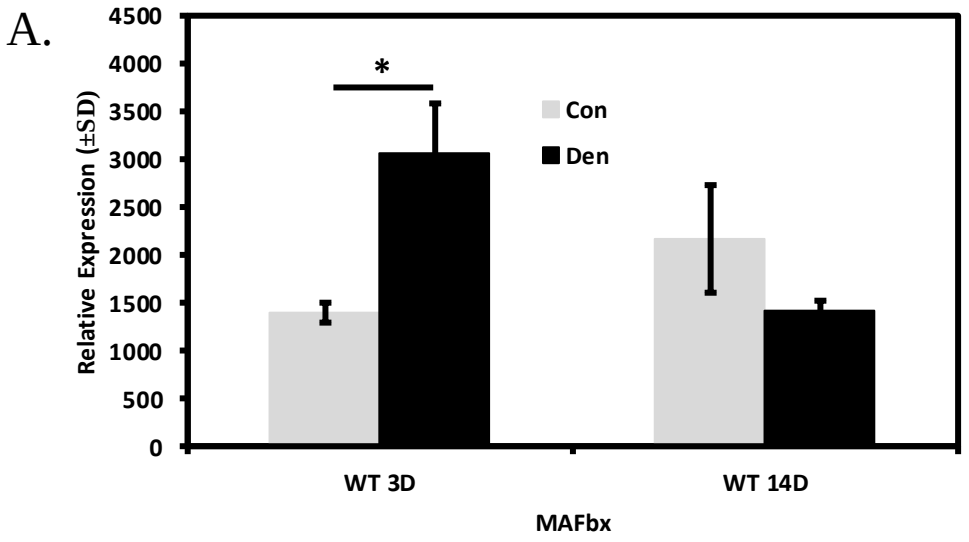

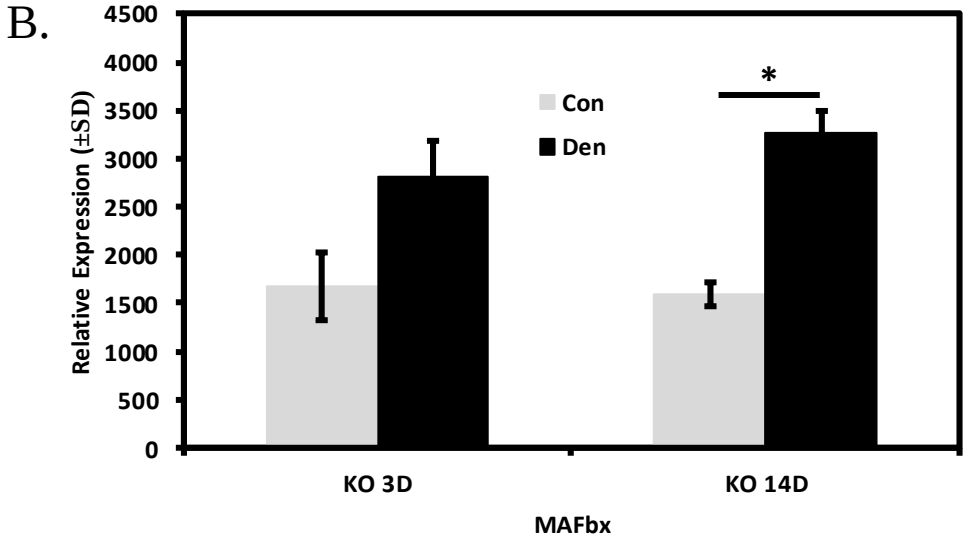

Figure 4. Transcriptional activity of MAFbx in WT and MuRF1 KO mice post-denervation. **(A)** Denervated WT mice showed an increase in MAFbx gene expression at day 3 (3D), but returned to baseline by day 14 (14D) post-denervation. **(B)** Denervated MuRF1 KO mice showed an increase in MAFbx gene expression at day 3 that remained elevated at day 14 post-denervation (Furlow, et al., 2013).

In addition to the differences in MuRF1 and MAFBx expression, a subset of genes showed differential expression when comparing the WT and KO cohorts following denervation (Furlow et al., 2015). Many of the differentially expressed genes have been shown to have a range of potential functions, including roles in muscle structure and function, signal transduction cascades, and metabolic pathways. Among the genes believed to be important in the regulation of muscle cell signaling cascades is one gene of particular interest: Tetratricopeptide 39c (Ttc39c).

Overview of Tetratricopeptide 39c

Ttc39c is a gene that encodes for a protein that contains several putative tetratricopeptide repeat (TPR) domains, a structural motif which has been shown to facilitate protein-protein interactions (D'Andrea and Regan, 2003). Other proteins that contain these domains have been shown to function in cell signaling pathways, apoptosis, and cell cycle regulation (Blatch and Lassle, 1999). Ttc39c has been shown to be critical for proper formation of motile and non-motile cilia in zebrafish, although its exact function remains unclear (Xu et al., 2015). Zebrafish embryos with Ttc39c knocked down exhibited several ciliopathic phenotypes, including abnormal body curvature, incorrect left-right patterning of organs, hydrocephalus, and abnormal otolith development (Xu et al., 2015)**.** This same study also observed via co-immunoprecipitation that Ttc39c had weak interactions with two proteins, IFT139 and IFT144, which are part of the IFT A complex that is responsible for retrograde intraflagellar transport in cilia (Xu et al., 2015). Importantly, while fully differentiated skeletal muscle fibers do not possess motile cilia, proliferating and differentiating muscle cells do possess primary cilia (Fu, et al., 2014).

The Primary Cilia and Cellular Signaling in Muscle Development

Primary cilia are non-motile, hair-like projections found on the surface of many cell types and have been shown to coordinate cell signaling during development and tissue homeostasis (Prevo et al., 2017; Satir et al., 2010). Primary cilia structure consists of nine microtubule doublets that are derived from a basal body, a transition zone which separates the cytoplasm from the cilium interior, and the ciliary membrane (Prevo et al., 2017; Satir et al., 2010, Bangs and Anderson, 2017). Intraflagellar transport (IFT) complexes are crucial for proper cargo transport up and down the ciliary axoneme, with IFT-A performing retrograde transport via dynein motors and IFT-B performing anterograde transport via kinesin motors (Fig. 5) (Bangs and Anderson, 2017; Prevo et al., 2017; Goetz and Anderson, 2010; Satir et al., 2010. Yuan and Yang, 2015). A complex of Bardet-Biedl syndrome (BBS) proteins comprising the BBSome are also required for proper IFT (Prevo, et al., 2017; Ye, et al., 2018; Liu and Lechtreck, 2018). Interestingly, primary cilia have been shown to be critical for proper Hedgehog (Hh) signaling, a pathway important for organ development and intercellular communication (Bangs and Anderson, 2017), as well as Wingless (Wnt), Notch, and mitogen-activated protein kinase (MAPK) signaling pathways (Prevo, et al., 2017; Satir, et al., 2010).

Properly regulated signaling, including the Hh pathway, is crucial for skeletal muscle development (Bentzinger, et al., 2012; Mok and Sweetman, 2011; Bismuth and Relaix, 2010; Fu, et al., 2014). Some studies have found that increased Hh signaling leads to attenuated myotube formation due to increased proliferation of satellite cells and inhibition of MyoD, a Myogenic Regulatory Factor (MRF), to activate the transcription of muscle-specific genes (Koleva et al., 2005; Gerber et al., 2007). Others have observed that an increase in Hh signaling actually increases myotube formation

of myoblasts already committed to differentiation (Duprez et al., 1998; Li, et al., 2004). Regardless of the exact role that Hh signaling plays in muscle cell differentiation, it is well established that primary cilia are critical for proper Hh signaling (Fu et al., 2014; Bangs and Anderson, 2017; Goetz and Anderson, 2010; Satir et al., 2010). Another study has shown that blocking the formation of primary cilia in C_2C_{12} mouse myoblasts by inhibiting the expression of proteins crucial for cilia formation resulted in aberrant Hh signaling, leading to a decrease in MRF expression and myoblast differentiation (Fu et al., 2014). This same study also found that primary cilia formation peaks in the transition between proliferation and differentiation of primary mouse myoblasts (Fu et al., 2014).

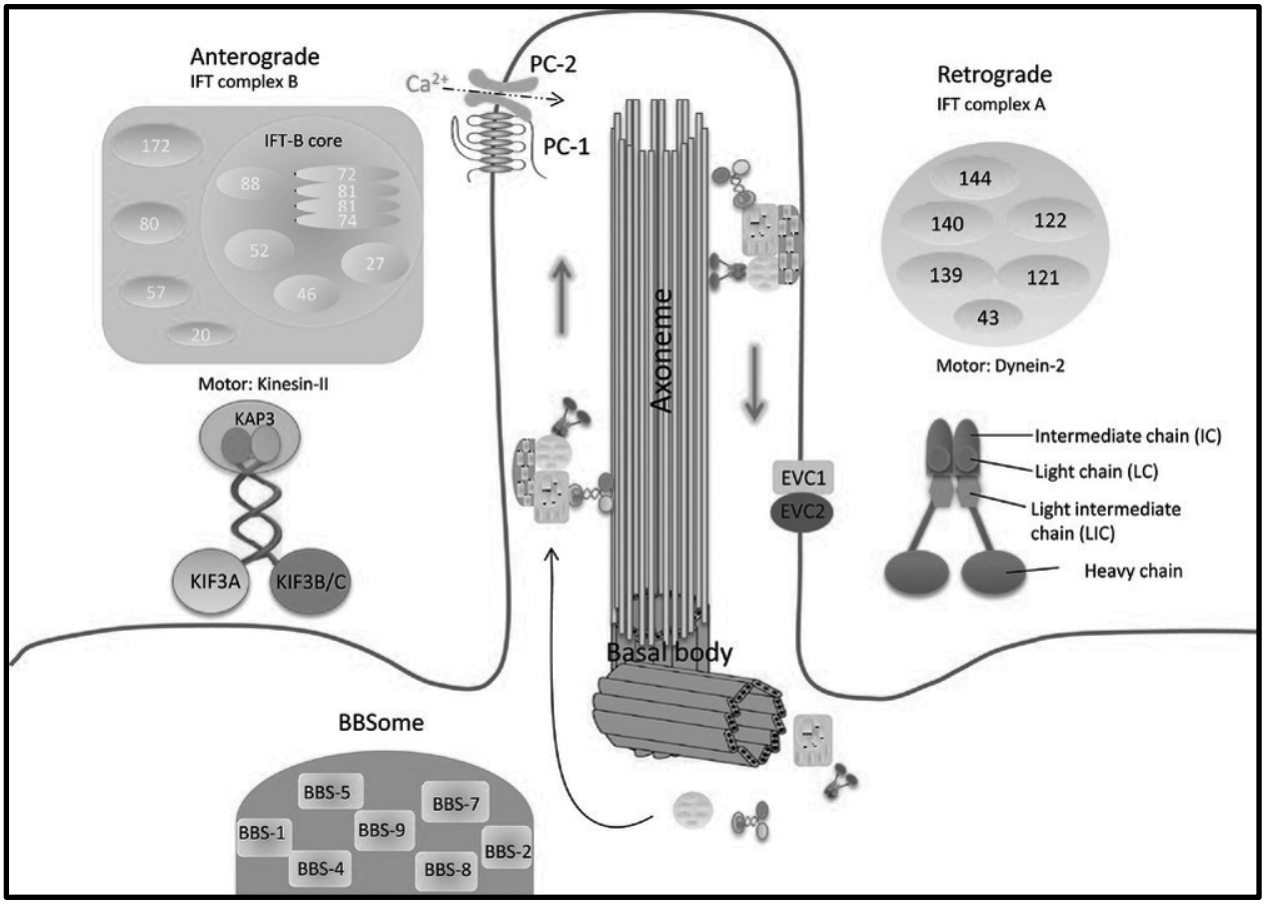

Figure 5. Primary cilia structure and intraflagellar (IFT) transport. IFT-A and IFT-B complexes, along with the BBSome complex, transport cargo up and down the ciliary axoneme that originates from the cell's basal body. IFT-A conducts retrograde transport via dynein motors, while IFT-B conducts anterograde via kinesin motors. (Adapted from Yuan and Yang, 2015)

In addition to Hh signaling, several receptor tyrosine kinases (RTKs) have been shown to localize within the primary cilium, including PDGFRa, EGFR, IGF-1R, and FGFR (Christensen et al., 2012). Upon binding of the appropriate growth factor, these receptors will activate several pathways such as mitogen-activated protein kinase (MAPK) pathways, including the MEK1/2-ERK1/2 pathway, which is known to control cell proliferation, migration, and cell differentiation (Christensen et al., 2012). ERK1/2 signaling is required for proper skeletal muscle development and has a nuanced effect on differentiating myoblasts (Knight and Kothary, 2011). ERK1/2 activity is critical for myoblast proliferation and preventing premature differentiation (Kook et al., 2007; Knight and Kothary, 2011), but the pathway activity decreases as myoblasts differentiate (Knight and Kothary, 2011). Furthermore, it has been observed that when ERK1/2 signaling activity is sustained, myoblast differentiation is inhibited (Sarbassov et al., 1997; Winter and Arnold, 2000; Rodriguez, et al., 2014). Even more interesting, ERK1/2 activity has been shown to increase again during terminal differentiation and has been found to be critical for proper myocyte fusion and survival (Adi et al., 2002; Bennett and Tonks, 1997; Sarbassov et al., 1997; Gredinger et al., 1998). The reliance of myoblasts on these disparate signaling pathways for proper differentiation displays the importance of proper regulation of signal transduction cascades, which appear to depend on proper assembly and function of the primary cilia.

Taken together, evidence linking Ttc39c to proper cilia formation and the role of primary cilia in skeletal muscle cell differentiation via cellular signaling cascades suggests a possible function of Ttc39c in muscle cell primary cilium formation and function that in-turn is crucial for proper differentiation of myoblasts into functional skeletal muscle tissue.

Chapter 2: Material and Methods, Results, and Discussion

Materials and Methods

Cell Culture

Cell culture was performed as previously described (Waddell et al., 2015). Briefly, the C_2C_{12} immortalized mouse myoblast cell line (CRL-1772) was obtained from the American Type Culture Collection (Manassas, VA) and maintained in DMEM (Life Technologies, Grand Island, NY) supplemented with 10% Fetal Bovine Serum (FBS) (GE Healthcare HyClone Laboratories, Logan, UT), non-essential amino acids, 1X Penicillin/Streptomycin and Gentamicin (all from Life Technologies, Grand Island, NY) and grown at 37˚C in a humidified chamber at 5% CO_2. Cells were switched to DMEM supplemented with 2% serum, non-essential amino acids, Penicillin/Streptomycin and Gentamicin in order to induce myoblast to myotube differentiation.

RNA isolation and cDNA synthesis

Total RNA was isolated from C_2C_{12} myoblast cells using the RNeasy Mini Kit (Qiagen, Valencia, CA) according to the manufacturer's protocol. Purified total RNA (0.75-1.5µg) was reverse-transcribed using Oligo-dT primers and Moloney Murine Leukemia Virus (M-MLV) Reverse Transcriptase according to the manufacturer's protocol (Life Technologies, Grand Island, NY).

Amplification and cloning of the full-length Ttc39c cDNA

For the amplification of *Ttc39c* cDNA, gene-specific primer pairs were designed (Table 1.) using the gene sequence from *Mus musculus* (*Ttc39c*, GenBank accession number: NM_028341). PCR was performed according to the manufacturer's protocol (Life Technologies, Grand Island, NY) using Taq DNA polymerase, gene specific primer pairs, and DNA template prepared by reverse

transcription of RNA isolated from C_2C_{12} cells as described in section 2.2. Amplicons were cloned into the pGEM-T Easy vector (Promega, Madison, WI) according the manufacturer's protocol and sequenced using the Big Dye Sanger terminator sequencing method (Eurofins MWG Operon, Huntsville, AL) to confirm amplification of the expected target and the absence of mutations. The *Ttc39c* cDNA was sub-cloned into the EcoRI restriction site of pcDNA3.1 (+) (Life Technologies, Grand Island, NY) and sequenced to confirm correct orientation and lack of mutations. The *Ttc39c* cDNA was also sub-cloned into the EcoRI restriction site of the pEGFP-C3 and pCS2+MT expression plasmids (Clontech, Mountain View, CA) and sequenced to confirm correct orientation and in frame fusion with GFP and the 6X-myc-tag, respectively.

Table 1. List of primers used in this study.

Primers	Sequence (5'-3')
Gene Cloning	
Ttc39c-F	GCGAATTCACTCGAGGCCTCGTGTGCCCATGG
Ttc39c-R	GCGAATTCGGGGCCACTGGGAGTTTATCACTGAGG
3'-UTR Cloning	
Ttc39c-3'UTR-F	GCACGCGTTAAACTCCCAGTGGCCCCTCCGTCC
Ttc39c-3'UTR-R	GCAAGCTTGGTCACTTAACCCTCTCCCAGGTCG
qPCR	
Ttc39c-AT1-qPCR-F	GCTGGCATCAATATGCTTCTC
Ttc39c-AT2-qPCR-F	GCCTCTGGTGATTTGCTACAG
Ttc39c-qPCR-R	ATGGCGTTCAAAAAGCTGACG
GAPDH-qPCR-F	CTCGTCCCGTAGACAAAATGG
GAPDH-qPCR-R	GGGTCGTTGATGGCAACAATC
Promoter Cloning	
Ttc39c-001-Pro-R1	GCAAGCTTGCCAGTCACTCCCAACTTCGTCCGG
Ttc39c-001-Pro-R2	GCAAGCTTCACGCGTGTCAGAACCCTTAGG
Ttc39c-001-Pro500-F	GCGCTAGCGGCAGGGAATATAGTCCATTTCGGC
Ttc39c-001-Pro1000-F	GCGCTAGCGCAATTACACAACCCAGAGGCCGAAGC
Ttc39c-001-Pro2000-F2	GCGCTAGCCAAGAGTGTCCCGAAGTTTGTACAACCC
Ttc39c-004-Pro-R	GCGCTAGCTGGGGGTGGGGGACGAATACAGG
Ttc39c-004-Pro500-F	GCGGTACCGGCTGACTCTTGCCTGCGTCCAGC
Ttc39c-004-Pro1000-F	GCGGTACCCGGCCACTGTTCTTGTCACTCAGGAGC
Ttc39c-004-Pro2000-F	GCGGTACCGCTGGGTTTCTGGGGAGGAGGTGG
Site-directed Mutagenesis	
Ttc39c-004-Ebox-Mut-F	CACTGAGCAAGACCCCTGGCAGGTTCCCCTGCTGC
Ttc39c-004-Ebox-Mut-R	GCAGCAGGGGAACCTGCCAGGGGTCTTGCTCAGTG
Ttc39c-001-Ebox1-Mut-F	CGCCCCTGCCGCCCGACCGCTTGAGGATTGGC
Ttc39c-001-Ebox1-Mut-R	GCCAATCCTCAAGCGGTCGGGCGGCAGGGGCG
Ttc39c-001-Ebox2-Mut-F	CATTTAGCTACGTGGCGTACGGATCCCTATCTCTC
Ttc39c-001-Ebox2-Mut-R	GAGAGATAGGGATCCGTACGCCACGTAGCTAAATG
Ttc39c-001-Ebox3-Mut-F	GGTGTTTTGCTGACGTTCGCTTATATAAAAACC
Ttc39c-001-Ebox3-Mut-R	GGTTTTTATATAAGCGAACGTCAGCAAAACACC
Sequencing	
Ttc39c-Seq-F	CTGTATCAGAAGAAGCTGACGG
Ttc39c-Seq-R	GACTCGTTCTTCAGCCTCTCC
siRNA Oligonucleotides	
Ttc39c-siRNA-2-F	GATCCCCGCACGTCTGTCTGTATGAATTCAAGAGATT CATACAGACAGACGTCGTTTTTA
Ttc39c-siRNA-2-R	TCGATAAAAAGCACGTCTGTCTGTATGAATCTCTTGA ATTCATACAGACAGACGTGCGGG

Promoter cloning of the Ttc39c gene

For the amplification of the proximal regulatory region of *Ttc39c*, genomic DNA was isolated from C_2C_{12} cells using the DNeasy Blood and Tissue Kit (Qiagen, Valencia, CA) according to the manufacturer's protocol. PCR was performed using *Ttc39c* promoter region-specific primer pairs (Table 1.) designed using mouse genomic sequences obtained from the Ensembl database (www.ensembl.org). PCR reactions were performed using 1µg of genomic DNA and Taq DNA polymerase according to the manufacturer's protocol (Life Technologies, Grand Island, NY). The PCR amplicons were cloned into the pGEM-T vector (Promega, Madison, WI) according to the manufacturer's protocol and sequenced to confirm amplification of the predicted target region and the absence of mutations. The Ttc39c promoter fragments were each sub-cloned into the NheI and Hind III sites of the pSEAP2-Basic reporter plasmid (Clontech, Mountain View, CA) to create the pSEAP-Ttc39c-Pro500, pSEAP-Ttc39c-Pro1000 and pSEAP-Ttc39c-Pro2000 reporter plasmids and sequenced to confirm correct orientation.

Site-directed Mutagenesis

The conserved E-box enhancer sequences located in the regulatory region of *Ttc39c* were mutated using the primer pairs listed in Table 1. The QuikChange II Site-Directed Mutagenesis protocol utilizing PfuTurbo DNA polymerase was performed according to the manufacturer's protocol (Agilent Technologies, Santa Clara, CA). The mutagenesis PCR reactions were digested with Dpn I (New England BioLabs, Ipswich, MA) and then transformed into sub-cloning efficiency competent cells (Life Technologies, Grand Island, NY). Clones were isolated and plasmids were purified and sequenced to confirm successful mutagenesis of the E-box enhancer sequences.

Transfections

C_2C_{12} myoblasts cells were plated into 12-well plates at a density of 50,000-75,000 cells/well and cultured overnight. Transfections were performed using TurboFect Transfection Reagent (Thermo Scientific, Rockford, IL) according to the manufacturer's protocol. Briefly, media was changed approximately 1-2 hours prior to transfection and 1μg of total DNA (250 ng/well of reporter plasmid, 125 ng/well of internal control plasmid, 125-250 ng/well of expression plasmids and empty pBluescript vector as filler DNA to 1 μg/well) was allowed to complex with the TurboFect transfection reagent for 20-30 minutes prior to overlaying the cells. Cells were incubated overnight with the TurboFect:DNA complexes. Cells were switched to differentiation media (2% serum) 24 hours post-transfection and incubated for an additional 24-72 hours prior to performing reporter assays.

Reporter gene assays

In order to monitor reporter gene activity, culture media was sampled at 24-72 hours following the switch to differentiation media and analyzed for SEAP activity using the Phospha-Light SEAP Reporter Gene Assay System according to the manufacturer's protocol (Life Technologies, Grand Island, NY). Glow luminescence levels were detected using a Synergy 2 microplate reader set for an endpoint read with a 2 second integration time. At the end of the assay, cells were lysed using Passive Lysis Buffer (Promega, Madison, WI), homogenates were cleared by centrifugation and analyzed for β-galactosidase (β-gal) activity. SEAP activity numbers were divided by β-gal activity numbers to correct for variations in transfection efficiency between replicate wells.

Bioinformatic analysis of Ttc39c

The nucleotide sequence corresponding to the regulatory regions of mouse, rat and human *Ttc39c* (Ensembl Transcript ID: ENSMUST00000025294.7, NSRNOT00000091424.1, and ENST00000317571.7, respectively) from -2000 through the first exon were downloaded from the Ensembl database (www.ensembl.org), aligned using the ClustalW2 alignment tool on the EMBL website (http://www.ebi.ac.uk/Tools/msa/clustalw2/), followed by Boxshade analysis of the ClustalW2 alignment output data (http://www.ch.embnet.org/software/BOX_form.html). The amino acid sequences for mouse Ttc39c were downloaded from the Ensembl database and aligned and shaded as described for the nucleotide sequences above.

Quantitative PCR

Total RNA was isolated from proliferating and differentiated C_2C_{12} cells as described in section 2.2. Purified total RNA (1.0µg) was reverse-transcribed using the iScript cDNA Synthesis Kit according to the manufacturer's protocol (Bio-Rad, Hercules, CA). The cDNA was them amplified using the iTaq Universal SYBR Green Reaction Supermix according the manufacturer's protocol (Bio-Rad, Hercules, CA) and quantitative analysis of *Ttc39c* expression was analyzed using the CFX Connect Real Time PCR Detection System (Bio-Rad, Hercules, CA). Each condition was performed in biological triplicates, each individual biological replicate was used for cDNA synthesis in duplicate, and each cDNA synthesis replicate was performed in technical triplicates (3 biological replicates x 2 cDNA synthesis replicates x 3 technical replicates = 18 individual reads per biological sample) and the experiment was repeated at least once. Relative *Ttc39c* gene expression was calculated using the $2^{-\Delta\Delta C_T}$ Livak method and GAPDH as the reference gene.

Protein purification and Western blot analysis

C_2C_{12} cells were differentiated over a 10 day time course by plating cells into 10cm culture dishes and maintaining them in proliferation media (DMEM + 10% serum) for 2 days followed by a switch to differentiation media (DMEM + 2% serum) at 2 days post-plating. The time course consisted of harvesting cells grown in proliferation media for 1 and 2 days, as well as, cells grown for 2 days in proliferation media followed by continued culturing for 1, 3, 5, 7, and 10 days in differentiation media. Harvested cells were spun down and stored at -80˚C until cell lysis and protein purification was performed.

Ttc39c was exogenously expressed in C_2C_{12} cells that were plated into 10cm culture dishes and transfected with the pcDNA3.1-Ttc39c expression plasmid 24 hours post-plating. The transfected cells were differentiated over a 5 day time course by maintaining them in proliferation media (DMEM + 10% serum) for 2 days followed by a switch to differentiation media (DMEM + 2% serum) at 2 days post-plating. The time course consisted of harvesting cells grown in proliferation media for 2 days, as well as, cells grown for 2 days in proliferation media followed by continued culturing for 1, 2, 3, 4 and 5 days in differentiation media. Harvested cells were spun down and stored at -80˚C until cell lysis and protein purification was performed.

Harvested cells were lysed on ice for 30 minutes in $ULB^{(+)}$ (50mM Tris, pH 7.5, 150mM NaCl, 50mM NaF, 0.5% NP-40, 1mM PMSF, 1mM DTT, 10mM β-glycerophosphate, 2mM sodium molbydate and a protease inhibitor cocktail). Cell lysates were cleared by centrifugation and protein concentrations were quantified using the Quick Start Bradford 1X Dye Reagent (Bio-Rad, Hercules, CA) according to the manufacturer's protocol.

Western blot analysis was performed by separating 25-100μg of total protein on a SDS-PAGE gel and then transferring the separated proteins overnight to Immobilon-P PVDF membrane (EMD Millipore, Billerica, MA). The membrane was Ponceau S stained to confirm equal protein loading and then blocked in blocking solution (5% w/v dry milk dissolved in Tris-buffered Saline (TBS) with 0.05% Tween-20). Blots were probed with anti-Ttc39c (G-6, Santa Cruz Biotechnology), anti-Myosin Heavy Chain (MYH1/2/4/6) (F59, Santa Cruz Biotechnology, Dallas, TX), anti-myogenin (F5D, Santa Cruz Biotechnology, Dallas, TX), anti-MyoD (5.8A, Santa Cruz Biotechnology, Dallas, TX), anti-p-ERK (E-4, Santa Cruz Biotechnology, Dallas, TX), anti-ERK (K-23, Santa Cruz Biotechnology, Dallas, TX), anti-IFT144 (ProteinTech, Rosemont, IL), anti-IFT88 (ProteinTech, Rosemont, IL), anti-acetylated tubulin (ProteinTech, Rosemont, IL), anti-Gli2 (ProteinTech, Rosemont, IL), or anti-α-tubulin (DM1A, Santa Cruz Biotechnology) primary antibodies followed by incubation with a species appropriate HRP-conjugated secondary antibody (Santa Cruz Biotechnology, Dallas, TX) and developed using ECL Western Blotting Substrate (Pierce/Thermo Scientific, Rockford, IL). Blots were stripped by incubating at room temperature for 10-15 minutes in Stripping Buffer (6M Guanidine Hydrochloride, 20mM Tris, pH 7.5, 0.2% Igepal CA-630, and 0.1M DTT), washed, and then blocked, re-probed and imaged as described above.

Confocal Fluorescence Microscopy

C_2C_{12} cells were plated into Cellvis 35mm glass bottom dishes with 20mm bottom well and transfected ~24 hours post-plating with pEGFP-C1 empty vector or pEGFP-Ttc39c complexed with TurboFect Transfection Reagent (Thermo Scientific, Rockford, IL) according to the

manufacturer's protocol. Cells were washed 2X with PBS ~24 hours post-transfection, fixed with 4% paraformaldehyde in 0.1M sodium cacodylate, pH 7.6, stained with DRAQ5 far-red fluorescent DNA dye (Biostatus, Leicestershire, UK) and mounted with VECTASHIELD HardSet Mounting Medium (Vector Laboratories, Burlingame, CA). All images shown were taken using an Olympus Fluoview FV-1000 confocal fluorescent microscope with either a Super Apochromat UPLSAPO 20X objective or a Super Apochromat UPLSAPO 60XW objective. The GFP and DRAQ5 images were merged using open access ImageJ software with the Open Microscopy Environment Bio-Formats software plugin tool.

siRNA Knockdown of Ttc39c

The murine Ttc39c transcript (GenBank accession number: NM_028341) was analyzed using the Whitehead Institute siRNA design tool (http://sirna.wi.mit.edu/) and two siRNA targeting sequences were selected. The sequences were used in the creation of two sets of complimentary oligonucleotides (Table 1.) that were then annealed together and cloned into the Bgl II and Hind III sites of the pSuper-Basic plasmid according the manufacturer's protocol (Oligoengine, Seattle, WA). Recombinant plasmids were sequenced to confirm proper orientation and absence of mutations. C_2C_{12} cells were then transfected with the pSuper-Ttc39c-siRNA-2 or pSuper-Ttc39c-siRNA-3 plasmid as described in section 2.6, cells were harvested 24-48 hours post-transfection, and Western blot analysis was performed as described in section 2.10 to confirm efficient Ttc39c knockdown.

Statistics

Data are presented as the mean ± standard deviation (SD). Statistical analysis was conducted using a two-tailed t-test and a difference was considered statistically significant at a P value < 0.05.

Results

Ttc39c is induced during skeletal muscle atrophy and is differentially expressed in MuRF1-null mice.

An Illumina mouse-6 v1.1 expression beadchip array was performed on RNA isolated from triceps surae (TS) muscle from mice undergoing neurogenic atrophy (i.e. denervation) as previously described (Furlow et al., 2013). Deeper analysis of the data SubSeries (GEO: GSE44205) deposited as part of a SuperSeries (GEO: GSE44259) submitted to the NCBI Gene Expression Omnibus (GEO) revealed a number of genes that have not previously been described in skeletal muscle and show differential expression patterns in response to denervation-induced skeletal muscle atrophy. *Ttc39c*, which was originally identified as a Riken gene (2810439F02RIK) in the Illumina beadchip array, showed relatively low basal expression in control muscle tissue, but was induced significantly in response to neurogenic atrophy at 3 days and 14 days post-denervation (Fig. 6A). In contrast, neurogenic atrophy had no effect on *Ttc39c* expression in muscle tissue isolated from MuRF1-null mice at 3 days or 14 days post-denervation (Fig. 6B).

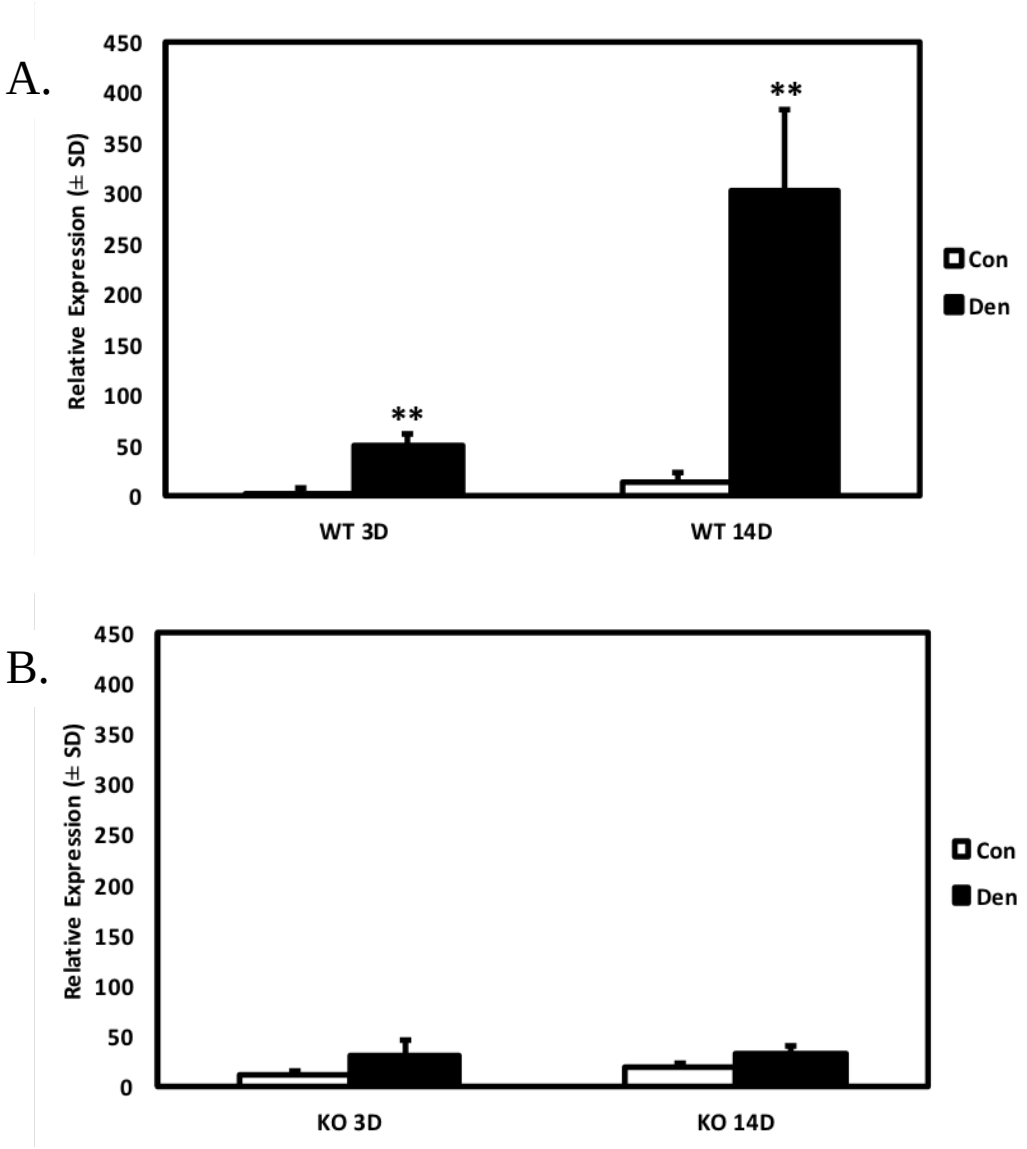

Figure 6. *Ttc39c* is induced during neurogenic skeletal muscle atrophy and is expressed in muscle cells. Whole genome expression analysis was conducted on triceps surae muscle from **(A)** wild-type (WT) and **(B)** MuRF1-null (KO) control (CON) mice after 3 days (3D) and 14 days (14D) of denervation (DEN). *Ttc39c* expression (array address 1410725) increased significantly at both 3 and 14 days of denervation in wild-type (WT) animals, but not in MuRF1-null animals. Each condition represents the average expression from three animals and error bars represent ± SD. White bars, controls; black bars, DEN. Significant difference between denervated mice and control mice in the same group, (**: $P < 0.01$).

.

Ttc39c expression is highest during early skeletal muscle cell differentiation.

Ttc39c is located on chromosome 18 in *M. musculus* and is predicted to have two alternative transcripts (identified in this manuscript as alternative transcript 1 (AT1) and alternative transcript 2 (AT2) that each consist of 14 exons. The AT1 isoform consists of 14 coding exons (Fig. 7A), while the AT2 isoform consists of 13 coding exons and one non-coding exon (Fig. 7B). To confirm that *Ttc39c* is expressed endogenously at the RNA level in muscle cells, qPCR was performed using RNA isolated from proliferating myoblasts and myotubes at early and late stages of differentiation. The results demonstrate that Ttc39c expression is elevated in early differentiation compared to expression levels in proliferating myoblasts and fully differentiated myotubes (Fig. 7C).

A.

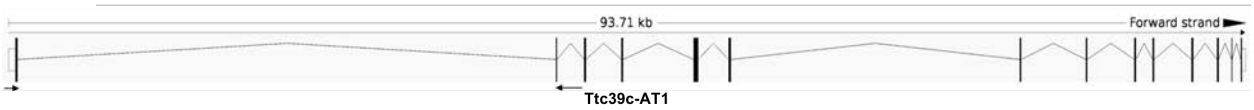

B.

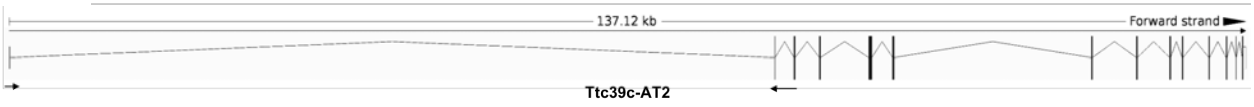

C.

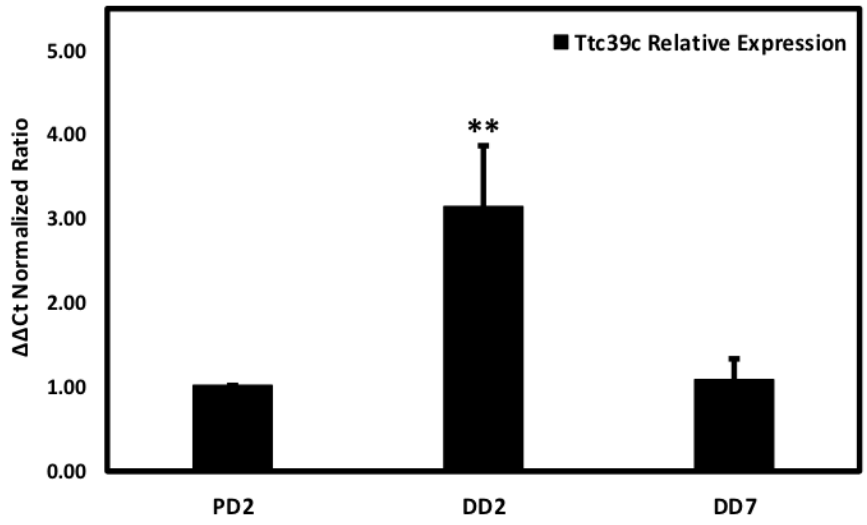

Figure 7. Schematics for the alternative transcripts of Ttc39c and endogenous expression profile of Ttc39c in C_2C_{12} myoblasts. Schematics of the **(A)** *Ttc39c-AT1* and **(B)** *Ttc39c-AT2* alternative transcripts of the *Ttc39* gene locus in mouse. Darkened rectangles represent exons containing translated region, open rectangles represent exons containing the untranslated regions and the lines connecting the rectangles represent introns. The arrows signify the location of the qPCR primers used to quantify the expression of the *Ttc39c* transcript. **(C)** *Ttc39c* increases in expression in early differentiation and then decreases as C_2C_{12} myoblasts differentiate. qPCR was performed on RNA isolated from proliferating (P) and differentiated (D) C_2C_{12} cells harvested over a 7 day differentiation time course. Cells were maintained in proliferation media (10% serum) and harvested 2 days post-plating (PD2) and the remaining cells were then switched to differentiation media (2% serum) and harvested at 2 (DD2) and 7 (DD7) days post-media change. Ttc39c expression was calculated using the $\Delta\Delta C_T$ method with normalization to GAPDH expression. Significant difference between Ttc39c expression at DD2 compared PD2, (**: $P < 0.01$)

To assess the effectiveness of a commercially available primary mouse monoclonal Ttc39c antibody (G6, Santa Cruz Biotechnology used at 1:1000 dilution) to detect mouse Ttc39c, 293T cells were transfected with expression plasmids that contained untagged murine Ttc39c, GFP-tagged Ttc39c and 6X-myc-tagged Ttc39c. Cells transfected with the mouse *Ttc39c* expression plasmids showed elevated levels of Ttc39c protein and also demonstrated a doublet that likely represents two alternative protein isoforms (Fig. 8). C_2C_{12} cells were differentiated and harvested over a 10 day time course and cell lysates were analyzed by Western blotting for endogenous Ttc39c protein expression levels (Fig. 9). Ttc39c protein levels peaked during late proliferation and early differentiation and then decreased by day 3 of differentiation. To monitor the differentiation status of C_2C_{12} cells over the differentiation time course, blots were also probed using a mouse monoclonal myosin heavy chain antibody (1:500 dilution). Myosin heavy chain increases as C_2C_{12} cells begin to differentiate from myoblasts to myotubes and peaks and stabilizes at about differentiation day 2 (Fig. 9). To confirm equal protein loading, the blots were also probed using a mouse monoclonal α-tubulin antibody (1:500 dilution) (Fig. 9).

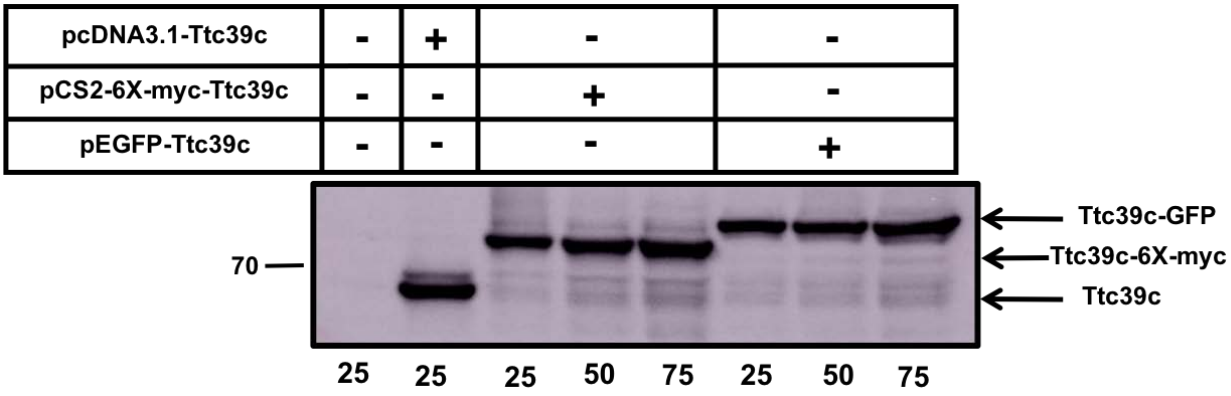

Figure 8. Validation of the Ttc39c mouse monoclonal antibody. Western blot analysis of ectopically expressed Ttc39c in 293T cells. 293T cells were transiently transfected with pcDNA3.1-Ttc39c, pCS2-6X-myc-Ttc39c, or pEGFP-Ttc39c. The gel was loaded with 25ug of protein lysate isolated from control cells and pcDNA3.1-Ttc39c transfected cells and three concentrations (25 µg, 50 µg and 75 µg) of protein lysate from cells transfected with pCS2-6X-myc-Ttc39c or pEGFP-Ttc39c were analyzed by Western blot.

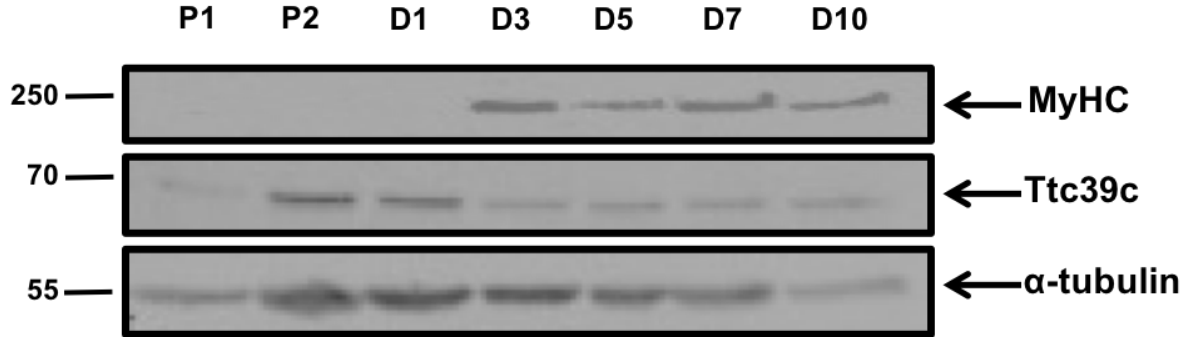

Figure 9. Ttc39c protein expression profile in C_2C_{12} myoblasts. Western blot analysis was performed using an antibody against Ttc39c on protein homogenates isolated from proliferating (P) and differentiated (D) C_2C_{12} cells harvested over a 10 day differentiation time course. Cells were maintained in proliferation media (10% serum) and harvested 1 and 2 days post-plating and the remaining cells were then switched to differentiation media (2% serum) and harvested at 1, 3, 5, 7 and 10 days post-media change. Myosin Heavy Chain (MyHC) was analyzed as a marker for differentiation and α-tubulin was analyzed to confirm equal protein loading.

Identified putative functional domains of Ttc39c possibly facilitate protein-protein interactions.

Mouse Ttc39c has two putative protein isoforms that are 580 amino acids (Ttc39c-580) or 522 amino acids (Ttc39c-522) in length and have predicted molecular weights of ~65.5kDA and ~59kDA, respectively. These two Ttc39c protein isoforms are validated in human and are predicted in mouse and are produced by the use of alternative start codons, which are indicated with an asterisk and highlighted in blue in the protein sequence alignment (Fig. 10). The Ttc39c

amino acid sequence is highly conserved from rodents to humans, with human Ttc39c sharing 94% identity with mouse and rat Ttc39c. Using the SMART database and the NCBI Conserved Domain Database (CDD), both Ttc39c isoforms are predicted to have a large domain of unknown function (DUF) spanning amino acids 31-495 that includes at least 4 tetratricopeptide repeat (TPR) domains (highlighted in red) (Fig. 10). The TPR domain has been shown to play an important role in protein-protein interactions and is proposed to be important for proteins that act as scaffolds for the assembly of larger protein complexes (Zeytuni and Zarivach, 2012).

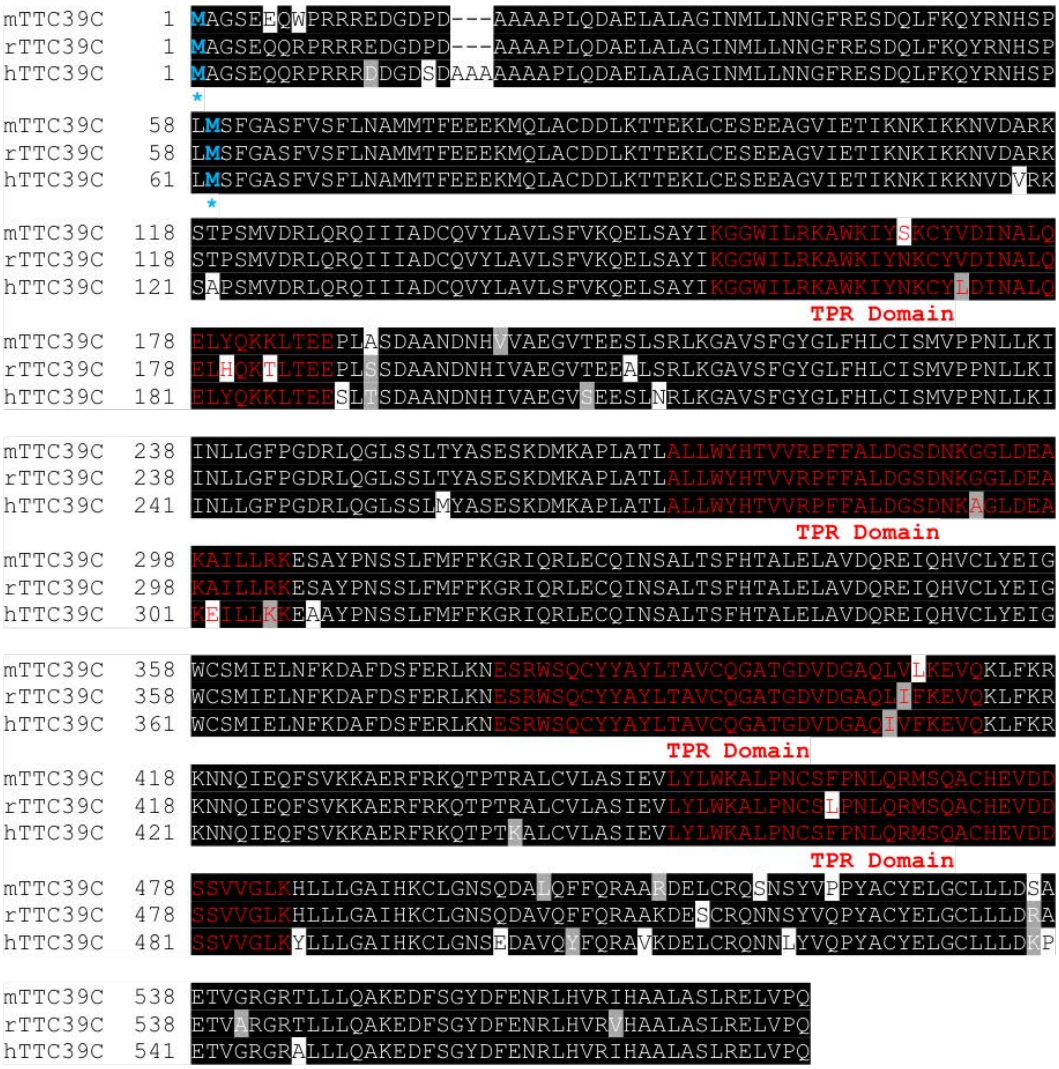

Figure 10. Protein sequence alignment of Ttc39c in mouse, rat, and human. Sequences of the mouse, rat and human Ttc39c protein were downloaded from the Ensembl database and aligned using the ClustalW2 algorithm. Approximate positions of the putative Tetratricopeptide Repeat (TPR) domains are highlighted in red in the alignment. The alternative start codons for Ttc39c-580 and Ttc39c-522 are highlighted in blue and indicated with an asterisk. The gene structure schematic images were downloaded from the Ensembl database (www.ensembl.org).

Cloning and analysis of the proximal regulatory regions of Ttc39c alternative transcripts.

Transcription initiation of the Ttc39c locus is predicted to occur from two alternative regions resulting in a two different transcripts with alternative first exons (Fig. 7A and Fig 7B). In order to assess the level of conservation between the common promoter regions of mouse, rat and human Ttc39c-AT1 and mouse and rat (Tct39c-AT2) and to identify potential transcriptional regulatory elements, the genomic sequences corresponding to the regulatory regions of these two alternative transcripts for mouse, rat and human were aligned (Fig. 11A and 12A). Several putative enhancer elements were identified, including a conserved E-box sequence in each putative promoter, and are indicated in the promoter schematics with an asterisk (Fig. 11A and 12A). In addition to the conserved E-box, the proximal regulatory region of *Ttc39c-AT1* contains a FoxO consensus element and TFIIB binding element, while the proximal regulatory region of *Ttc39c-AT2* contains a putative Elk1 consensus element, a consensus AP-1 element, a Runx1 element and a TFIIB binding element (Fig. 11A and 12A).

To confirm that the regulatory regions of both alternative transcripts possess transcriptional activity, 500, 1000 and 2000 bp fragments of the proximal regulatory regions of each transcript was cloned using the primer pairs listed in Table 1. The promoter fragments were fused with the secreted alkaline phosphatase (SEAP) reporter gene to create the pSEAP-Ttc39c-AT1-Pro500, pSEAP-Ttc39c-AT1-Pro1000, pSEAP-Ttc39c-AT1-Pro2000, pSEAP-Ttc39c-AT2-Pro500, pSEAP-Ttc39c-AT2-Pro1000, and pSEAP-Ttc39c-AT2-Pro2000 reporter plasmids. C_2C_{12} mouse

myoblast cells were transiently transfected with the *Ttc39c-AT1* and *Ttc39c-AT2* reporter plasmids and SEAP activity levels were analyzed 48-72 hours following the switch to differentiation media and compared to SEAP activity levels from cells transfected with the empty pSEAP2-Basic plasmid. The *Ttc39c-AT1* and *Ttc39c-AT2* reporter plasmids each showed robust transcriptional activity and had significantly higher activity compared to the empty reporter plasmid alone (Fig. 11B-D and 12B-D).

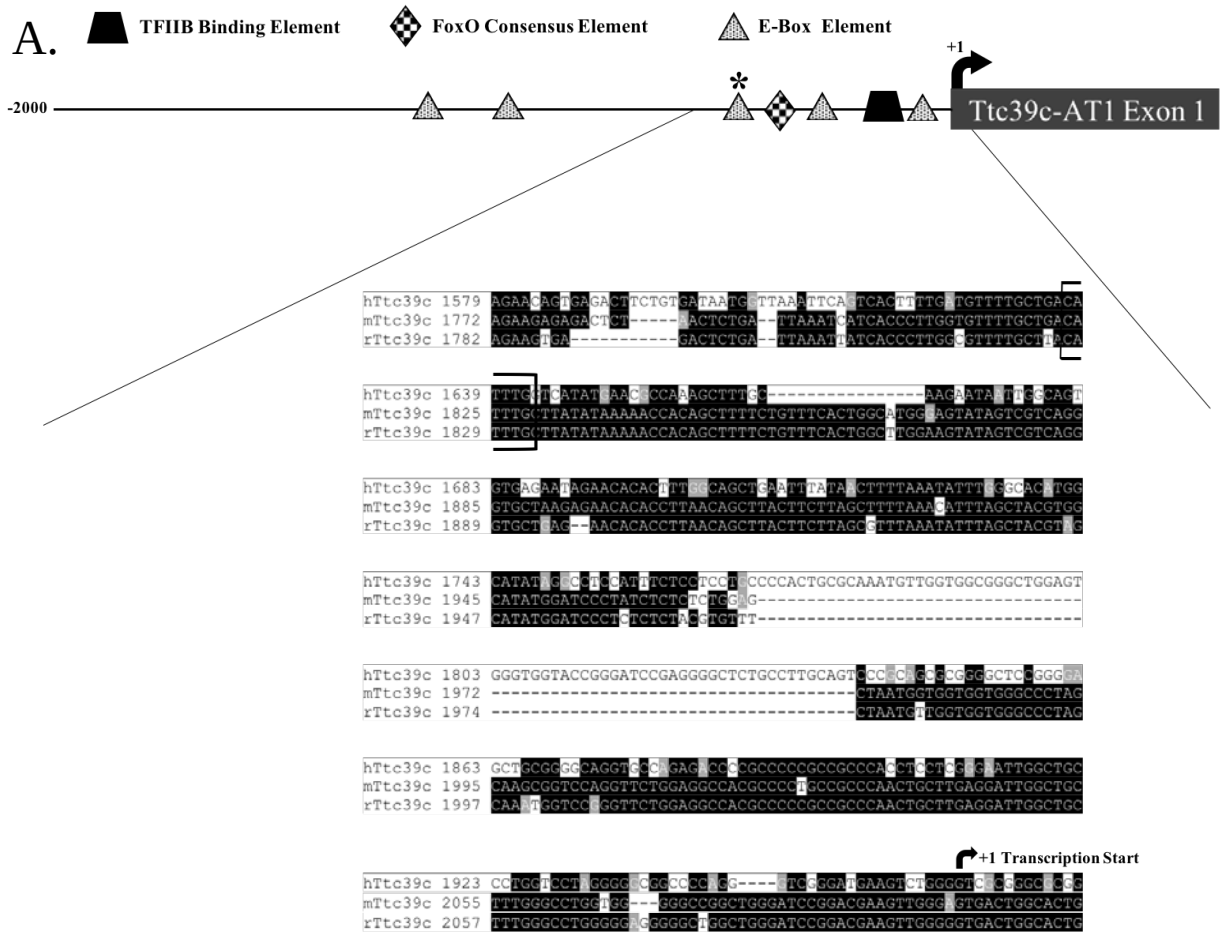

B.

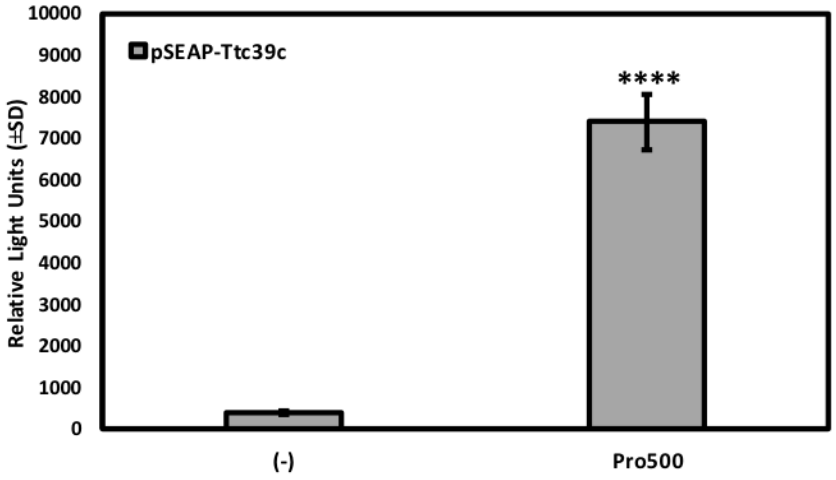
pSEAP-Ttc39c
Relative Light Units (±SD)
10000
9000
8000
7000
6000
5000
4000
3000
2000
1000
0
****
(-)
Pro500

C.

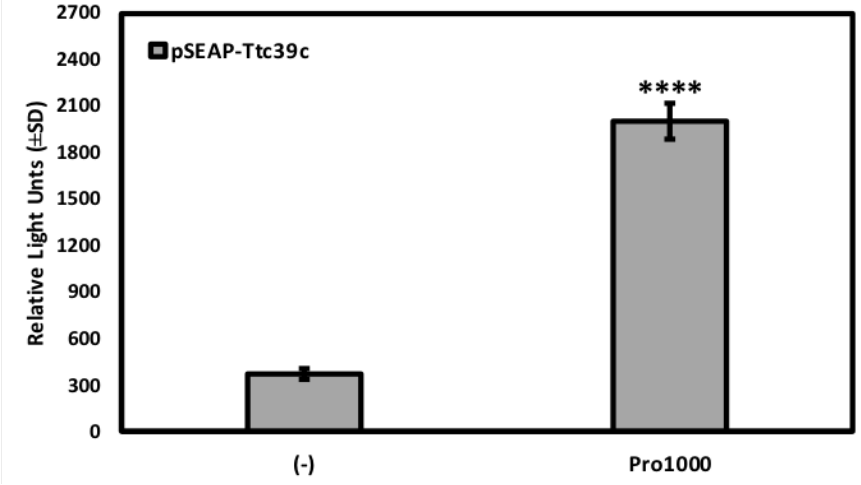
pSEAP-Ttc39c
Relative Light Unts (±SD)
2700
2400
2100
1800
1500
1200
900
600
300
0
****
(-)
Pro1000

D.

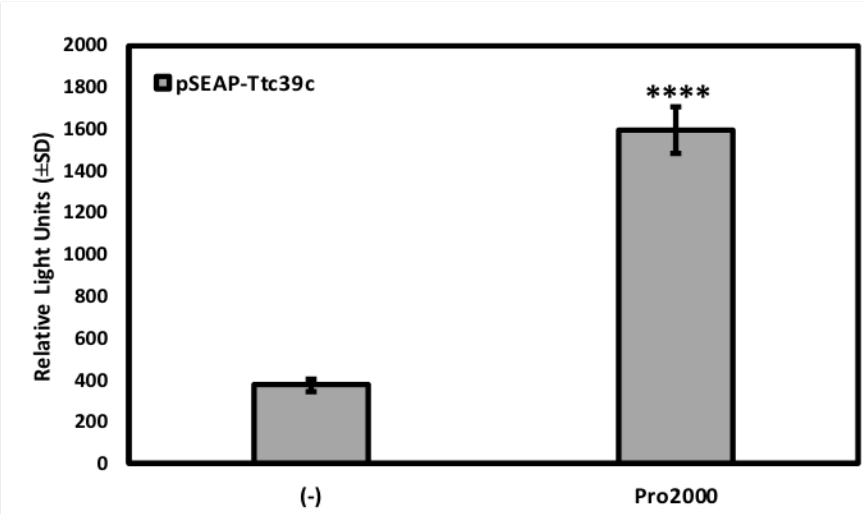
pSEAP-Ttc39c
Relative Light Units (±SD)
2000
1800
1600
1400
1200
1000
800
600
400
200
0
****
(-)
Pro2000

Figure 11. Schematic, sequence alignment, and analysis of the *Ttc39c-AT1*alternative transcript promoter region. Promoter sequences from mouse, rat, and human *Ttc39c-AT1* (2000 base pairs upstream of the start of the transcription start site (+1) through the first exon) were downloaded from the Ensembl database (www.ensembl.org) and aligned using the ClustalW algorithm. Approximate positions of putative transcription factor binding sites are indicated in the schematic of the **(A)** *Ttc39c-AT1* regulatory region at the top. Putative TFIIB Response Element (BRE) 5'-(G/C)(G/C(G/A)CGCC-3' (shaded trapezoid), predicted FoxO binding element 5'-(G/A)TAAA(T/C)AA-3" (checkered diamond), and putative consensus E-box elements 5'-CANNTG-3' (dotted triangle) are indicated. N represents any nucleotide. Conserved nucleotides are highlighted in black, transitions are highlighted in gray and transversions are highlighted in white. The black arrow indicates the position of the transcription initiation start site. Cloning and analysis of the proximal regulatory region of *Ttc39c-AT1* was conducted by transfecting C_2C_{12} myoblasts with either an empty reporter plasmid or a reporter plasmid containing **(B)** ~500 bp, **(C)** ~1000 bp or **(D)** ~2000 bp of the *Ttc39c-AT1* promoter fused to the Secreted Alkaline Phosphatase (SEAP) reporter gene. Each condition was performed in triplicate and each experiment was repeated at least once. The graphs are of a representative experiment and values correspond to the mean relative light unit (RLU) values ± SD. Significant difference between the control empty reporter plasmid (pSEAP2-Basic) and either the pSEAP-Ttc39c-Pro500-AT1, pSEAP-Ttc39c-Pro1000-AT1, or pSEAP-Ttc39c-Pro2000-AT1 reporter constructs (****: P < 0.001).

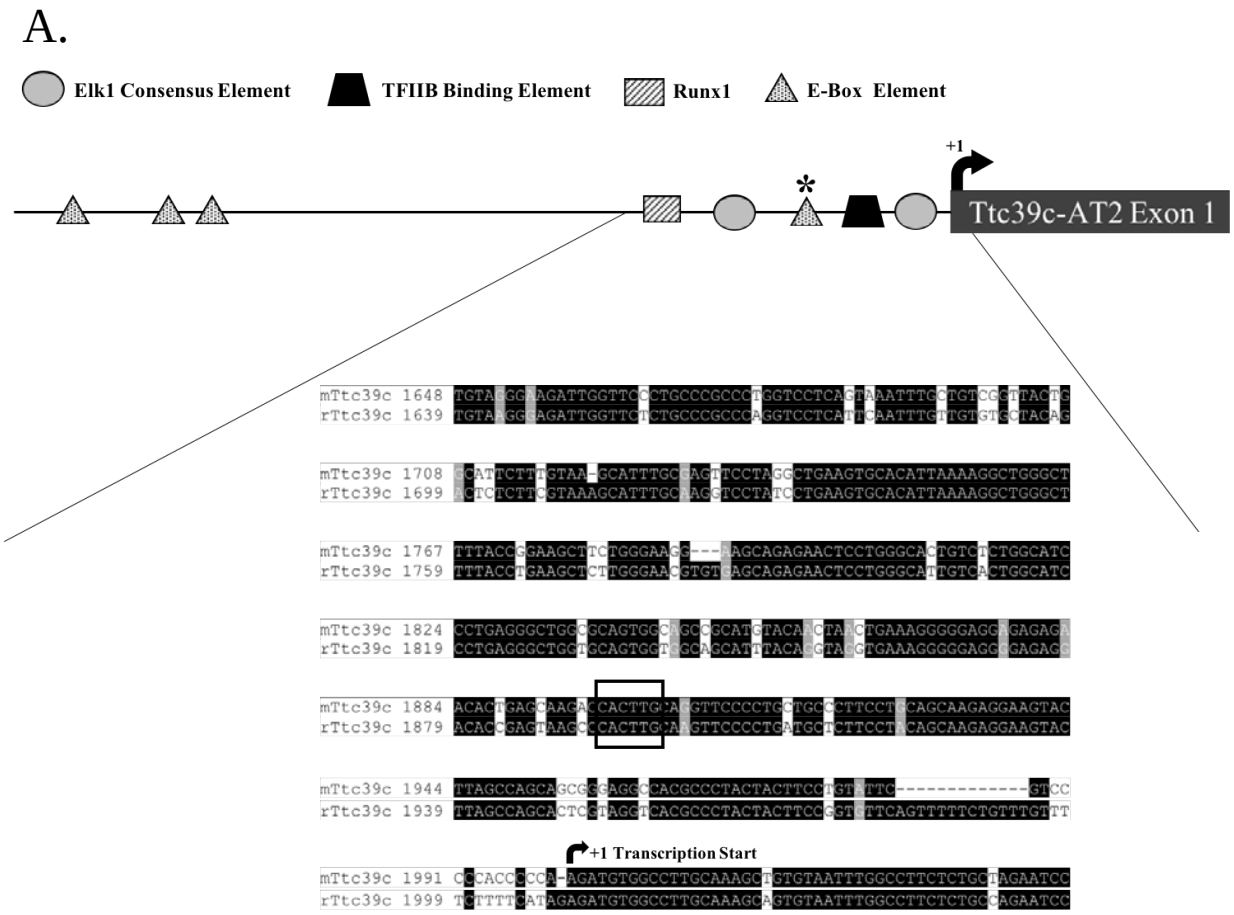

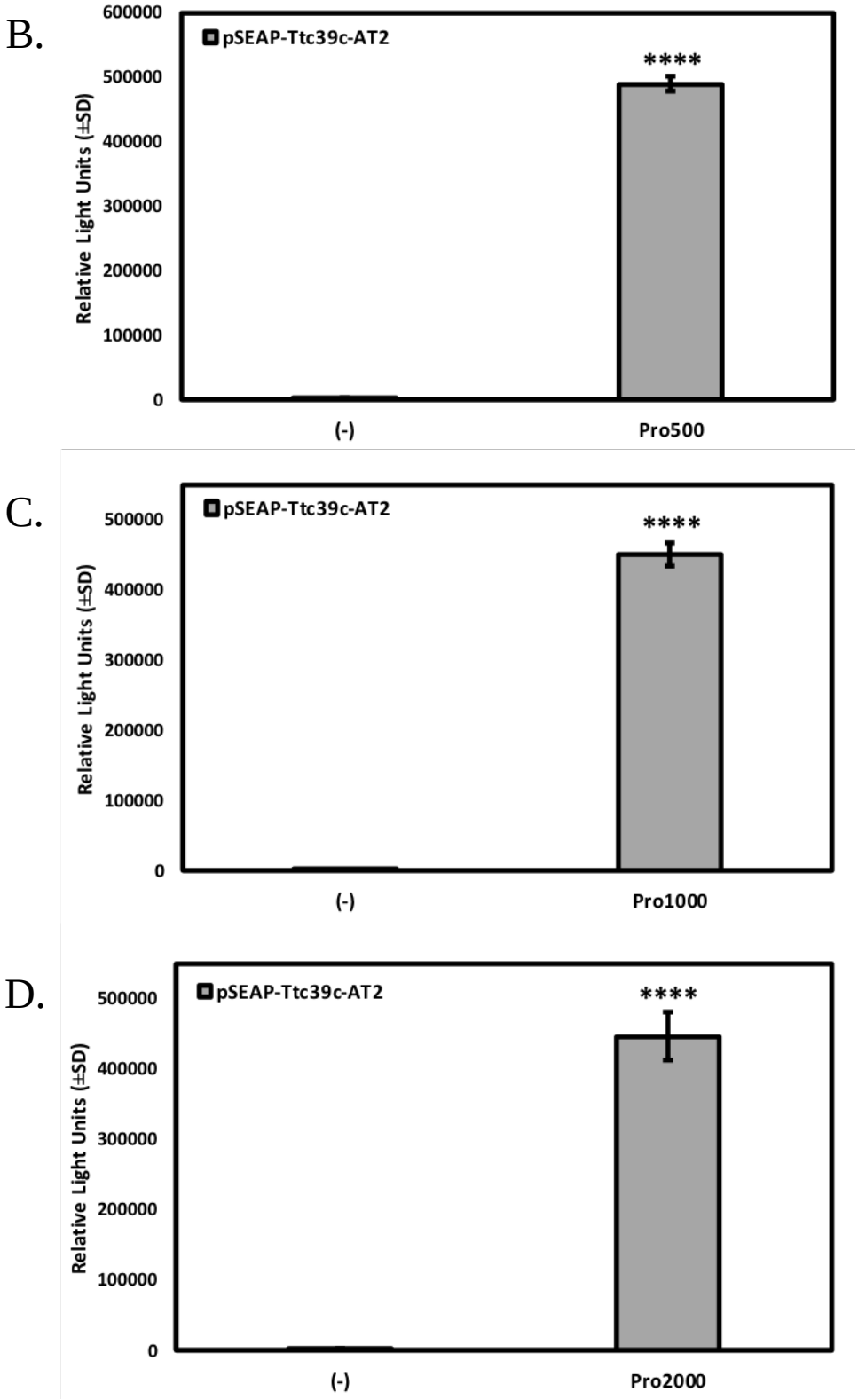

Figure 12. Schematic, sequence alignment, and analysis of the *Ttc39c-AT2* alternative transcript promoter region. Promoter sequences from mouse and rat *Ttc39c-AT2* (2000 base pairs upstream of the start of the transcription start

site (+1) through the first exon) were downloaded from the Ensembl database (www.ensembl.org) and aligned using the ClustalW algorithm. Approximate positions of putative transcription factor binding sites are indicated in the schematic of the **(A)** *Ttc39c-AT2* regulatory region at the top. Putative TFIIB Response Element (BRE) 5'-(G/C)(G/C(G/A)CGCC-3' (shaded trapezoid), predicted Elk-1 binding element, 5'-CC(A/T)$_6$GG-3' (gray circle), predicted Runx1 binding element 5'-TGTGGT-3' (stripped square), and putative consensus E-box elements 5'-CANNTG-3' (dotted triangle) are indicated. N represents any nucleotide. Conserved nucleotides are highlighted in black, transitions are highlighted in gray and transversions are highlighted in white. The black arrow indicates the position of the transcription initiation start site. Cloning and analysis of the proximal regulatory region of *Ttc39c-AT2* was conducted by transfecting C_2C_{12} myoblasts with either an empty reporter plasmid or a reporter plasmid **(B)** ~500 bp, **(C)** ~1000 bp or **(D)** ~2000 bp of the *Ttc39c-AT2* promoter fused to the Secreted Alkaline Phosphatase (SEAP) reporter gene. Each condition was performed in triplicate and each experiment was repeated at least once. The graphs are of a representative experiment and values correspond to the mean relative light unit (RLU) values ± SD. Significant difference between the control empty reporter plasmid (pSEAP2-Basic) and either the pSEAP-Ttc39c-Pro500-AT2, pSEAP-Ttc39c-Pro1000-AT2, or pSEAP-Ttc39c-Pro2000-AT2 reporter constructs (****: $P < 0.001$).

Ttc39c reporter gene activity is repressed in response to ectopic MRF expression

Myogenic regulatory factors (MRF's) are transcription factors important in muscle tissue formation and are known to regulate gene activity by interacting with co-activators or co-repressors at the promoters of muscle-specific genes (Singh and Dilworth, 2013; Londhe and Davie, 2011**)**. MRFs are characterized by having a basic helix-loop-helix (bHLH) motif, which promotes binding to a canonical E-box consensus sequence of 5'-CANNTG-3' (where N can be any nucleotide base) (Singh and Dilworth, 2013; Londhe and Davie, 2011**)**. These E-box sequences are found in the promoter regions of most muscle specific genes, and MRFs can bind directly to these E-boxes to modulate the transcriptional activity of genes that possess these enhancers (Londhe and Davie, 2011).

Two MRFs important in skeletal muscle are MyoD and myogenin. MyoD acts as a marker of myogenic commitment to skeletal muscle and helps to maintain the differentiated state of muscle cells (Londhe and Davie, 2011). In addition, MyoD is important in the expression of myogenin in muscle cells, while myogenin also has a significant role in muscle cell differentiation and, unlike other MRFs, is required for cell viability (Londhe and Davie, 2011). Furthermore, it has been shown that the deletion of myogenin results in lower levels of MuRF1 in skeletal muscle and

resistance to muscle wasting in mice experiencing denervation-induced atrophy (Moresi, et al., 2010).

Neurogenic atrophy results in a dramatic increase in MRF expression, including significant increases in MyoD and myogenin expression (Merlie et al., 1994; Cohen et al., 2007; Tang et al., 2009; Williams et al., 2009; Moresi et al., 2010; Furlow et al., 2013). Furthermore, the conserved E-box sequence identified in the two alternative Ttc39c regulatory regions matches the canonical E-box sequence (Fig. 11A and 12A, boxed sequences), which is the preferred sequence for MRF binding (Cao et al., 2010). Therefore, since MyoD1 and myogenin are elevated during neurogenic atrophy and are capable of binding canonical E-box elements in muscle-specific genes, we evaluated the ability of the *Ttc39c* reporters to respond to ectopic expression of MyoD1 and myogenin in C_2C_{12} cells transiently transfected with the Ttc39c-AT1-Pro500 (Fig, 13A and 13B) and Ttc39c-AT2-Pro500 (Fig. 13C and 13D) wild-type reporter constructs. Interestingly, cells transiently transfected with MyoD1 (Fig. 13A and 13C) or myogenin (Fig. 13B and 13D) expression plasmids showed significantly lower *Ttc39c* reporter gene activity compared to cells that were not.

A.

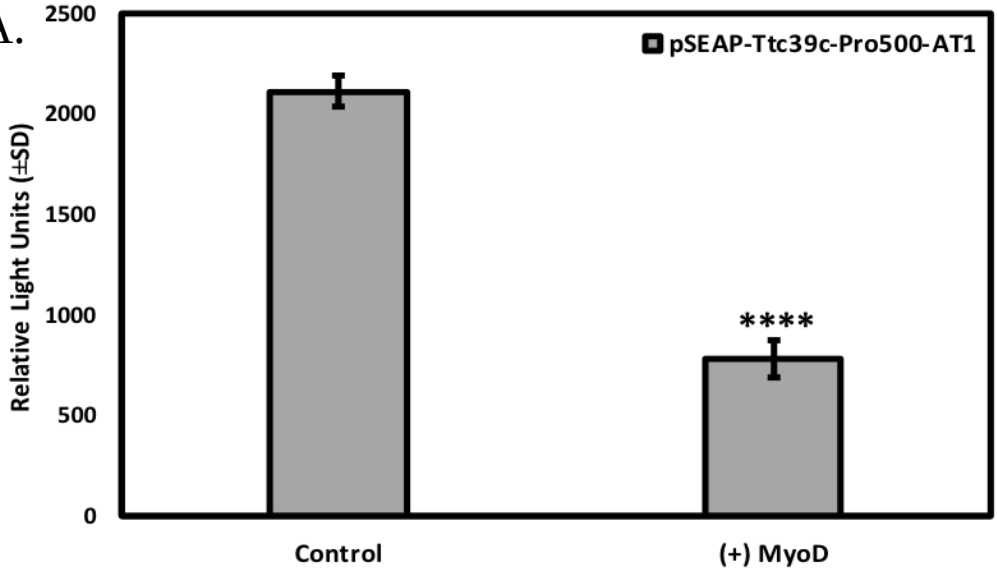
pSEAP-Ttc39c-Pro500-AT1
Relative Light Units (±SD)
2500
2000
1500
1000
500
0
****
Control
(+) MyoD

B.

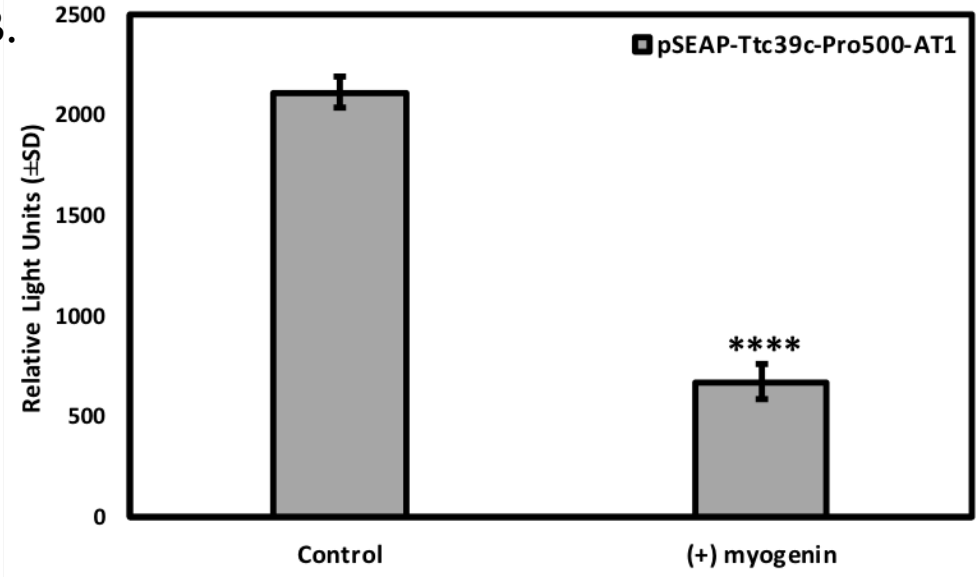
pSEAP-Ttc39c-Pro500-AT1
Relative Light Units (±SD)
2500
2000
1500
1000
500
0
****
Control
(+) myogenin

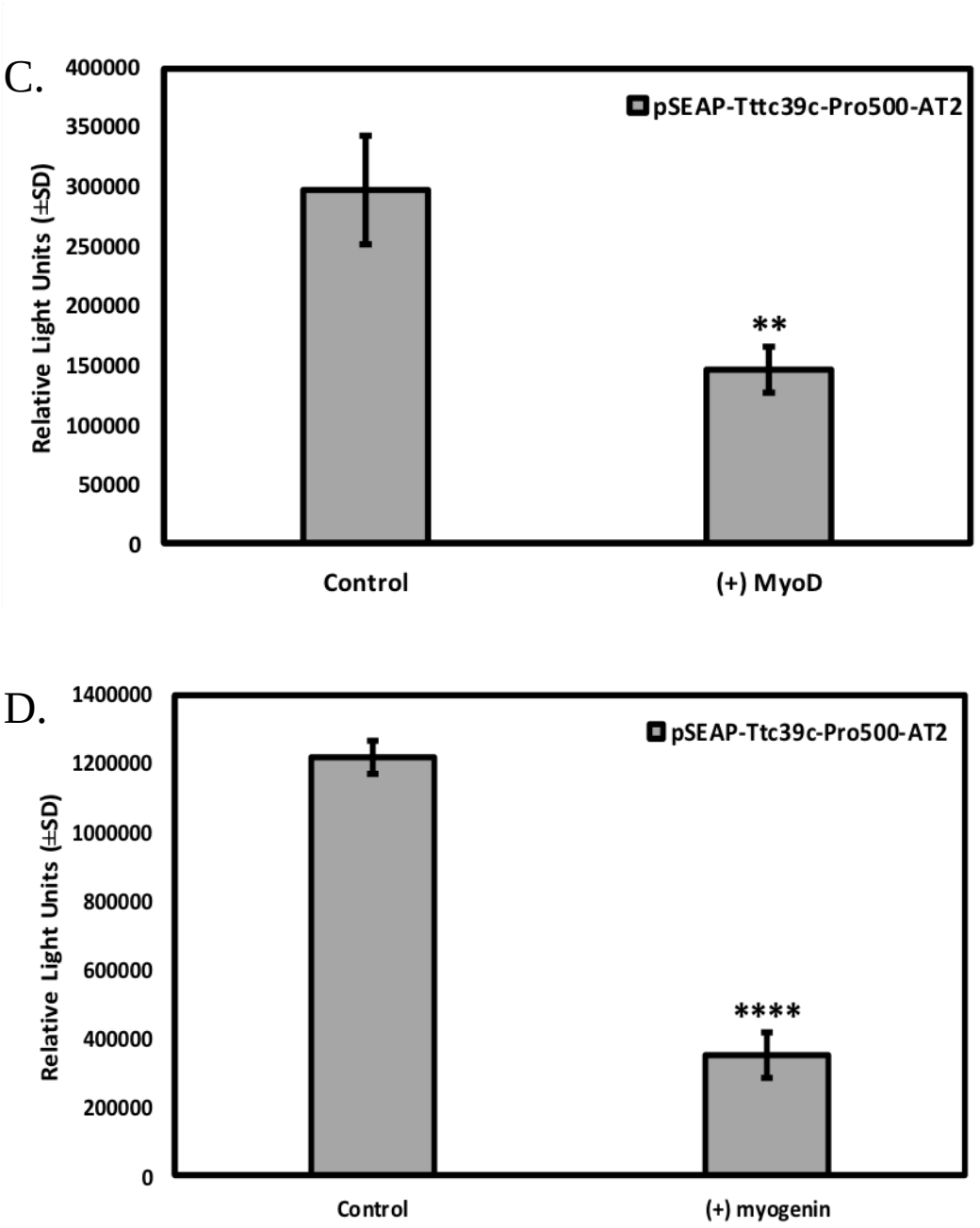

Figure 13. Myogenic regulatory factors repress Ttc39c reporter gene activity. C_2C_{12} myoblasts were transfected with the **(A and B)** pSEAP-Ttc39c-Pro500-AT1 or **(C and D)** pSEAP-Ttc39c-Pro500-AT2 reporter plasmids alone or in combination with **(A and C)** MyoD or **(B and D)** myogenin expression plasmids, a β-galactosidase reporter plasmid and filler DNA to 1µg/well of total DNA. The media was then assayed for SEAP activity at 72 hours following the switch to differentiation media and SEAP numbers were normalized to β-galactosidase activity to correct for variations in transfection efficiency. Each condition was performed in triplicate and each experiment was repeated at least once. The graphs are of a representative experiment and values correspond to the mean relative light unit (RLU) values ± SD. Significant differences between the activities of the pSEAP-Ttc39c-Pro500-AT1 and pSEAP-Ttc39c-Pro500-AT2 reporter constructs alone compared to reporter gene activity in response to MyoD or myogenin overexpression are indicated (****: $P < 0.001$).

Characterization of conserved E-box elements in the regulatory regions of Ttc39c-AT1 and Ttc39c-AT2.

A sequence matching the canonical E-box element sequence (5'-CANNTG-3') was identified in the proximal promoter region of both *Ttc39c* alternative transcripts and found to be conserved in rodents and humans (Fig. 14A and 15A). Furthermore, additional consensus E-box elements were also identified in the proximal 2000 base pair regulatory regions of the two Ttc39c alternative transcripts (Fig. 14B and 15B). To determine if the conserved putative E-box elements are necessary for proper *Ttc39c* promoter activity, a site-directed mutagenesis strategy was developed and performed using the 500 base pair promoter fragments of the alternative Ttc39c reporter plasmids, resulting in the generation of the pSEAP-Ttc39c-Pro500-E-Box1, E-Box-2 and E-Box-2 mutants for AT1 (Fig. 14C) and the pSEAP-Ttc9c-Pro500 E-box mutant for AT2 (Fig. 15C). Mutation of the conserved E-box in the Ttc39c-Pro500-AT1 promoter construct resulted in significantly lower reporter gene activity compared to the wild-type reporter construct, while constructs containing mutations of the non-conserved E-box elements had no significant effect on reporter gene activity in transiently transfected C_2C_{12} cells (Fig. 14D). Additionally, mutation of the conserved E-box in the Ttc39c-Pro500-AT2 promoter construct also resulted in significantly lower reporter gene activity compared to the wild-type reporter construct in transiently transfected C_2C_{12} cells (Fig. 15D).

A.

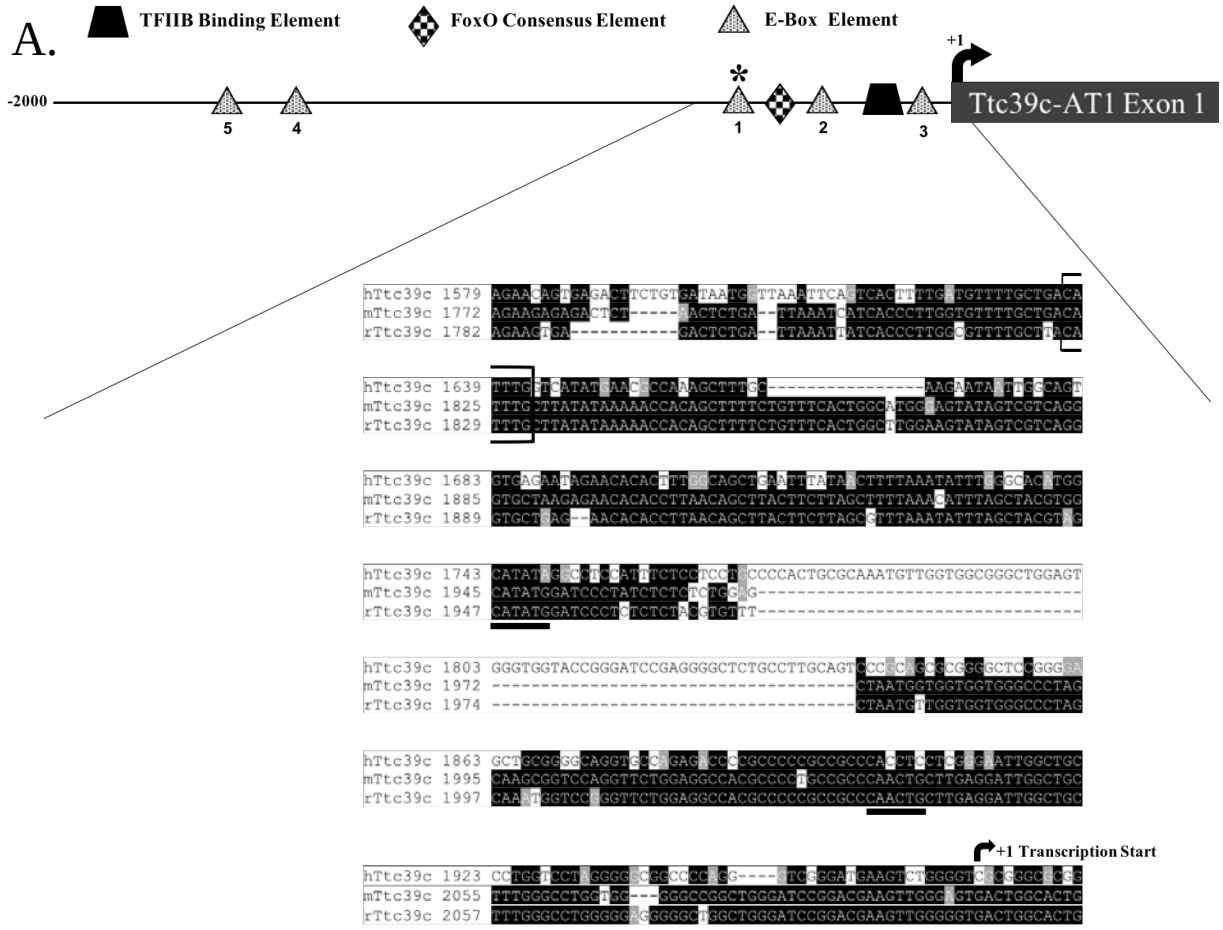

B.

E-box Sequence	E-Box Location
CATTTG*	-1325 to -1320
CAACTG*	-1165 to -1161
CATTTG**	-277 to -272
CATATG*	-155 to -150
CAACTG*	-67 to -62

* conserved in mouse and rat

** conserved in mouse, rat and human

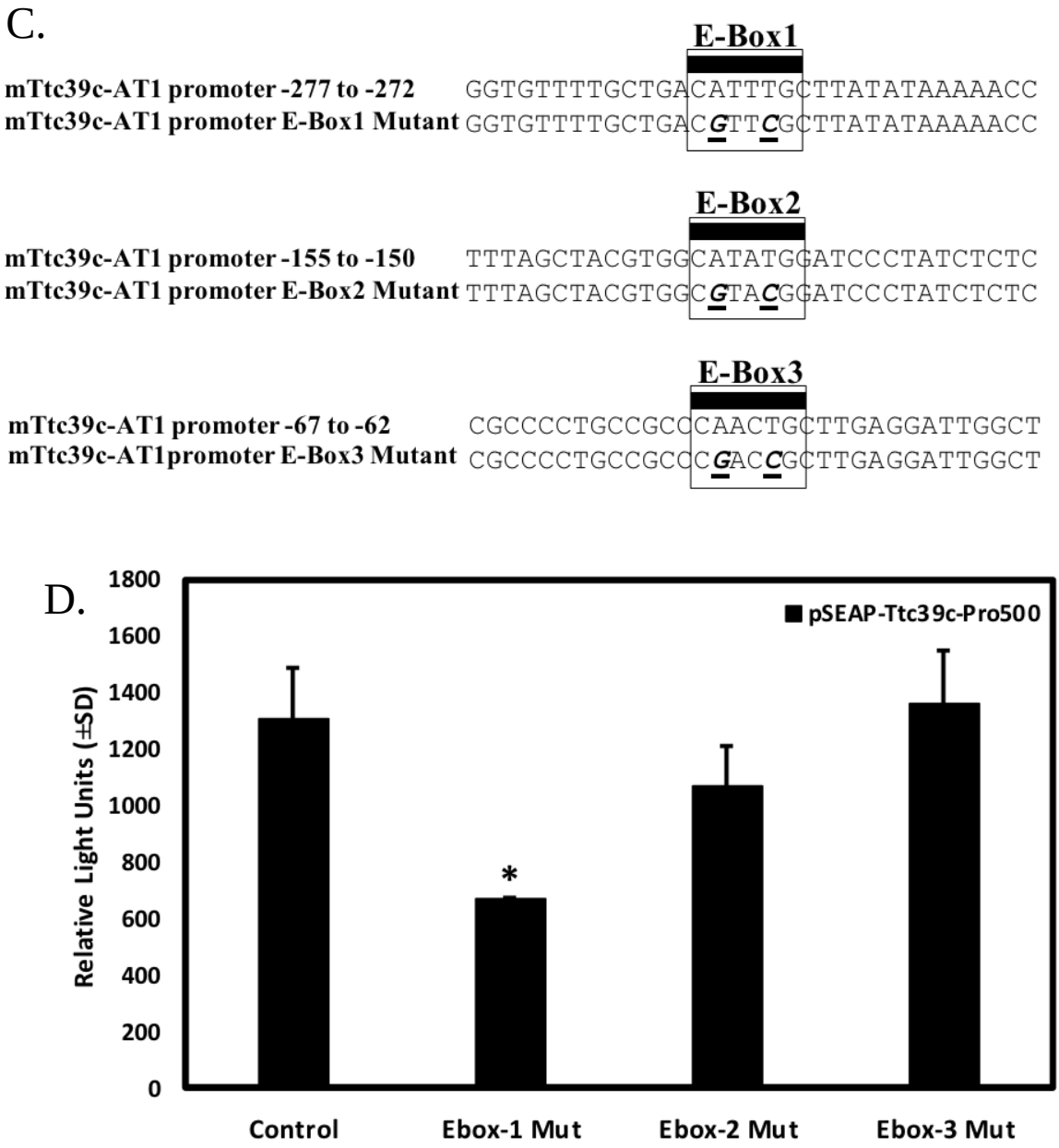

Figure 14. Conserved E-boxes in the proximal regulatory region of *Ttc39c-AT1* necessary for full reporter gene activity. Schematic, sequence alignment and analysis of the **(A)** *Ttc39c-AT1* promoter region containing multiple putative consensus E-box elements 5'-CANNTG-3' (dotted triangles). The starred triangle represents the conserved E-Box elements in the *Ttc39c-AT1* regulatory region schematic and the sequences are boxed in the alignment. N represents any nucleotide. The *Ttc39c-AT1* sequence alignment includes the proximal promoter region that contains three of the five putative E-boxes, the boxed sequence identifies the E-box conserved from human to rodents, and the underlined sequences identify the E-boxes conserved in rodents only. The sequences and locations of the putative consensus E-box elements in the **(B)** *Ttc39c-AT1* regulatory region. Schematics of the site-directed mutagenesis strategy and corresponding nucleotide changes made to the proximal E-box elements in the **(C)** *Ttc39c-Pro500-AT1* reporter plasmid. **(D)** C_2C_{12} myoblasts were transfected with the pSEAP-Ttc39c-Pro500-AT1 wild-type, pSEAP-Ttc39c-Pro500-AT1-Ebox-1, pSEAP-Ttc39c-Pro500-AT1-Ebox-2, or pSEAP-Ttc39c-Pro500-AT1-Ebox-3 reporter plasmids, a β-galactosidase reporter plasmid and filler DNA to 1µg/well of total DNA. The media

was then assayed for SEAP activity at 72 hours following the switch to differentiation media and SEAP numbers were normalized to β-galactosidase activity to correct for variations in transfection efficiency. All conditions were performed in triplicate and each experiment was repeated at least once. The graphs are of a representative experiment and values correspond to the mean relative light unit (RLU) values ± SD. Significant differences between the activities of the pSEAP-Ttc39c-Pro500 wild-type reporter constructs and the pSEAP-Ttc39c-Pro500 E-box mutant reporter constructs, (**: $P < 0.001$).

A.

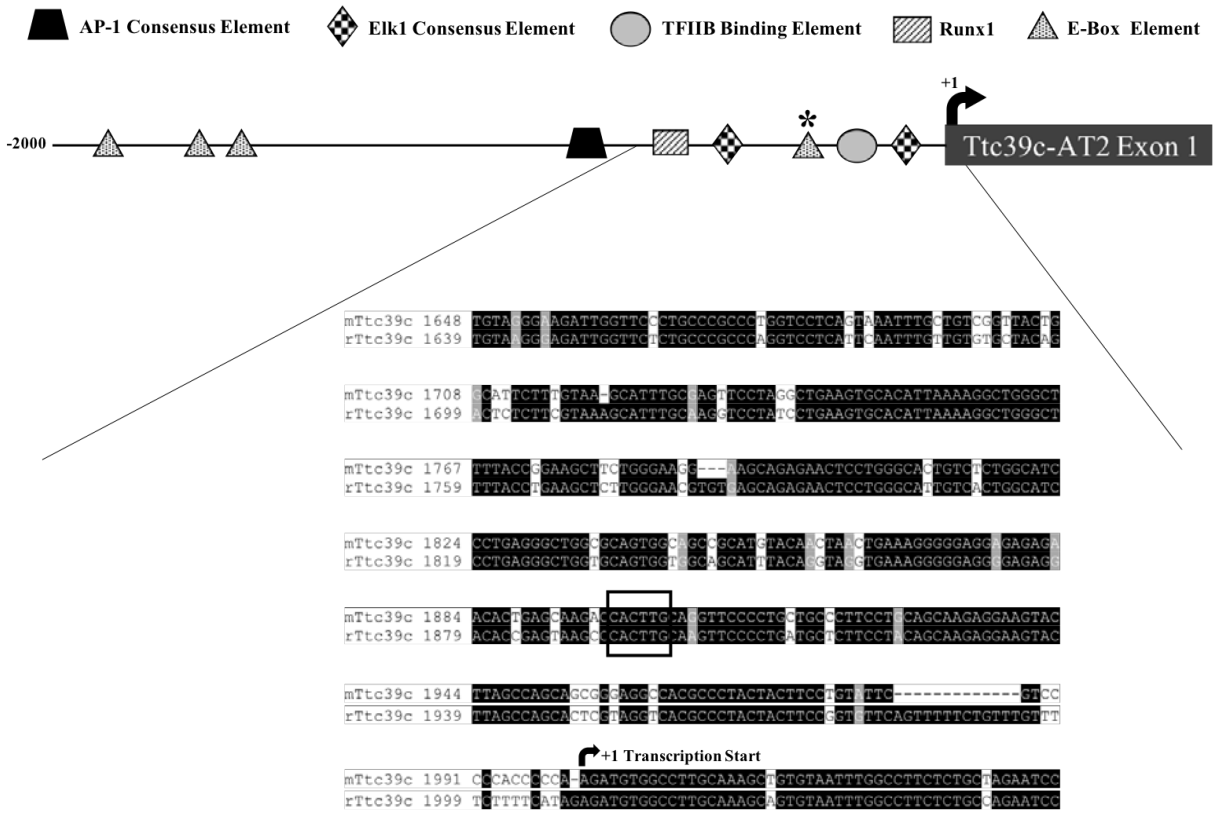

B.

E-box Sequence	E-Box Location
CAGATG*	-1949 to -1944
CAGTTG*	-1308 to -1303
CACGTG*	-1238 to -1233
CACTTG*	-103 to -98

*** conserved in mouse and rat**

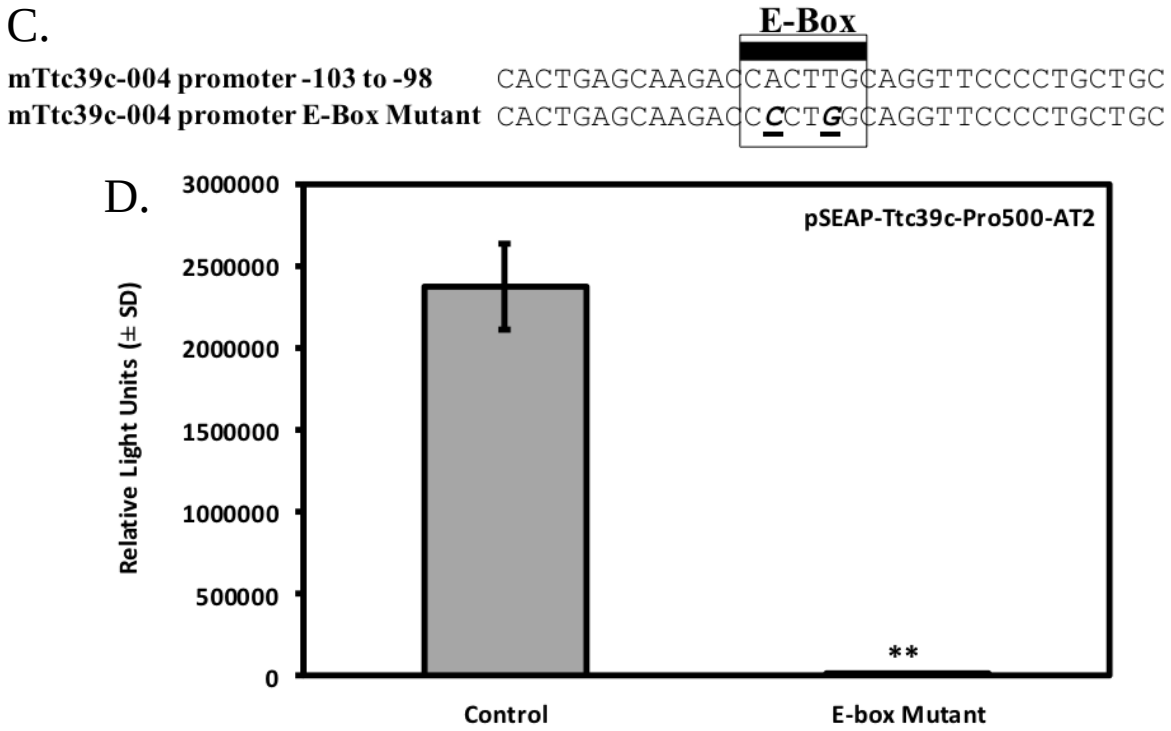

Figure 15. Conserved E-boxes in the proximal regulatory region of *Ttc39c-AT2* are necessary for full reporter gene activity. Schematic, sequence alignment and analysis of the **(A)** *Ttc39c-AT2* promoter region containing multiple putative consensus E-box elements 5'-CANNTG-3' (dotted triangles). The starred triangle represents the conserved E-Box element in the *Ttc39c-AT2* regulatory region schematic and the sequence is boxed in the alignment. N represents any nucleotide. The sequences and locations of the putative consensus E-box elements in the **(B)** *Ttc39c-AT2* regulatory region. Schematic of the site-directed mutagenesis strategy and corresponding nucleotide changes made to the proximal E-box element in the **(C)** *Ttc39c-Pro500-AT2* reporter plasmid. **(D)** C_2C_{12} myoblasts were transfected with the pSEAP-Ttc39c-Pro500-AT2 wild-type or pSEAP-Ttc39c-Pro500-AT2-Ebox mutant reporter plasmids, a β-galactosidase reporter plasmid and filler DNA to 1μg/well of total DNA. The media was then assayed for SEAP activity at 72 hours following the switch to differentiation media and SEAP numbers were normalized to β-galactosidase activity to correct for variations in transfection efficiency. All conditions were performed in triplicate and each experiment was repeated at least once. The graphs are of a representative experiment and values correspond to the mean relative light unit (RLU) values ± SD. Significant differences between the activities of the pSEAP-Ttc39c-Pro500 wild-type reporter constructs and the pSEAP-Ttc39c-Pro500 E-box mutant reporter constructs, (**: $P < 0.001$).

Ttc39c is regulated post-transcriptionally during muscle differentiation.

Ttc39c expression reaches peak levels between late proliferation and early differentiation of muscle cells (Fig. 7C and 9). To determine if Ttc39c is being regulated at the post-transcriptional level, a 228 base pair fragment of the 3' untranslated region (UTR) was cloned and fused to the 3'end of the SEAP reporter gene to create the pSEAP-Report-Ttc39c-3'UTR reporter plasmid. The proximal Ttc39c 3'UTR is predicted to have seed sites for several poorly conserved mammalian

miRNA families and one conserved mammalian miRNA family (Fig. 16A). To determine if the Ttc39c 3'UTR has any regulatory capability, C_2C_{12} myoblast cells were transfected with the pSEAP-Report-Ttc39c-3'UTR reporter plasmid and culture media was then analyzed for SEAP activity 24 hours post-transfection. Cells were then switched to differentiation media (2% serum) and culture media was further assayed at 24, 72, and 120 hours post-switch. Cells transfected with the pSEAP-Report-Ttc39c-3'UTR reporter plasmid showed decreasing SEAP activity as the cells differentiated compared to cells transfected with the pSEAP-Report control plasmid (Fig. 16B). These results suggest that the 3'UTR of Ttc39c may function in the post-transcriptional regulation of Ttc39c expression and is likely regulated by a poorly conserved mammalian miRNA or an unknown muscle-specific miRNA that is upregulated during muscle cell differentiation. The conserved miR-1193 microRNA is not likely to regulate Ttc39c expression, since the 3'UTR fragment only contains a portion of the miR-1193 complimentary seed sequence.

A.

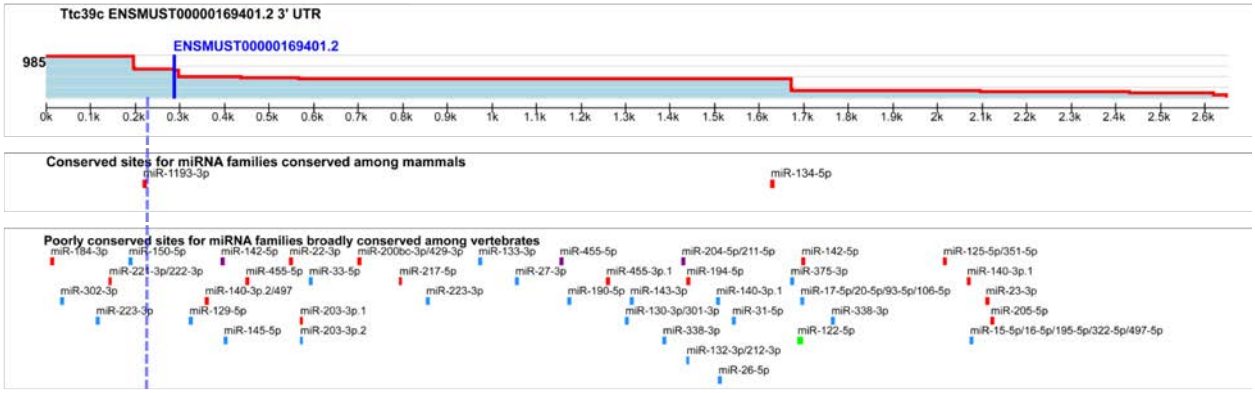

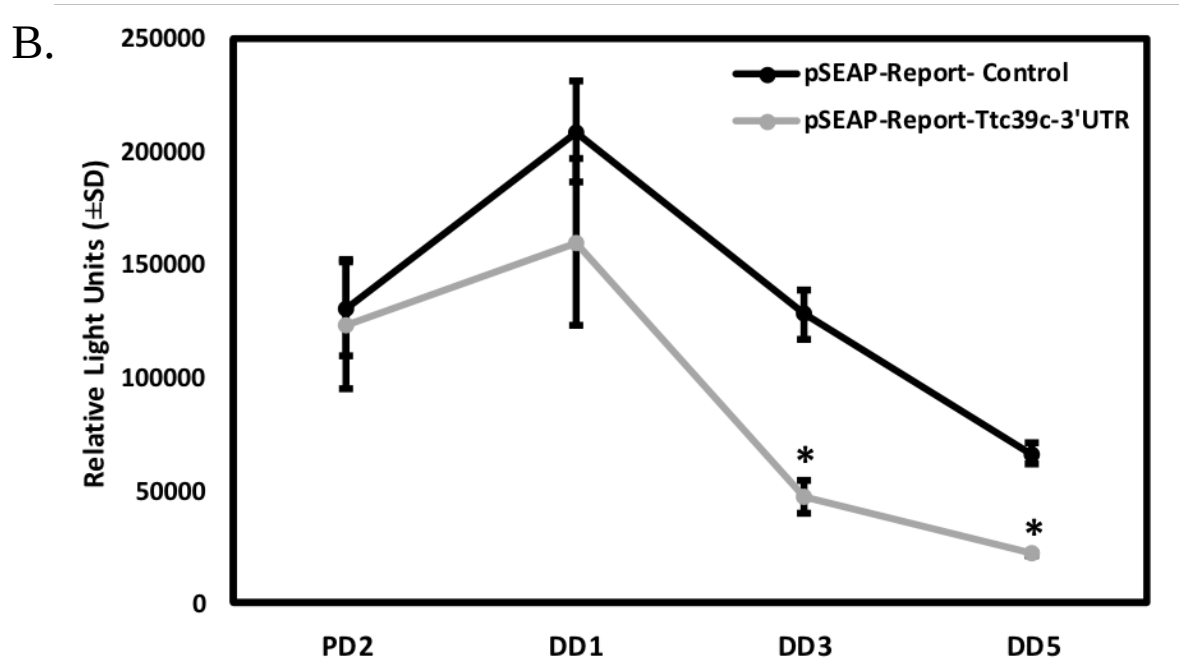

Figure 16. Ttc39c 3'untranslated region (3'-UTR) negatively regulates SEAP reporter gene activity during muscle cell differentiation. **(A)** Schematic of the mouse Ttc39c 3'-UTR showing the location of conserved mammalian miRNA seed sequences and broadly conserved vertebrate miRNA seed sequences. **(B)** 228 base pairs of the 3'-UTR of the mouse Ttc39c gene was cloned and fused with the 3'-end of the SEAP gene in the pSEAP-Report plasmid. C_2C_{12} cells were transfected with either the pSEAP-Report plasmid or the pSEAP-Report-Ttc39c-3'-UTR plasmid and culture media was then assayed after day 2 (PD2) in proliferation media prior to switching the cells to differentiation media (2% serum) and analyzing at day 1 (DD1), day 3 (DD3) and day 5 (DD5) post-media switch. Cells transfected with the pSEAP-Report-Ttc39c-3'-UTR plasmid showed significantly lower SEAP activity as the cells differentiated compared to cells transfected with the pSEAP-Report control plasmid. Significant differences between the activities of the pSEAP-Report empty control plasmid and the pSEAP-Report-Ttc39c-3'-UTR plasmid, (****: $P < 0.001$). The schematic image of the murine Ttc39c 3'-UTR was downloaded from the TargetScan database Release 7.1 (www.targetscan.org).

Sub-cellular localization of Ttc39c.

This study is one of the first to describe Ttc39c in muscle and as a consequence very little has been reported for this protein. Therefore, in order to further characterize Ttc39c in muscle cells, sub-cellular localization was analyzed by fusing the *Ttc39c* cDNA in frame with the *GFP* cDNA. C_2C_{12} cells were then transfected with either the pEGFP control plasmid or the pEGFP-Ttc39c expression plasmid and cells were subsequently imaged by confocal fluorescent microscopy. C_2C_{12} cells transfected with the pEGFP control vector showed uniform intracellular distribution of GFP in

both proliferating myoblasts (Fig. 17, panels A-C and J-L) and differentiating myotubes (Fig. 18, panels A-C and J-L). In contrast, C_2C_{12} cells transfected with the pEGFP-Ttc39c expression plasmid resulted in strong cytoplasmic localization and nuclear exclusion in both proliferating myoblasts (Fig. 17, panels D-I and M-R) and in differentiating myotubes (Fig. 18, panels D-I and M-R). Interestingly, C_2C_{12} cells transfected with GFP-Ttc39c appear to show fluorescence at the centrosome and association with microtubules radiating out from the centrosome (Fig. 18, panels M-O, white arrows). Furthermore, cells overexpressing GFP-Ttc39c developed elongated protrusions (Fig. 18, panels D-I and M-R, red arrows) that were not observed in cells transfected with the pEGFP-control plasmid (Fig. 18, panels A-C and J-L).

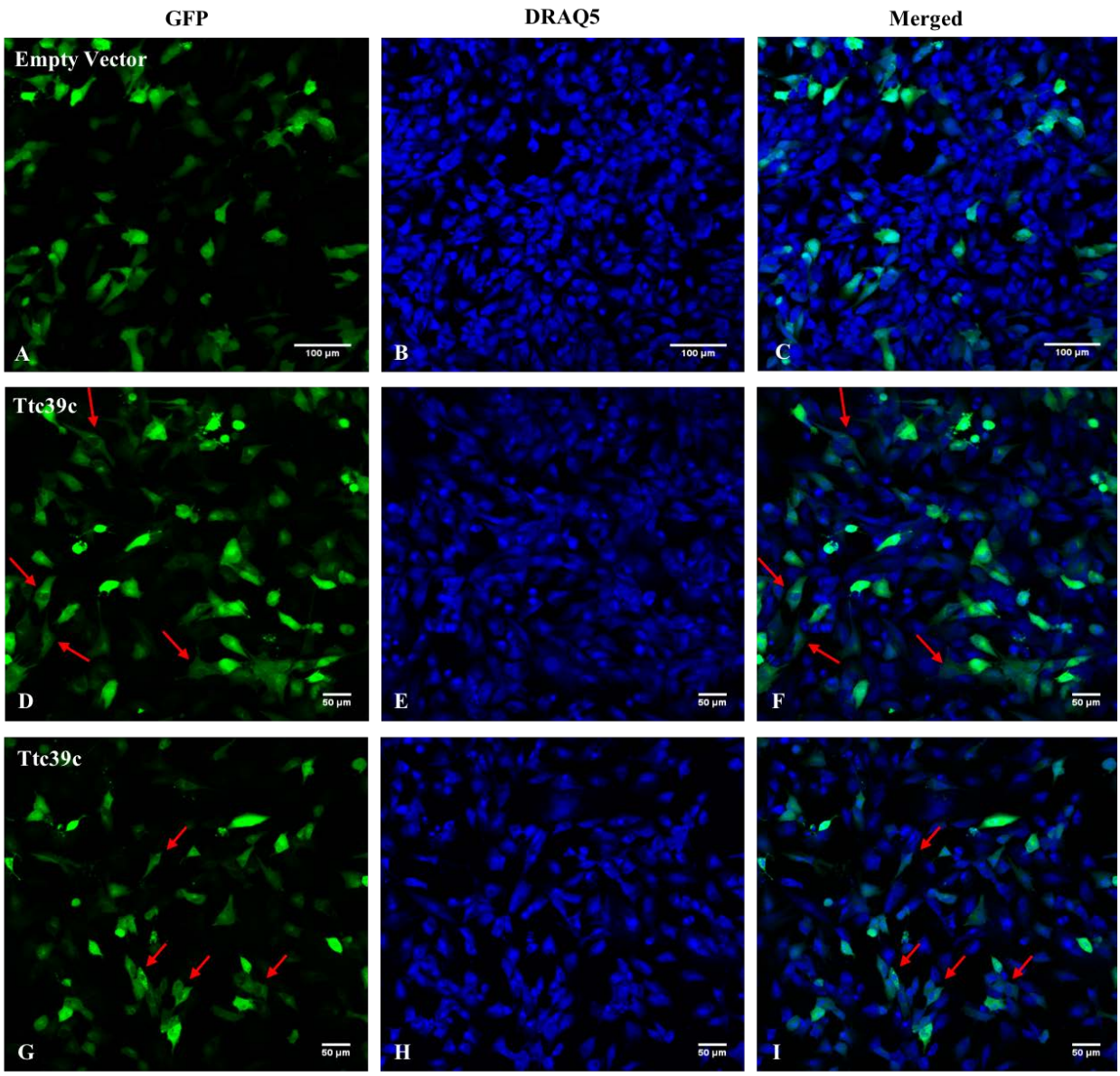
GFP
DRAQ5
Merged
Empty Vector
A
100 µm
B
100 µm
C
100 µm
Ttc39c
D
50 µm
E
50 µm
F
50 µm
Ttc39c
G
50 µm
H
50 µm
I
50 µm

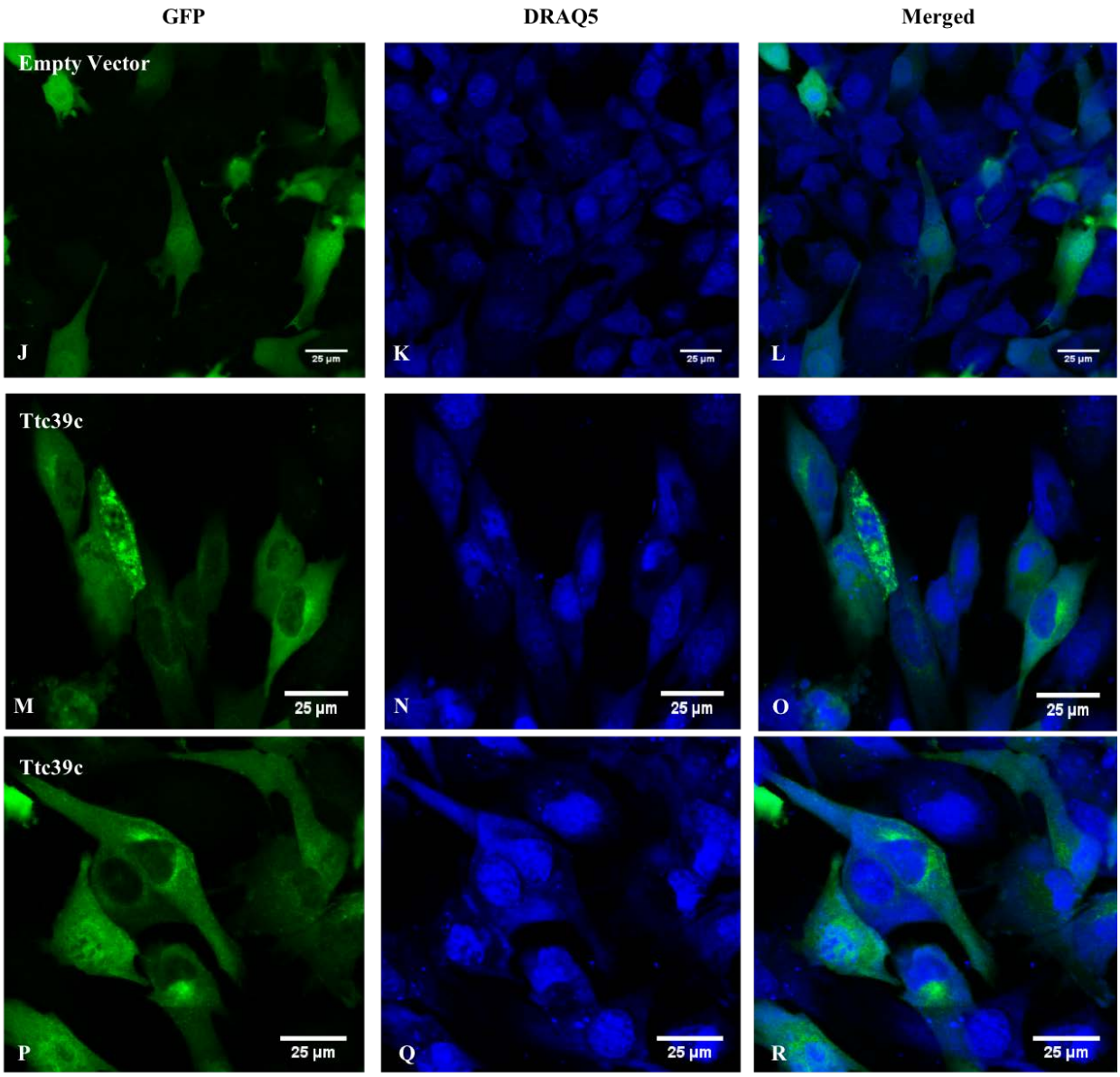

Figure 17. Ttc39c localizes to the cytoplasm in C_2C_{12} myoblast cells. Proliferating C_2C_{12} cells transfected with the empty pEGFP-C1 expression vector were imaged at 20X **(A-C)** and 60X **(J-L)** magnification and uniform cellular localization of GFP was observed. Representative C_2C_{12} cells transfected with a pEGFP-Ttc39c expression plasmid were imaged at 20X **(D-I)** and 60X **(M-R)** magnification and cytoplasmic fluorescence was observed.

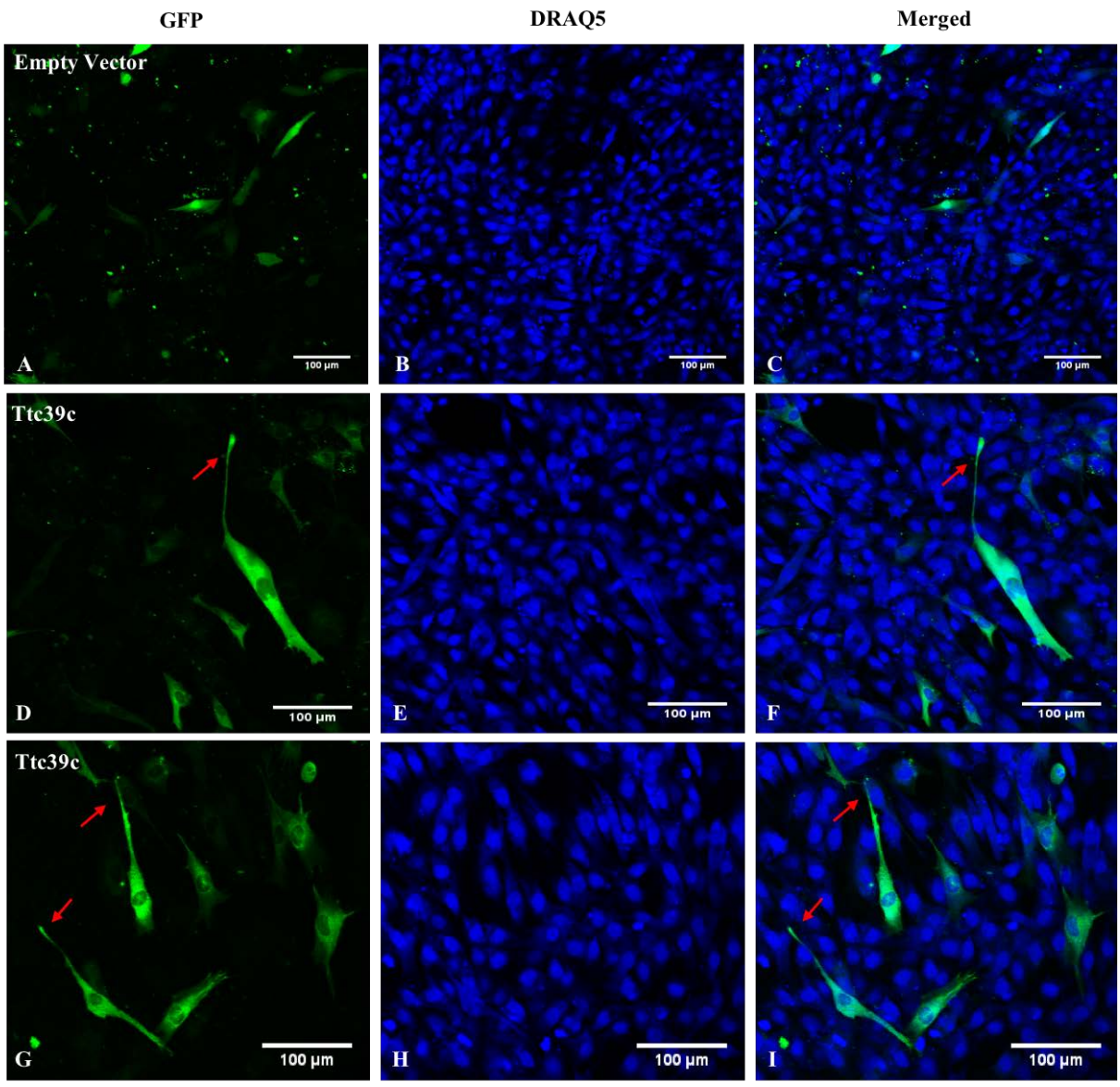
GFP
DRAQ5
Merged
Empty Vector
A
100 µm
B
100 µm
C
100 µm
Ttc39c
D
100 µm
E
100 µm
F
100 µm
Ttc39c
G
100 µm
H
100 µm
I
100 µm

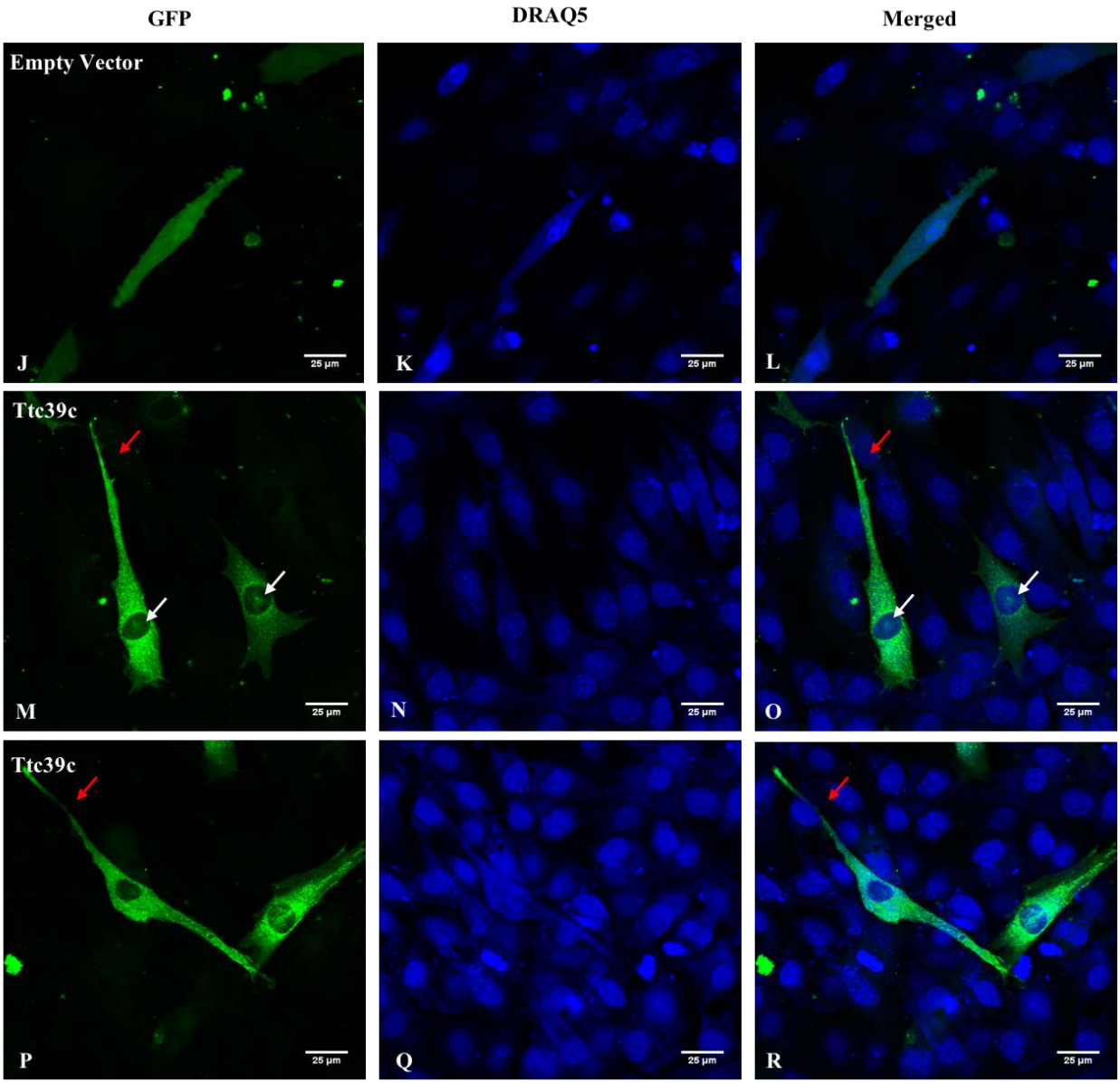

Figure 18. Ttc39c overexpression alters primary cilia structure in differentiating C_2C_{12} muscle cells. Differentiating C_2C_{12} cells transfected with the empty pEGFP-C1 expression vector were imaged at 20X **(A-C)** and 60X **(J-L)** magnification and displayed uniform cellular localization of GFP and normal myofiber formation. Representative C_2C_{12} cells transfected with a pEGFP-Ttc39c expression plasmid were imaged at 20X **(D-I)** and 60X **(M-R)** magnification and displayed cytoplasmic fluorescence, elongated primary cilia (red arrows) and association with the centrosome and microtubules (white arrows).

Ectopic expression of Ttc39c inhibits muscle cell differentiation.

The pcDNA3-Ttc39c expression plasmid was transfected into C_2C_{12} mouse myoblasts and cells were then harvested at 24 hours post-transfection (PD2), while the remaining cells were switched to differentiation media (2% serum) and harvested at 24, 48, 72, and 96 hours post-media switch.

Western blots were then performed to analyze markers of muscle cell differentiation over the time course. Mouse monoclonal antibodies against Myosin Heavy Chain (MyHC), myogenin (1:500 dilution) and MyoD (1:500 dilution) were used to analyze the expression of these canonical markers of muscle cell differentiation in control muscle cells and cells ectopically expressing Ttc39c. Overexpression of Ttc39c resulted in decreased expression of MyHC, myogenin and MyoD in early differentiation (DD1 and DD2), but did not prevent muscle cells from eventually differentiating (DD3 and DD4) (Fig. 19). Interestingly, Ttc39c overexpression, analyzed using a mouse monoclonal antibody against Ttc39c (1:1000 dilution), decreased dramatically as cells differentiated, which correlates with the increased expression of muscle cell differentiation markers (Fig. 19) and suggests that Ttc39c is likely post-translationally regulated during muscle cell differentiation. Acetylated tubulin, an additional marker of muscle cell differentiation, was also analyzed using a mouse monoclonal antibody (1:1000 dilution) that recognizes acetylation of the lysine 40 residue of α-tubulin and was found to show decreased levels of acetylation throughout differentiation (Fig 19). α-tubulin protein levels were analyzed to confirm equal protein loading and demonstrated that α-tubulin subunit levels remained constant from proliferation through differentiation (Fig. 19).

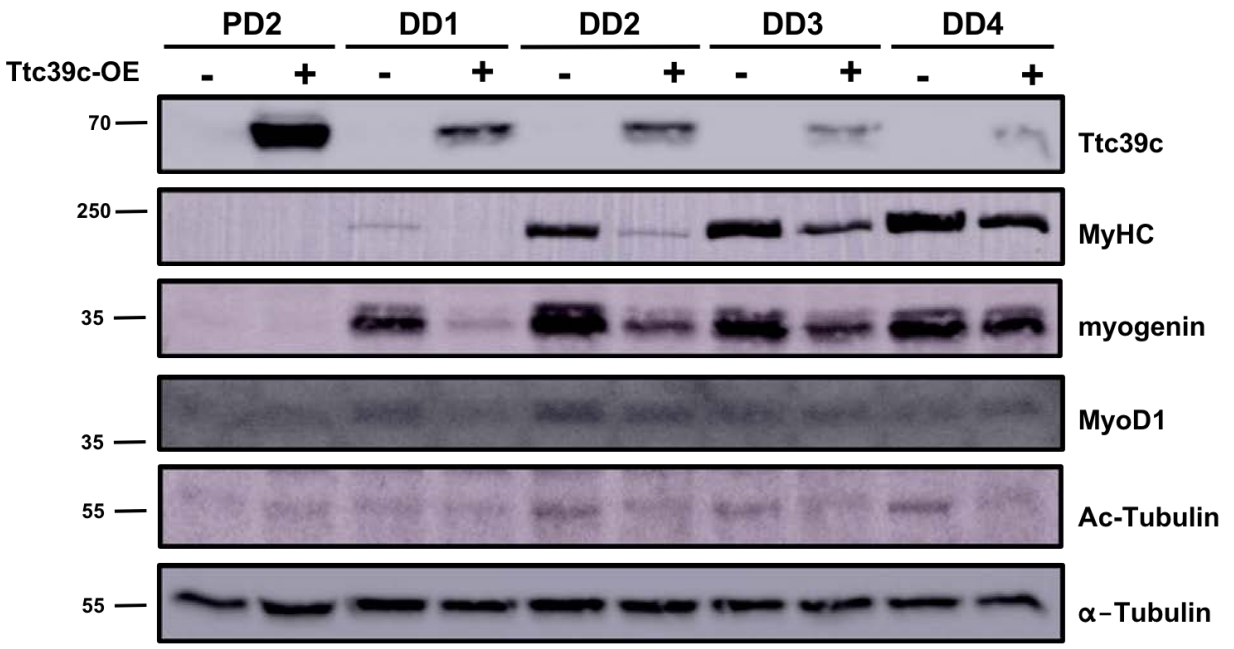

Figure 19. Ectopic expression of Ttc39c in C_2C_{12} muscle cells represses muscle cell differentiation. Proliferating (PD) and differentiated (DD) control C_2C_{12} cells and cells overexpressing Ttc39c were harvested over a 4 day differentiation time course and protein lysates were then analyzed by Western blot. Cells were maintained in proliferation media (10% serum) and harvested 2 days post-plating and the remaining cells were then switched to differentiation media (2% serum) and harvested at 1, 2, 3 and 4 days post-media change. Cells transfected with the Ttc39c expression plasmid showed dramatically higher levels of Ttc39c expression compared to control cells when blots were probed using an antibody against Ttc39c. Myosin Heavy Chain (MyHC) was analyzed as a marker of muscle cell differentiation and found to be inhibited in cells overexpression Ttc39c. Myogenic regulatory factors, myogenin and MyoD, were also found to have lower expression in muscle cells overexpressing Ttc39c during early differentiation, while acetylated tubulin, another marker of muscle differentiation, also displayed lower levels in cells overexpressing Ttc39c. α-tubulin was analyzed to confirm equal protein loading. The experiments were repeated at least once and the western blots are representative examples of the results obtained.

To confirm that muscle cells overexpressing Ttc39c had lower levels of MyoD and myogenin available to regulate muscle-specific gene expression, a reporter gene construct was created by fusing 4 canonical E-box elements with a minimal SV40 promoter to create the pSEAP-Pro-Ebox-4X reporter plasmid. The E-box reporter was transfected into C_2C_{12} cells with or without Ttc39c ectopic expression and reporter gene activity was measured over a 7 day differentiation time course by sampling the growth media every 48 hours and analyzing the level of secreted alkaline phosphatase (SEAP) activity. Muscle cells overexpressing Ttc39c showed significantly lower MRF reporter gene activity compared to control cells over the entire 7 day time course (Fig. 20).

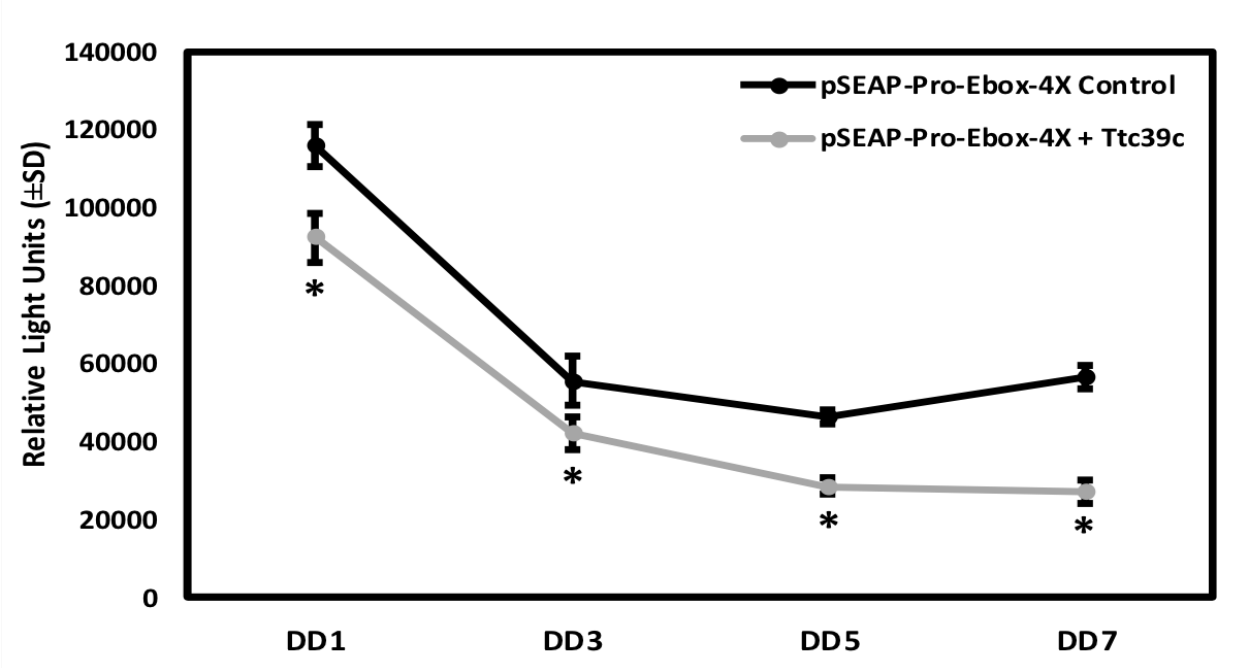

Figure 20. Ectopic overexpression of Ttc39c in C_2C_{12} muscle cells represses myogenic regulatory factor activity. Myogenic regulatory factor activity was analyzed using a reporter gene that consisted of a minimal SV40 promoter fused with 4 concatemerized E-box consensus elements. C_2C_{12} cells were transfected with either the reporter alone (black line) or in combination with the pcDNA3-Ttc39c expression plasmid (gray line) and culture media was analyzed over a 7 day time course post-media switch. Cells ectopically expression Ttc39c showed a significantly lower levels of myogenic regulatory factor activation of the E-box reporter construct compared to control cells. Significant differences between reporter gene activity in control cells compared to cells ectopically expressing Ttc39c, (*: $P < 0.001$).

Ectopic expression of Ttc39c attenuates MAP Kinase and Hedgehog signaling pathways in muscle cells.

Ttc39c was overexpressed in C_2C_{12} myoblasts and cells were then harvested at 24 hours post-transfection (PD2), while the remaining cells were switched to differentiation media (2% serum) and harvested at 24, 48, 72, 96 and 120 hours post-media switch. Western blots were then performed to evaluate markers of MAP Kinase signaling pathway activity over the time course. A mouse monoclonal antibody against phosphorylated ERK (p-ERK) that recognizes an epitope that includes phosphorylated Tyrosine 204 (1:500 dilution) was used to analyze the level of p-ERK in muscle cells ectopically expressing Ttc39c compared to control cells. Overexpression of Ttc39c resulted in significantly lower levels of p-ERK in cells overexpressing Ttc39c (Fig. 21A).

Interestingly, when overall ERK protein levels were assessed using a rabbit polyclonal antibody (1:500), cells overexpressing Ttc39c actually showed elevated ERK expression compared to control cells at later stages of differentiation (DD3-DD5) (Fig. 21A).

In addition to the MAP kinase signaling pathway, Western blots were also performed to evaluate the activity of the Hedgehog (Hh) signaling pathway over the time course. A rabbit polyclonal antibody against Gli2 (1:1000 dilution) was used to analyze the level of Gli2 repressor and a proteolytic cleavage product of Gli2 in muscle cells ectopically expressing Ttc39c compared to control cells. Overexpression of Ttc39c resulted in significantly higher levels of repressor Gli2 in cells overexpressing Ttc39c during differentiation (DD2-DD4) (Fig. 21B). Interestingly, a proteolytic cleavage product of Gli2 was detected in muscle cells and this product also showed elevated levels in cells overexpressing Ttc39c during differentiation (DD2-DD4) (Fig. 21B). As expected, Ttc39c expression was higher in cells transfected with the Ttc39c expression plasmid, but decreased dramatically as muscle cells differentiated, while α-tubulin protein levels remained constant from proliferation through differentiation (Fig. 21A and 21B).

A.

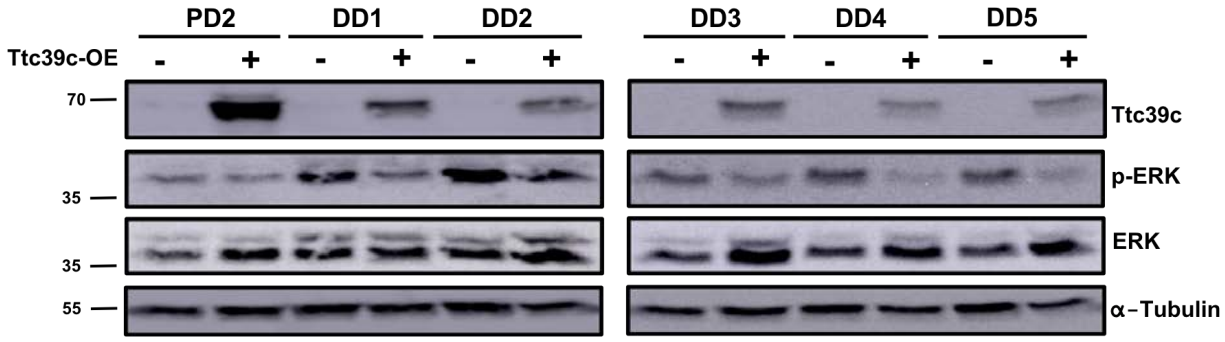

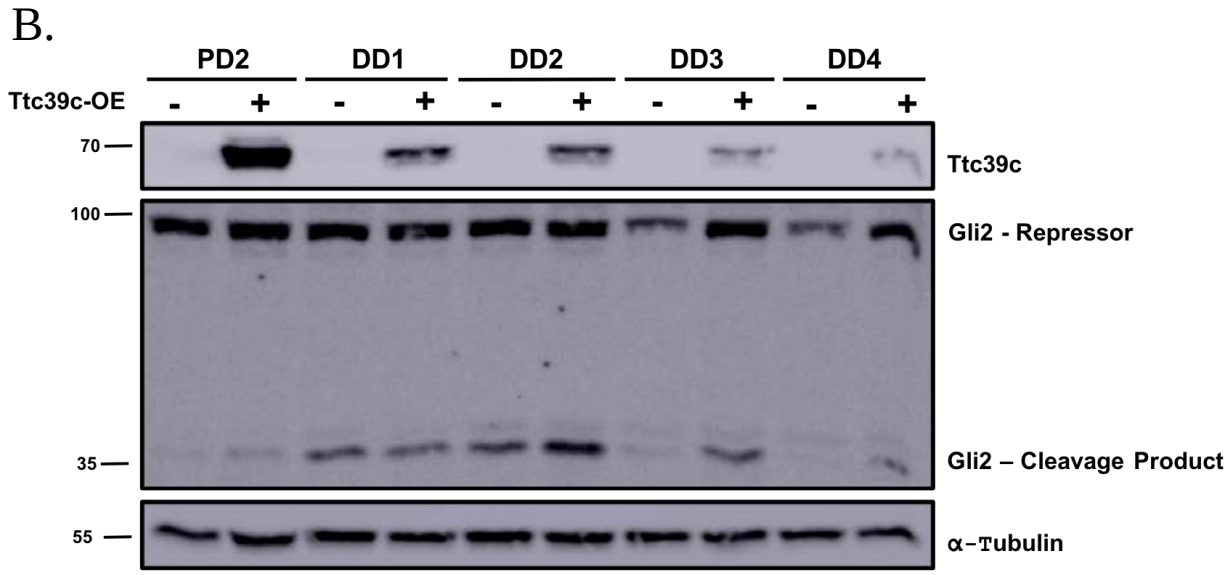

Figure 21. Ectopic expression of Ttc39c in C_2C_{12} muscle cells attenuates MAP Kinase and Hedgehog Signaling Pathways. Proliferating (PD) and differentiated (DD) control C_2C_{12} cells and cells overexpressing Ttc39c were harvested over a 4 day differentiation time course and protein lysates were then analyzed by Western blot. Cells were maintained in proliferation media (10% serum) and harvested 2 days post-plating and the remaining cells were then switched to differentiation media (2% serum) and harvested at 1, 2, 3, and 4 (Hedgehog Signaling) or 1, 2, 3, 4 and 5 days (MAP Kinase Signaling) post-media change. Cells transfected with the Ttc39c expression plasmid showed significantly higher levels of Ttc39c expression compared to control cells. **(A)** Phosphorylated Erk was significantly lower in Ttc39c overexpressing cells during muscle cell differentiation, while the levels of the Erk protein were elevated in cells ectopically expressing Ttc39c. **(B)** The Gli2 repressor isoform is elevated in C_2C_{12} cells overexpressing Ttc39c in later differentiation. α-tubulin was analyzed to confirm equal protein loading. These experiments were repeated at least once and the Western blots are representative examples of the results obtained.

To confirm that muscle cells overexpressing Ttc39c had decreased MAP kinase signaling, a reporter gene construct was created by fusing a canonical AP-1 element with a minimal SV40 promoter to create the pSEAP-Pro-AP-1 reporter plasmid. The AP-1 reporter was transfected into C_2C_{12} cells with or without Ttc39c ectopic expression and reporter gene activity was measured over a 7 days differentiation time course by sampling the growth media every 48 hours and analyzing the level of secreted alkaline phosphatase (SEAP) activity (Fig. 22A). Muscle cells overexpressing Ttc39c showed significantly lower AP-1 reporter gene activity compared to control cells over the entire 7 day time course (Fig. 22B). In addition, Hh signaling was also assessed in

muscle cells overexpressing Ttc39c revealing decreased signaling activity. To monitor Hh signaling, a reporter gene construct was created by fusing a Gli consensus binding element with a minimal SV40 promoter to create the pSEAP-Pro-Gli reporter plasmid. The Gli reporter was transfected into C_2C_{12} cells with or without Ttc39c ectopic expression and reporter gene activity was measured over a 7 days differentiation time course by sampling the growth media every 48 hours and analyzing the level of secreted alkaline phosphatase (SEAP) activity (Fig 22A). Muscle cells overexpressing Ttc39c showed significantly lower Gli reporter gene activity compared to control cells over the entire 7 day time course (Fig. 22C).

A.

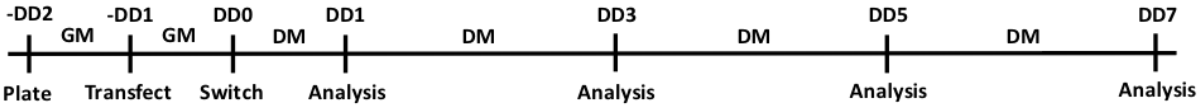

B.

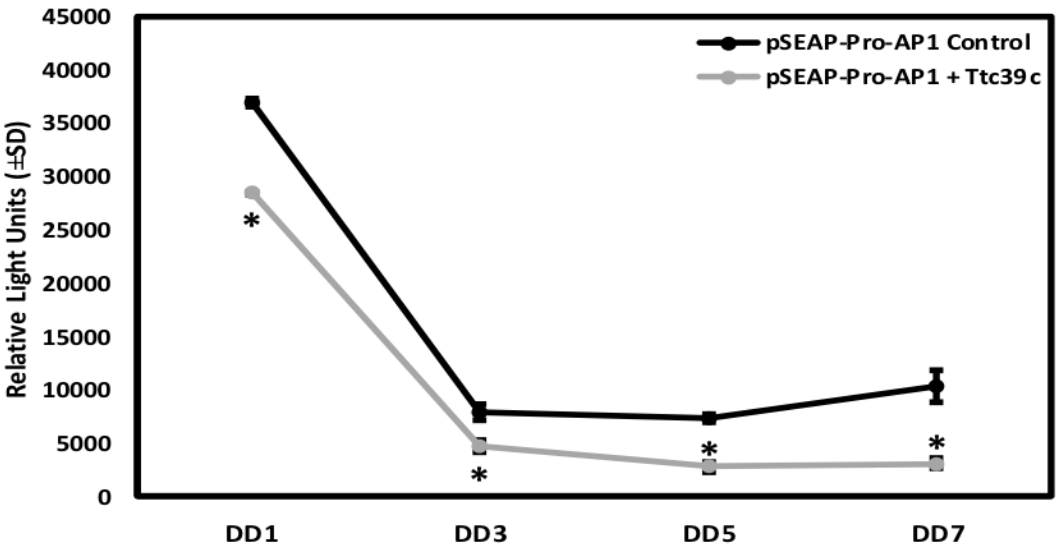

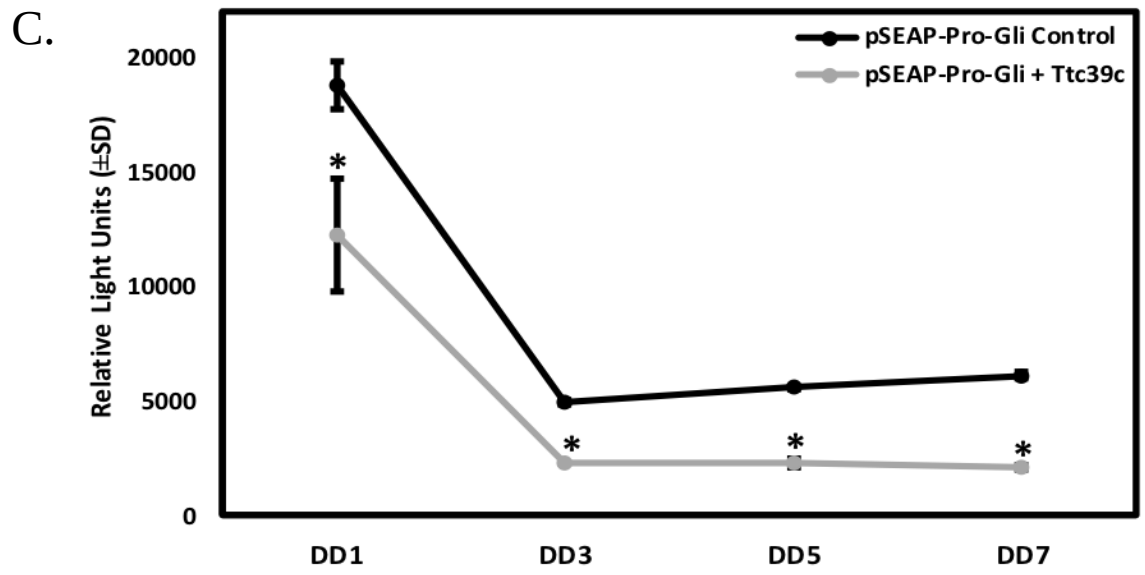

Figure 22. Ectopic expression of Ttc39c in C_2C_{12} muscle cells represses AP-1 and Gli reporter activity. **(A)** Schematic of the signaling pathway reporter gene experimental design. C_2C_{12} cells were transfected one day post-plating and maintained in proliferation media for an additional 24 hours post-transfection. The cells were then changed to differentiation media (2% serum) and analyzed for reporter gene actively at 1, 3, 5, and 7 days post-media switch. **(B)** The MAP Kinase signaling pathway was analyzed using a reporter gene that consisted of a minimal SV40 promoter fused with an AP-1 consensus element. C_2C_{12} cells were transfected with either the reporter alone (black line) or in combination with the pcDNA3-Ttc39c expression plasmid (gray line) and culture media was analyzed over a 7 day time course post-media switch. Cells ectopically expression Ttc39c showed a significantly lower level of MAP Kinase signaling compared to control cells. **(C)** The Hedgehog signaling pathway was analyzed using a reporter gene that consisted of a minimal SV40 promoter fused with a Gli consensus element. C_2C_{12} cells were transfected with either the reporter alone (black line) or in combination with the pcDNA3-Ttc39c expression plasmid (gray line) and culture media was analyzed over a 7 day time course post-media switch. Cells ectopically expressing Ttc39c showed a significantly lower level of Hedgehog signaling compared to control cells. Significant differences between reporter gene activity in control cells compared to cells ectopically expressing Ttc39c, (*: $P < 0.001$).

Ttc39c overexpression results in increased IFT144 protein levels in muscle cells.

Ttc39c was overexpressed in C_2C_{12} mouse myoblasts and cells were then harvested at 24 hours post-transfection (PD2), while the remaining cells were switched to differentiation media (2% serum) and harvested at 24, 48, 72, 96 and 120 hours post-media switch. Western blots were performed to analyze the expression level of IFT88, a component of the anterograde intraflagellar transport (IFT) complex B, and IFT144, a component of the retrograde intraflagellar transport complex A in muscle cells. Since previous research has shown that Ttc39c interacts with IFT144, a rabbit polyclonal antibody against IFT144 (1:1000 dilution) was used to analyze the expression

level of IFT144 in response to Ttc39c ectopic expression. Overexpression of Ttc39c resulted in an increase in expression of IFT144 as cells differentiated (DD3-DD5) (Fig. 23). Interestingly, Ttc39c overexpression did not significantly impact IFT88 protein levels in proliferating or differentiated muscle cells (Fig. 23). Ttc39c expression was again found to decrease dramatically as muscle cells differentiated, while α-tubulin protein levels remained constant from proliferation through differentiation (Fig. 23).

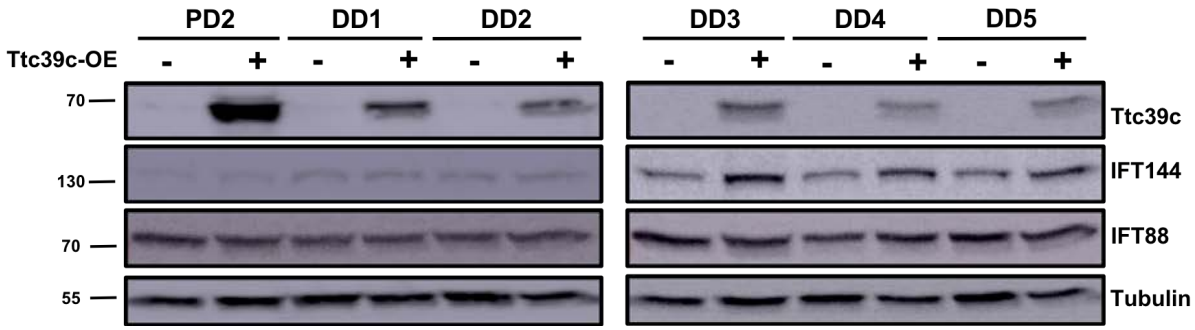

Figure 23. Ectopic expression of Ttc39c in C_2C_{12} muscle cells increases IFT144 protein levels. C_2C_{12} cells were transfected with the pcDNA3-Ttc39c expression plasmid and western blot analysis was performed using an antibody against Ttc39c on protein homogenates from differentiated (DD) C_2C_{12} cells harvested over a 5 day differentiation time course. Cells were maintained in proliferation media (10% serum) 2 days post-plating and then switched to differentiation media (2% serum) and harvested at 1, 2, 3, 4 and 5 days post-media change. Cells transfected with the pcDNA3-Ttc39c expression plasmid showed significantly higher levels of Ttc39c expression compared to control cells. IFT144 is part of the Intraflagellar Transport system and is a component of Complex A, which participates in retrograde transport in the primary cilia. Ttc39c overexpression results in elevated IFT144 protein levels in differentiating muscle cells. Conversely, IFT88 is also part of the Intraflagellar Transport system and is a component of Complex B, which participates in anterograde transport in the primary cilia. Ttc39c overexpression did not impact IFT88 protein levels in proliferating or differentiating muscle cells. α-tubulin was analyzed to confirm equal protein loading. These experiments were repeated at least once and the western blots are representative examples of the results obtained.

siRNA knockdown of Ttc39c alters myoblast cell morphology.

The cDNA of Ttc39c was cloned from mouse muscle cells, sequenced in both directions and found to contain no mutations or unknown polymorphisms based on comparisons to the sequence on deposit in the Ensembl database (*Ttc39c*) (Fig 24A). This Ttc39c cDNA sequence was then analyzed for potential siRNA targeting sequences and two target sites (highlighted in red) were identified and used to create siRNA oligonucleotides that were subsequently cloned into the

pSuper-Basic expression plasmid. C_2C_{12} cells were transfected with the pSuper-Basic plasmid or the pSuper-Ttc39c-siRNA-2 or the pSuper-Ttc39c-siRNA-3 plasmids and cells were harvested 48 hours post-transfection. Protein lysates purified from transfected cells were then analyzed by Western blot to determine the efficiency of siRNA knockdown of Ttc39c and the targeting sequences were found to dramatically reduce Ttc39c levels in cells transfected with the Ttc3c-siRNA expression plasmids compared to control cells and cells transfected with the pSuper-Basic control plasmid (Fig. 24B). Interestingly, C_2C_{12} cells transfected with the Ttc39c-siRNA-3 plasmid also demonstrated dramatic morphological changes (Fig. 24D and 24F), compared to control cells transfected with the pSuper-Basic control plasmid (Fig. 24C and 24E).

A.

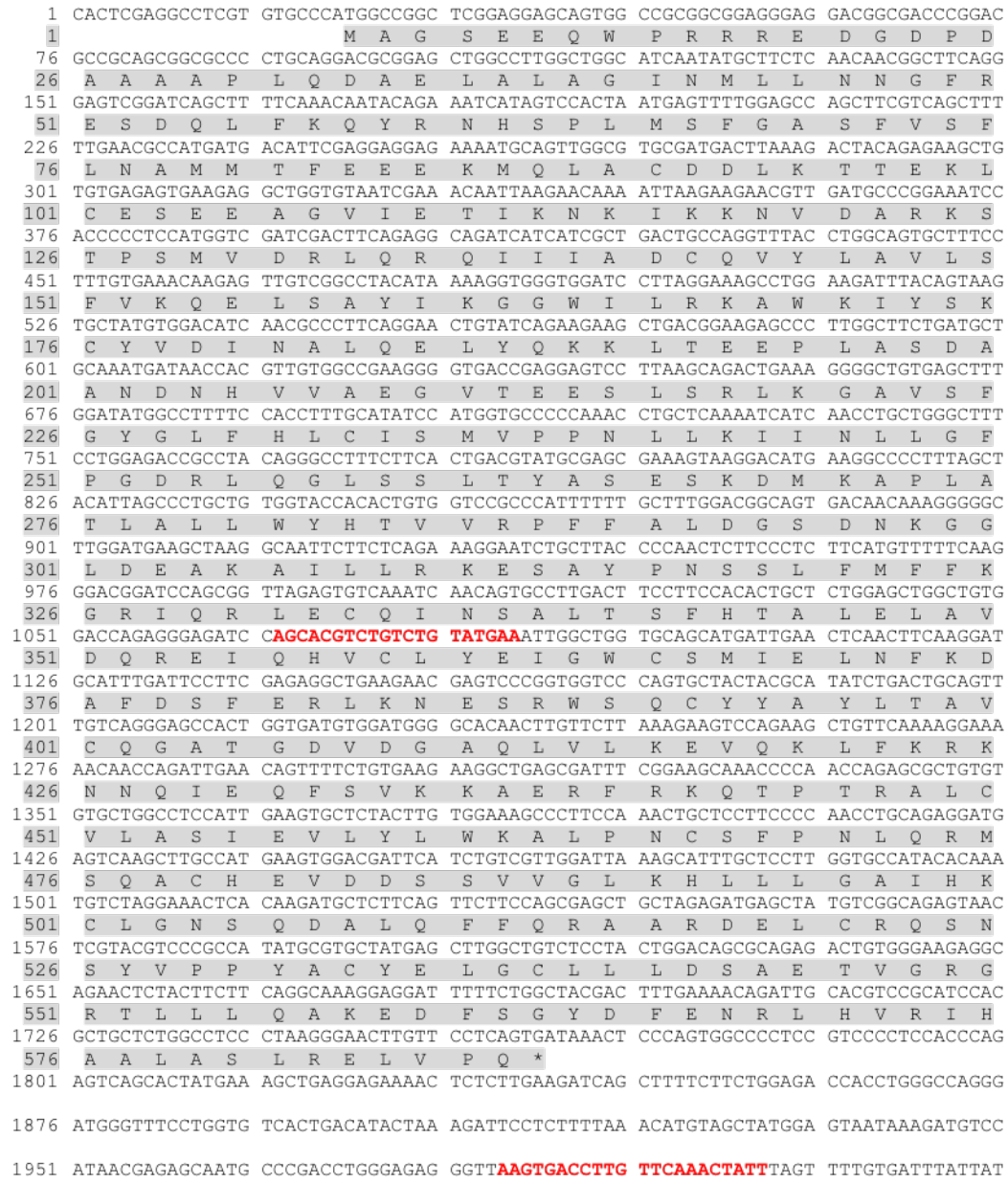
1 CACTCGAGGCCTCGT GTGCCCATGGCCGGC TCGGAGGAGCAGTGG CCGCGGCGGAGGGAG GACGGCGACCCGGAC
1 M A G S E E Q W P R R R E D G D P D
76 GCCGCAGCGGCGCCC CTGCAGGACGCGGAG CTGGCCTTGGCTGGC ATCAATATGCTTCTC AACAACGGCTTCAGG
26 A A A A P L Q D A E L A L A G I N M L L N N G F R
151 GAGTCGGATCAGCTT TTCAAACAATACAGA AATCATAGTCCACTA ATGAGTTTTGGAGCC AGCTTCGTCAGCTTT
51 E S D Q L F K Q Y R N H S P L M S F G A S F V S F
226 TTGAACGCCATGATG ACATTCGAGGAGGAG AAAATGCAGTTGGCG TGCGATGACTTAAAG ACTACAGAGAAGCTG
76 L N A M M T F E E E K M Q L A C D D L K T T E K L
301 TGTGAGAGTGAAGAG GCTGGTGTAATCGAA ACAATTAAGAACAAA ATTAAGAAGAACGTT GATGCCCGGAAATCC
101 C E S E E A G V I E T I K N K I K K N V D A R K S
376 ACCCCCTCCATGGTC GATCGACTTCAGAGG CAGATCATCATCGCT GACTGCCAGGTTTAC CTGGCAGTGCTTTCC
126 T P S M V D R L Q R Q I I I A D C Q V Y L A V L S
451 TTTGTGAAACAAGAG TTGTCGGCCTACATA AAAGGTGGGTGGATC CTTAGGAAAGCCTGG AAGATTTACAGTAAG
151 F V K Q E L S A Y I K G G W I L R K A W K I Y S K
526 TGCTATGTGGACATC AACGCCCTTCAGGAA CTGTATCAGAAGAAG CTGACGGAAGAGCCC TTGGCTTCTGATGCT
176 C Y V D I N A L Q E L Y Q K K L T E E P L A S D A
601 GCAAATGATAACCAC GTTGTGGCCGAAGGG GTGACCGAGGAGTCC TTAAGCAGACTGAAA GGGGCTGTGAGCTTT
201 A N D N H V V A E G V T E E S L S R L K G A V S F
676 GGATATGGCCTTTTC CACCTTTGCATATCC ATGGTGCCCCCAAAC CTGCTCAAAATCATC AACCTGCTGGGCTTT
226 G Y G L F H L C I S M V P P N L L K I I N L L G F
751 CCTGGAGACCGCCTA CAGGGCCTTTCTTCA CTGACGTATGCGAGC GAAAGTAAGGACATG AAGGCCCCTTTAGCT
251 P G D R L Q G L S S L T Y A S E S K D M K A P L A
826 ACATTAGCCCTGCTG TGGTACCACACTGTG GTCCGCCCATTTTTT GCTTTGGACGGCAGT GACAACAAAGGGGGC
276 T L A L L W Y H T V V R P F F A L D G S D N K G G
901 TTGGATGAAGCTAAG GCAATTCTTCTCAGA AAGGAATCTGCTTAC CCCAACTCTTCCCTC TTCATGTTTTTCAAG
301 L D E A K A I L L R K E S A Y P N S S L F M F F K
976 GGACGGATCCAGCGG TTAGAGTGTCAAATC AACAGTGCCTTGACT TCCTTCCACACTGCT CTGGAGCTGGCTGTG
326 G R I Q R L E C Q I N S A L T S F H T A L E L A V
1051 GACCAGAGGGAGATC CAGCACGTCTGTCTG TATGAAATTGGCTGG TGCAGCATGATTGAA CTCAACTTCAAGGAT
351 D Q R E I Q H V C L Y E I G W C S M I E L N F K D
1126 GCATTTGATTCCTTC GAGAGGCTGAAGAAC GAGTCCCGGTGGTCC CAGTGCTACTACGCA TATCTGACTGCAGTT
376 A F D S F E R L K N E S R W S Q C Y Y A Y L T A V
1201 TGTCAGGGAGCCACT GGTGATGTGGATGGG GCACAACTTGTTCTT AAAGAAGTCCAGAAG CTGTTCAAAAGGAAA
401 C Q G A T G D V D G A Q L V L K E V Q K L F K R K
1276 AACAACCAGATTGAA CAGTTTTCTGTGAAG AAGGCTGAGCGATTT CGGAAGCAAACCCCA ACCAGAGCGCTGTGT
426 N N Q I E Q F S V K K A E R F R K Q T P T R A L C
1351 GTGCTGGCCTCCATT GAAGTGCTCTACTTG TGGAAAGCCCTTCCA AACTGCTCCTTCCCC AACCTGCAGAGGATG
451 V L A S I E V L Y L W K A L P N C S F P N L Q R M
1426 AGTCAAGCTTGCCAT GAAGTGGACGATTCA TCTGTCGTTGGATTA AAGCATTTGCTCCTT GGTGCCATACACAAA
476 S Q A C H E V D D S S V V G L K H L L L G A I H K
1501 TGTCTAGGAAACTCA CAAGATGCTCTTCAG TTCTTCCAGCGAGCT GCTAGAGATGAGCTA TGTCGGCAGAGTAAC
501 C L G N S Q D A L Q F F Q R A A R D E L C R Q S N
1576 TCGTACGTCCCGCCA TATGCGTGCTATGAG CTTGGCTGTCTCCTA CTGGACAGCGCAGAG ACTGTGGGAAGAGGC
526 S Y V P P Y A C Y E L G C L L L D S A E T V G R G
1651 AGAACTCTACTTCTT CAGGCAAAGGAGGAT TTTTCTGGCTACGAC TTTGAAAACAGATTG CACGTCCGCATCCAC
551 R T L L L Q A K E D F S G Y D F E N R L H V R I H
1726 GCTGCTCTGGCCTCC CTAAGGGAACTTGTT CCTCAGTGATAAACT CCCAGTGGCCCCTCC GTCCCCTCCACCCAG
576 A A L A S L R E L V P Q *
1801 AGTCAGCACTATGAA AGCTGAGGAGAAAAC TCTCTTGAAGATCAG CTTTTCTTCTGGAGA CCACCTGGGCCAGGG
1876 ATGGGTTTCCTGGTG TCACTGACATACTAA AGATTCCTCTTTTAA ACATGTAGCTATGGA GTAATAAAGATGTCC
1951 ATAACGAGAGCAATG CCCGACCTGGGAGAG GGTTAAGTGACCTTG TTCAAACTATTTAGT TTTGTGATTTATTAT

B.

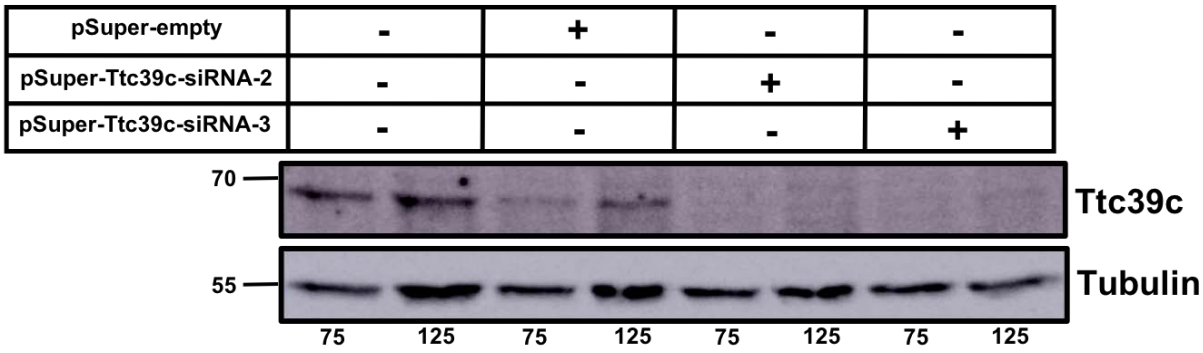

pSuper-Empty PD2 4X Objective

C.

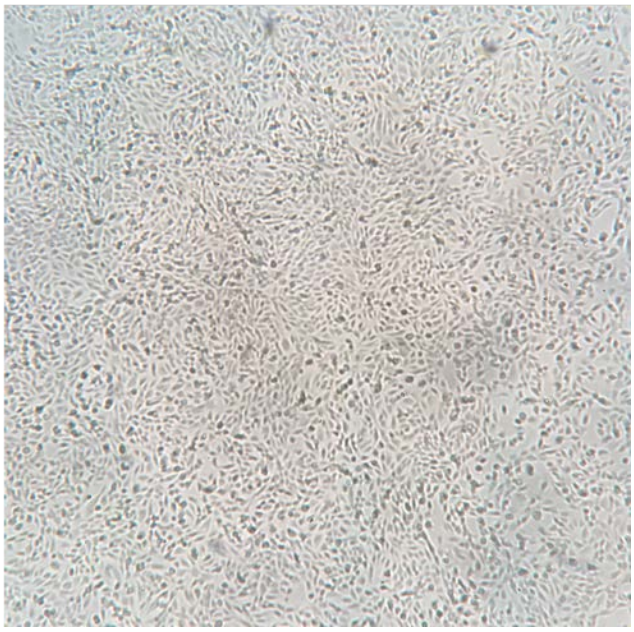

Ttc39c-siRNA PD2 4X Objective

D.

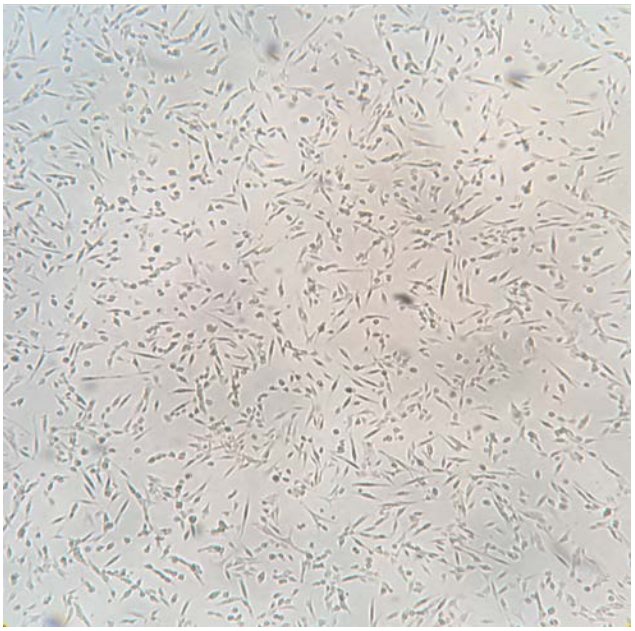

pSuper-Empty PD2 10X Objective

E.

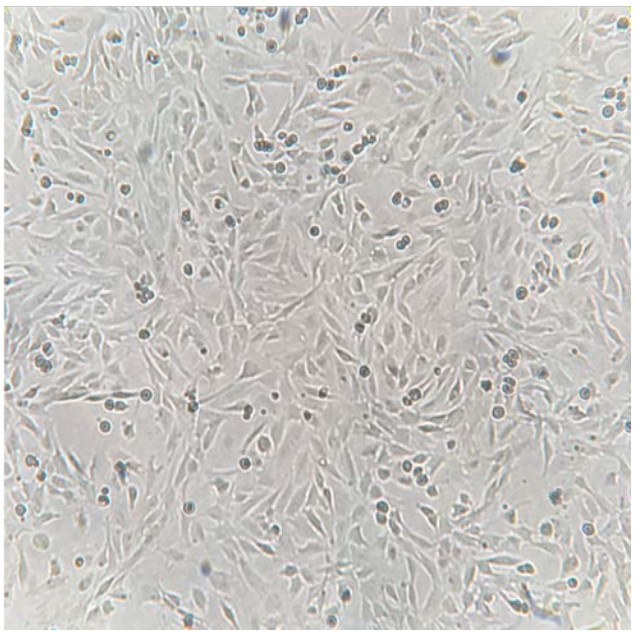

F.

Figure 24. Knockdown of Ttc39c expression in C_2C_{12} muscle cells results in changes in muscle cell morphology. **(A)** Sequence of the cDNA of Ttc39c cloned from mouse muscle cells and the location of the siRNA targeting sequences (highlighted in red). **(B)** C_2C_{12} cells were transfected with either the pSuper empty plasmid or pSuper plasmids that contained oligonucleotide sequences for targeting the Ttc39c mRNA transcript for transient knockdown (pSuper-Ttc39c-siRNA-2 and pSuper-Ttc39c-siRNA-3). Phase microscopic analysis of C_2C_{12} cells transfected with either the pSuper-empty plasmid at **(C)** 4X and **(E)** 10X or the pSuper-Ttc39c-3 siRNA expression plasmid at **(D)** 4X and **(F)** 10X.

Ttc39 knockdown inhibits muscle cell differentiation.

The sSuper-Ttc39c-siRNA-3 expression plasmid was transfected into C_2C_{12} mouse myoblasts and cells were switched to differentiation media (2% serum) and harvested at 24, 48, 72 and 96 hours post-media switch. Western blots were then performed to evaluate the expression levels of markers of muscle cell differentiation over the time course. Knockdown of Ttc39c resulted in significant reduction of MyHC and myogenin throughout differentiation (DD1-DD4) (Fig. 25). Effective siRNA knockdown of Ttc39c expression was confirmed, while α-tubulin protein levels remained relatively constant from proliferation through differentiation (Fig. 25).

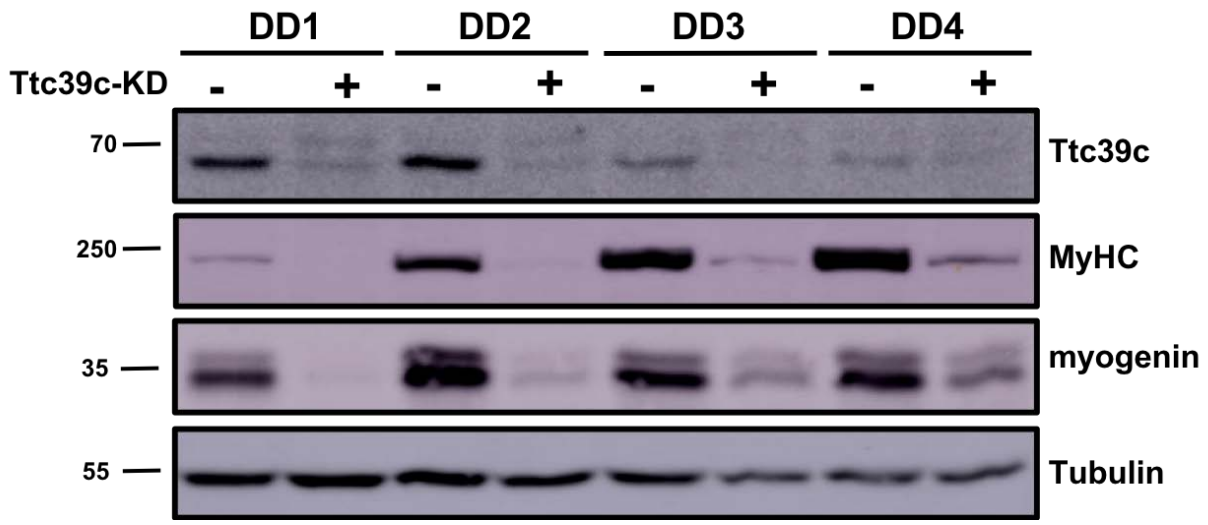

Figure 25. Loss of Ttc39c expression in C_2C_{12} muscle cells represses muscle cell differentiation. C_2C_{12} cells were transfected with the pSuper-siRNA control plasmid or the pSuper-Ttc39c-3 siRNA expression plasmid and Western blot analysis was performed on protein homogenates from differentiated (DD) C_2C_{12} cells harvested over a 4 day differentiation time course. Cells were maintained in proliferation media (10% serum) 2 days post-plating and then switched to differentiation media (2% serum) and harvested at 1, 2, 3, and 4 days post-media change. Cells transfected with the pSuper-Ttc39c-3 siRNA expression plasmid showed significantly lower levels of Ttc39c expression compared to control cells (top panel). Myosin Heavy Chain (MyHC) was analyzed as a marker of muscle cell differentiation and found to be significantly lower in cells with reduced Ttc39c expression (second panel from top). The myogenic regulatory factor, myogenin, also showed lower expression in Ttc39c knockdown cells (third panel from the top). α-tubulin was analyzed to confirm equal protein loading (bottom panel). The experiments were repeated at least once and the western blots presented are representative examples.

To assess the impact that Ttc39c knockdown has on muscle differentiation, the pSEAP-Pro-Ebox-4X reporter plasmid was transfected into C_2C_{12} cells with or without Ttc39c repression and reporter gene activity was measured over a 5 day differentiation time course by sampling the growth media every 48 hours and analyzing the level of secreted alkaline phosphatase (SEAP) activity. Muscle cells with repressed Ttc39c expression showed significantly lower MRF reporter gene activity compared to control cells over the entire 5 day time course (Fig. 26).

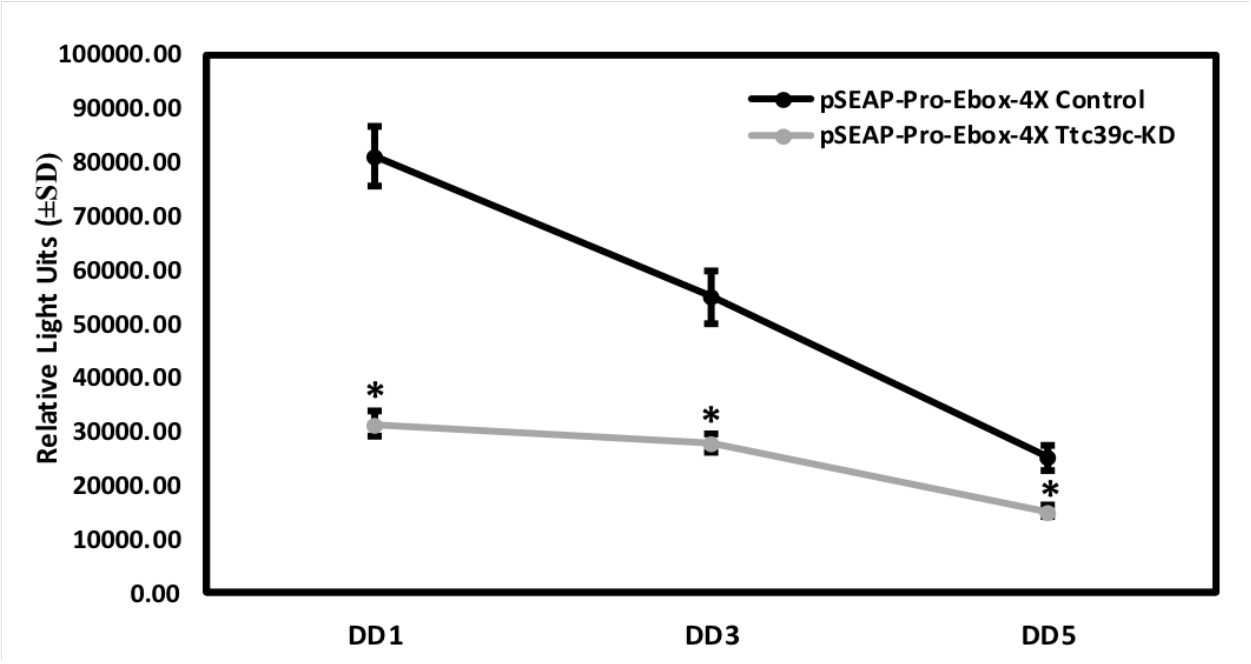

Figure 26. Loss of Ttc39c in C_2C_{12} muscle cells represses myogenic regulatory factor activity. Myogenic regulatory factor activity was analyzed using a reporter gene that consisted of a minimal SV40 promoter fused with 4 concatemerized E-box consensus elements. C_2C_{12} cells were transfected with either the reporter alone (black line) or in combination with the pSuper-Ttc39c-3 siRNA expression plasmid (gray line) and culture media was analyzed over a 5 day time course post-media switch. Cells with decreased Ttc39c protein levels showed significantly lower levels of myogenic regulatory factor activation of the E-box reporter construct compared to control cells. Significant differences between reporter gene activity in control cells compared to Ttc39c knockdown cells, (*: $P < 0.001$).

Knockdown of Ttc39c expression attenuates MAP Kinase and Hedgehog signaling pathways in muscle cells.

Ttc39c was transiently knocked down in C_2C_{12} myoblasts and cells were then switched to differentiation media (2% serum) and harvested at 24, 48, 72, and 96 hours post-media switch. Western blots were then performed to analyze markers of MAP Kinase signaling pathway activity over the time course. Knockdown of Ttc39c resulted in significantly lower levels of p-ERK in cells with lower levels of Ttc39c, while overall ERK protein levels remained unchanged in Ttc39c knockdown cells (Fig. 27). In addition to the MAP kinase signaling pathway, Western blots were also performed to evaluate the activity of the Hedgehog (Hh) signaling pathway over the time course. Ttc39c repression resulted in lower levels of the repressor Gli2 and the Gli2 proteolytic

cleavage product in Ttc39c knockdown cells during early differentiation (DD2) (Fig. 27). As expected, Ttc39c knockdown was effectively achieved in cells transfected with the pSuper-Ttc39c-siRNA-3 expression plasmid, while α-tubulin protein levels remained relatively constant from proliferation through differentiation (Fig. 27).

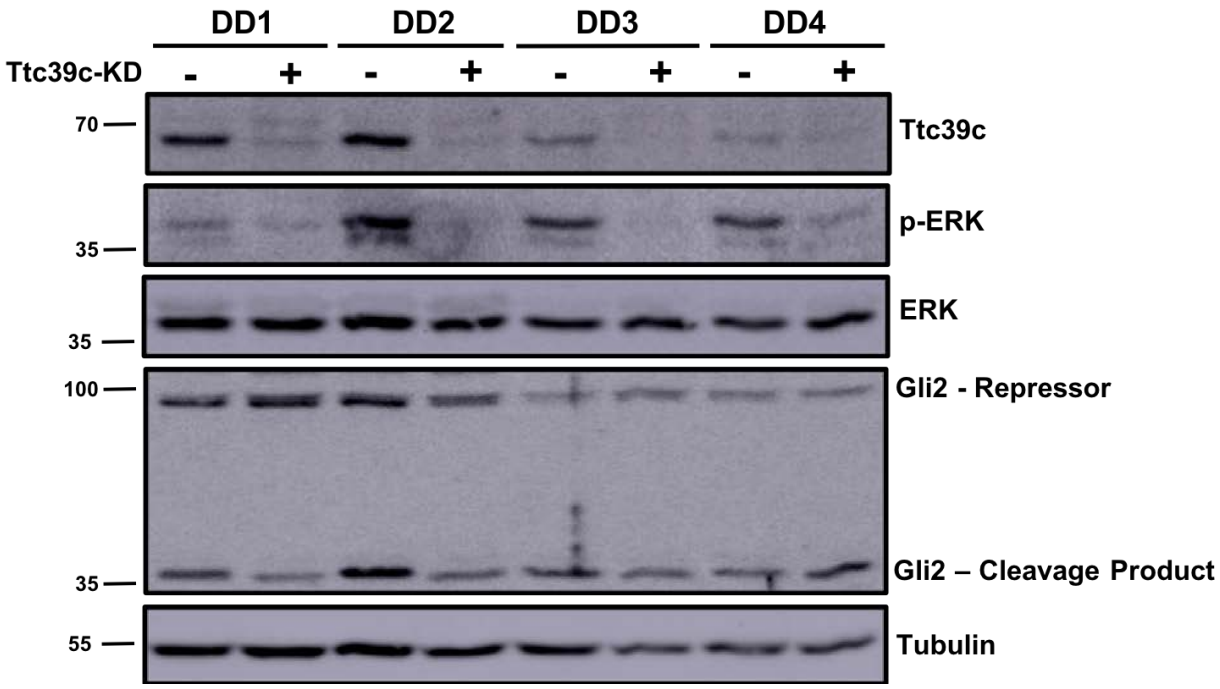

Figure 27. Loss of Ttc39c in C_2C_{12} muscle cells attenuates MAP Kinase and Hedgehog Signaling Pathways in muscle cells. C_2C_{12} cells were transfected with the pSuper-siRNA control plasmid or the pSuper-Ttc39c-3 siRNA expression plasmid and Western blot analysis was performed on protein homogenates from differentiated (DD) C_2C_{12} cells harvested over a 4 day differentiation time course. Cells were maintained in proliferation media (10% serum) 2 days post-plating and then switched to differentiation media (2% serum) and harvested at 1, 2, 3, and 4 days post-media change. **(A)** Cells transfected with the Ttc39c siRNA expression plasmid showed significantly lower levels of Ttc39c expression compared to control cells (top panel). Levels of phosphorylated Erk (panel second from top) were significantly lower in Ttc39c knockdown cells during muscle cell differentiation, while the levels of the Erk protein (panel third from top) remained constant in control cells and Ttc39c knockdown cells. The Gli2 repressor isoform is higher in C_2C_{12} control cells in early differentiation compared to Ttc39c knockdown cells (panel fourth from top). α-tubulin was analyzed to confirm equal protein loading (bottom panel). These experiments were repeated at least once and the Western blots are representative examples of the results obtained.

To determine the level of MAP kinase signaling in muscle cells with repressed Ttc39c expression, the pSEAP-Pro-AP-1 reporter plasmid was transfected into C_2C_{12} cells with or without the Ttc39c-siRNA-3 expression plasmid and reporter gene activity was measured over a 5 day differentiation

time course by sampling the growth media every 48 hours and analyzing the level of secreted alkaline phosphatase (SEAP) activity (Fig 28A). Muscle cells with Ttc39c knocked down showed significantly lower AP-1 reporter gene activity compared to control cells over the entire 5 day time course (Fig. 28B). In addition, Hh signaling was also assessed in muscle cells with repressed Ttc39c expression. To monitor Hh signaling pathway activity, the pSEAP-Pro-Gli reporter plasmid was transfected into C_2C_{12} cells with or without the Ttc39c-siRNA-3 expression plasmid and reporter gene activity was measured over a 5 day differentiation time course by sampling the growth media every 48 hours and analyzing the level of secreted alkaline phosphatase (SEAP) activity (Fig 28A). Muscle cells with Ttc39c repression showed significantly lower Gli reporter gene activity compared to control cells over the entire 5 day time course (Fig. 28C).

A.

B.

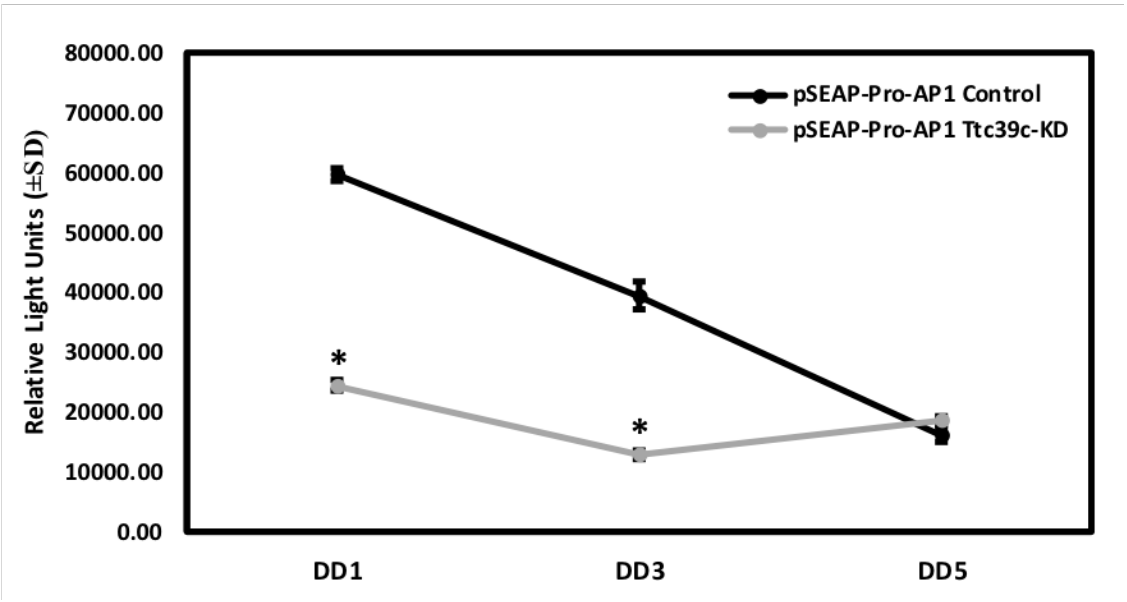

C.

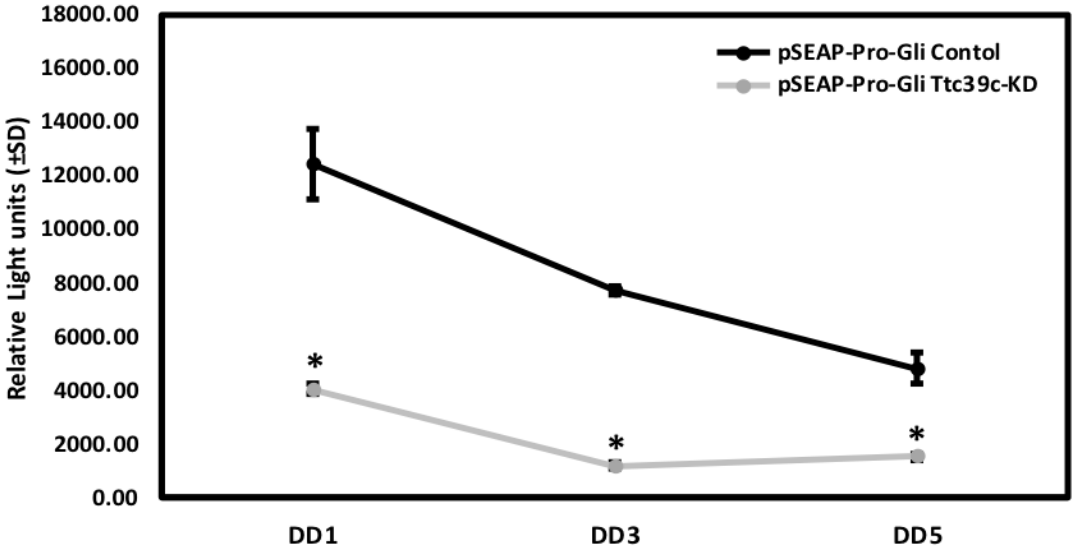

Figure 28. Loss of Ttc39c in C_2C_{12} muscle cells repressed AP-1 and Gli reporter activity. **(A)** Schematic of the signaling pathway reporter gene experimental design. C_2C_{12} cells were transfected one day post-plating and maintained in proliferation media for an additional 24 hours post-transfection. The cells were then changed to differentiation media (2% serum) and analyzed for reporter gene actively at 1, 3, and 5 days post-media switch. **(B)** The MAP Kinase signaling pathway was analyzed using a reporter gene that consisted of a minimal SV40 promoter fused with an AP-1 consensus element. C_2C_{12} cells were transfected with either the reporter alone (black line) or in combination with the pSuper-Ttc39c-3 siRNA expression plasmid (gray line) and culture media was analyzed over a 5 day time course post-media switch. Cells with decreased Ttc39c protein levels showed significantly lower levels of MAP Kinase signaling compared to control cells. **(C)** The Hedgehog signaling pathway was analyzed using a reporter gene that consisted of a minimal SV40 promoter fused with a Gli consensus element. C_2C_{12} cells were transfected with either the reporter alone (black line) or in combination with the pSuper-Ttc39c-3 siRNA expression plasmid (gray line) and culture media was analyzed over a 5 day time course post-media switch. Cells with lower Ttc39c expression showed significantly lower levels of Hedgehog signaling compared to control cells. Significant differences between reporter gene activity in control cells compared to Ttc39c knockdown cells, (*: $P < 0.001$).

Ttc39c knockdown does not affect IFT88 or IFT144 protein levels in muscle cells.

Ttc39c expression was transiently knocked down in C_2C_{12} mouse myoblasts and cells were then switched to differentiation media (2% serum) and harvested at 24, 48, 72 and 96 hours post-media switch. Western blots were again performed to analyze the expression level of IFT88 and IFT144, in muscle cells with repressed Ttc39c expression. Knockdown of Ttc39c had no significant impact on IFT144 or IFT88 protein levels in muscle cells (Fig. 29). siRNA knockdown of Ttc39c was confirmed to be highly effective, while α-tubulin protein levels remained relatively constant from proliferation through differentiation (Fig. 29).

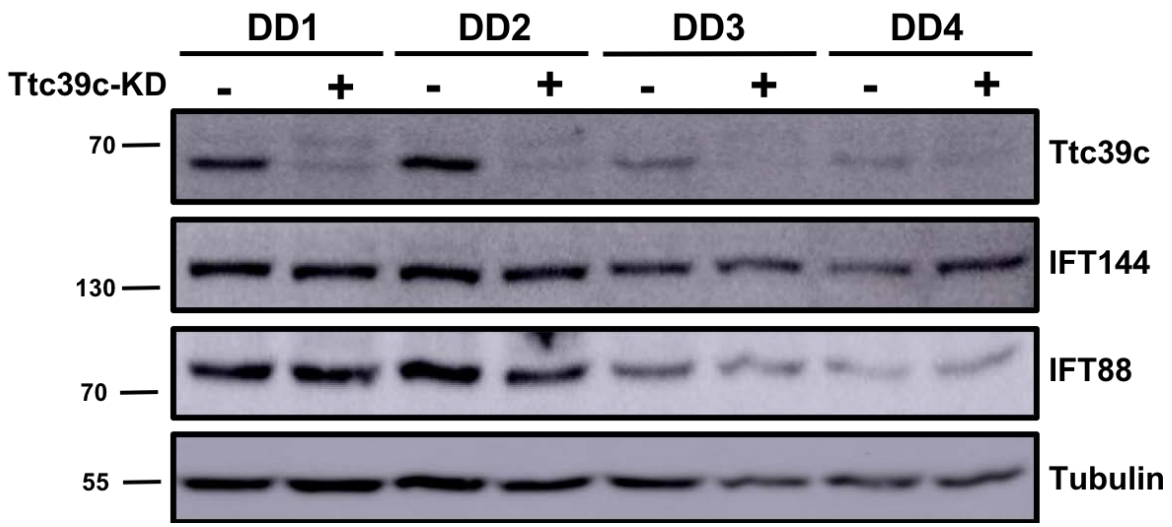

Figure 29. Knockdown of Ttc39c in C_2C_{12} muscle cells does not affect IFT88 or IFT144 protein levels. C_2C_{12} cells were transfected with the pSuper-siRNA control plasmid or the pSuper-Ttc39c-3 siRNA expression plasmid and western blot analysis was performed using an antibody against Ttc39c on protein homogenates from differentiated (DD) C_2C_{12} cells harvested over a 4 day differentiation time course. Cells were maintained in proliferation media (10% serum) 2 days post-plating and then switched to differentiation media (2% serum) and harvested at 1, 2, 3, and 4 days post-media change. Cells transfected with the pSuper-Ttc39c-3 siRNA expression plasmid showed significantly lower levels of Ttc39c expression compared to control cells. IFT144 is part of the Intraflagellar Transport system and is a component of Complex A, which participates in retrograde transport in the primary cilia. IFT88 is part of the Intraflagellar Transport system and is a component of Complex B, which participates in anterograde transport in the primary cilia.Ttc39c knockdown had no effect on IFT144 or IFT88 protein levels in differentiating muscle cells. α-tubulin was analyzed to confirm equal protein loading. These experiments were repeated at least once and the Western blots presented are representative examples.

Discussion

Ttc39c is upregulated in neurogenic skeletal muscle atrophy.

When skeletal muscle tissue is damaged or lost due to atrophy, muscle stem cells, called satellite cells, are activated and divide in an attempt to compensate for the loss of muscle tissue (Bentzinger, et al., 2012; Dasarathy, et al., 2004). MuRF1 has long been believed to be a major regulator of skeletal muscle atrophy by functioning as an E3 ubiquitin ligase that targets proteins for degradation, while more recent data suggests that MuRF1 may also act as a transcriptional regulator of gene expression during atrophy conditions (Bodine, et al., 2001; Bodine and Baehr, 2014; Furlow et al., 2013). Interestingly, microarray data presented in this study shows that Ttc39c expression is increased both 3 days and 14 days post-denervation in wild-type animals, but in

MuRF1-null mice, Ttc39c expression is not significantly induced at 3 days or 14 days post-denervation (Fig. 6A and 6B). These data suggest that Ttc39c expression is reliant on MuRF1 expression during neurogenic skeletal muscle atrophy conditions and that Ttc39c is involved in the atrophy pathway.

Ttc39c is expressed at the mRNA and protein level in skeletal muscle.

Since Ttc39c was observed being upregulated in neurogenic atrophy, this study wanted to validate its expression profile in differentiating skeletal muscle cells. Data presented in this study shows the expression profile for Ttc39c *in vitro,* as the qPCR data from C_2C_{12} myoblasts show elevated mRNA expression at differentiation day 2 (DD2) compared to proliferation day 2 (PD2), but by differentiation day 7 (DD7) the mRNA expression levels returned to baseline (Fig. 7C). Western blot analysis confirmed these time points, as Ttc39c protein expression in C_2C_{12} myoblasts is highest at PD2 through DD2, but then drops off dramatically by DD3 (Fig. 9). This study also confirmed through reporter gene analysis that the proximal promoter regions of both alternative transcripts of Ttc39c show activity in skeletal muscle cells, as these regions contain several conserved regulatory elements (Fig. 11B-D, 12B-D). This shows Ttc39c expression is induced via the promoter regions of each transcript and suggests that Ttc39c has a narrow window of function within early muscle cell differentiation.

Ttc39c is regulated transcriptionally via muscle-specific transcription factors and post-transcriptionally via its 3'UTR in vitro.

As previously described, MRFs are muscle-specific transcription factors responsible for regulating gene expression during myogenesis and do so via binding canonical E-box consensus sequences

in the promoter regions of these genes (Singh and Dilworth, 2013; Londhe and Davie, 2011). MRFs can bind E-box sequences by forming homodimers or by forming heterodimers with ubiquitously expressed E-proteins such as TCF3 and TCF12 (Singh and Dilworth, 2013; Londhe and Davie, 2011). Both transcripts of Ttc39c contain conserved E-box sequences in their 500 bp proximal promoters, so reporter assays were conducted to test the effect of MRFs on these promoter fragments. MyoD and myogenin exhibited repression of reporter gene activity for both Ttc39c transcripts (Fig. 13A-D). For the Ttc39c-580 and the Ttc39c-522 transcripts, both MyoD and myogenin repressed promoter activity (Fig. 13A-D). Both transcripts also showed differential promoter activity compared to the WT promoter when these conserved E-box sequences were mutagenized to inhibit the binding of MRFs (Fig. 14D and 15D). This data suggests the expression of Ttc39c in skeletal muscle is regulated by MRFs, and it is the binding of MRFs to conserved E-box sequences that facilitates this transcriptional regulation.

In addition to containing conserved E-box sequences in its promoter region, Ttc39c also possesses a short 3'UTR region which is likely bound by miRNAs to post-transcriptionally regulate the expression of Ttc39c. To see if the 3'UTR had any possible regulatory effects on Ttc39c, this segment of the gene was cloned into a reporter plasmid and transfected into C_2C_{12} myoblasts. The data shows that, as differentiation proceeds, the reporter activity of the Ttc39c 3'UTR construct decreases when compared to the control reporter construct (Fig. 16B). This suggests that the expression of Ttc39c is regulated at both the transcriptional and post-transcriptional level in differentiating muscle cells.

The TPR domains of Ttc39c may facilitate protein-protein interactions.

As the exact function of Ttc39c has yet to be elucidated, this study wanted to identify putative functional domains of Ttc39c. This study's analysis of the functional domains of the 580 amino acid and 522 amino acid isoforms of Ttc39c reveals that both transcripts contain a DUF region that includes 4 putative TPR domains (Fig. 10). The presence of these TPR domains points to the potential function of Ttc39c as a scaffolding protein that could facilitate protein-protein interactions and help assemble protein complexes. Indeed, previous research has shown that TPR domains do facilitate protein-protein interactions and can act as scaffolds for larger protein complexes (Zeytuni and Zarivach, 2012). This potential function of Ttc39c as a scaffolding protein warranted further study into where Ttc39c is localizing and what it is possibly associating with in skeletal muscle cells.

Ttc39c localizes to the cytoplasm and associates with the centrosome in skeletal muscle cells.

This study is the first to describe Ttc39c in skeletal muscle, so confocal fluorescent microscopy was utilized to observe the subcellular localization of the Ttc93c protein. Ttc39c was fused in frame with GFP, transfected into C_2C_{12} myoblasts, and visualized at proliferation and differentiation time points. The transfected Ttc39c-GFP cells showed localization to the cytoplasm and nuclear exclusion, while also showing possible association with the centrosome and the microtubules radiating from it (Fig. 17D-I, 17M-R, 18D-I, and 18M-R). Furthermore, the images show aberrant protrusions growing from differentiating cells transfected with the Ttc39c-GFP expression plasmid (Fig. 18D-I and 18M-R). This result could be due to aberrant microtubule growth, but the exact mechanism remains unclear. Further investigation is required to confirm the associations with the centrosome and elucidate what is causing the aberrant protrusions.

Regardless, the overexpression of Ttc39c results in aberrant morphology of skeletal muscle cells and a lack of proper skeletal muscle cell differentiation.

Ectopic overexpression of Ttc39c inhibits myoblast differentiation

Confocal fluorescent microscopy revealed that overexpressing Ttc39c results in aberrant skeletal muscle cell morphology during differentiation. To observe if Ttc39c has any effect on myogenesis, Ttc39c was ectopically expressed in C_2C_{12} myoblasts over a time course ranging from proliferation to late differentiation. Protein lysates from these cells were then analyzed via Western blot, probing for MyHC, MyoD, and myogenin as markers of muscle cell differentiation. Compared to the control cells, the cells overexpressing Ttc39c showed a dramatic reduction in MyHC, MyoD, and myogenin (Fig. 19), suggesting that overexpression of Ttc39c inhibits myoblast differentiation *in vitro.*

To confirm that overexpressing Ttc39c results in lower levels of MyoD and myogenin, an E-box reporter construct was transfected into C_2C_{12} myoblasts with or without Ttc39c overexpression and the reporter activity was measured over a 7 day time course. As expected, the E-box reporter activity in the cells overexpressing Ttc39c was significantly lower than the control cells (Fig. 20), suggesting that reduction in MRF expression due to Ttc39c overexpression inhibited differentiation by reducing muscle-specific gene expression required for myogenesis *in vitro*.

Ectopic overexpression of Ttc39c attenuates MAPK and Hh signaling in myoblasts.

Several signaling pathways are required for proper myogenesis, including the ERK1/2 pathway of the MAPK signaling cascade and the Hh signaling pathway (Bentzinger, et al., 2012; Mok and Sweetman, 2011; Bismuth and Relaix, 2010; Fu, et al., 2014; Knight and Kothary, 2011). If the

signaling of these pathways is impaired, proper myogenesis cannot occur (Koleva, et al., 2005; Li, et al., 2004; Sarbassov, et al., 1997; Winter and Arnold, 2000). To observe any effects on these signaling pathways in the Ttc39c overexpression cells, Western blots were probed for ERK, p-ERK, and Gli2 repressor. Activation of the ERK1/2 pathway leads to the phosphorylation and activation of ERK. Phosphorylated ERK (p-ERK) then acts downstream to control cell proliferation, migration, and cell differentiation (Christensen et al., 2012). Compared to control cells, p-ERK levels were significantly reduced in the Ttc39c overexpression samples, while overall ERK levels remained relatively constant (Fig. 21A). These findings suggest that overexpression of Ttc39c affects the activation of the MAPK pathway and does not simply reduce the amount of overall ERK that is available to be phosphorylated. In Hh signaling, Gli proteins are proteolytically processed into a repressor form that blocks the transcription of Hh target genes (Bangs and Anderson, 2017). When the pathway is activated, this proteolytic processing of the Gli protein is blocked, allowing for the activator form of Gli to activate the transcription of Hh target genes (Bangs and Anderson, 2017). For the Gli2 repressor probe, the cells overexpressing Ttc39c showed significantly higher amounts of Gli2 repressor at later differentiation time points when compared to the control cells (Fig. 21B). This suggests the overexpression of Ttc39c also causes a decrease in Hh signaling due to an increase in the repressor form of Gli2 *in vitro.*

To confirm these observations, reporter assays were performed to quantify the effects of Ttc39c overexpression on both of these signaling pathways. For MAPK signaling, an AP-1 reporter construct was transfected into C_2C_{12} myoblasts with and without Ttc39c overexpression and its activity was measured over a 7 day time course. In accordance with the Western blot data, AP-1 reporter activity was significantly lower in the cells overexpressing Ttc39c (Fig. 22B). For Hh signaling, a Gli reporter construct was transfected into C_2C_{12} myoblasts and its activity was also

measured over 7 days of differentiation. The results of the reporter assays confirmed the Western blot data, by showing significantly reduced reporter activity in the cells overexpressing Ttc39c (Fig. 22C). Taking the Western blot and reporter data together, it is apparent Ttc39c overexpression inhibits myogenesis by attenuating signaling pathways required for proper muscle cell differentiation.

Knockdown of Ttc39c inhibits myoblast differentiation.

After observing that overexpression of Ttc39c inhibits myoblast differentiation and attenuates MAPK and Hh signaling in muscle cells, we next wanted to determine how knocking down the expression of Ttc39c via an siRNA would affect these same processes. Interestingly, as with the overexpression experiments, C_2C_{12} myoblast differentiation was significantly inhibited when Ttc39c was repressed. Compared to the control cells, MyHC and myogenin expression levels were dramatically lower (Fig. 25). We confirmed that the observed reduction in MRF expression was reflected in lower E-box reporter gene activity in C_2C_{12} cells with Ttc39c knocked down compared to control cells. As with the overexpression cells, the reporter activity was dramatically lower compared to the control cells, suggesting that aberrant Ttc39c expression (i.e. too high or too low) negatively affects muscle cell differentiation (Fig. 26).

Knockdown of Ttc39c attenuates MAPK and Hh signaling in myoblasts.

As with Ttc39c overexpression, the effect that knocking down Ttc39c has on the MAPK and Hh signaling pathways was evaluated. As with the overexpression cells, p-ERK was practically absent when Ttc39c was repressed, while overall ERK levels remained constant, again suggesting that activation of the MAPK pathway is inhibited in response to aberrant Ttc39c expression levels (Fig.

27). Interestingly, lower levels of Gli2 repressor were observed in the Ttc39c knockdown cells, which is the opposite of what was observed with overexpression of Ttc93c in muscle cells (Fig. 27). This observation suggests that repressing Ttc39c could possibly increase Hh signaling by reducing the repressor form of Gli2.

Finally, we evaluated the effects of Ttc39c knockdown on MAPK and Hh signaling by transfecting the AP-1 reporter or Gli Reporter into C_2C_{12} myoblasts with and without Ttc39c repression and measured reporter activity over a 5 day time course. Reporter activity for both constructs was dramatically lower in the knockdown cells, even more so than what was observed in the Ttc39c overexpression cells (Fig. 28B-C). While this supports the Western blot data for MAPK signaling, lower Hh signaling seems counterintuitive in light of the lower levels of repressor Gli2 on the Western blot in cells with Ttc39c repression. A possible explanation is the lack of Gli2 protein in the cells could be indicative of a general lack of expression of proteins involved in Hh signaling. Less components of the signaling pathway are present, thus there is less overall Gli2 available to be proteolytically processed, resulting in dramatically lower Hh signaling observed in the reporter assays. To fully elucidate this process, further investigation will be required. As with the Ttc39c overexpression data, these findings suggest that repressing Ttc39c inhibits myogenesis by dramatically attenuating signaling pathways required for proper muscle cell differentiation. The Ttc39c overexpression and knockdown data strongly support the hypothesis that Ttc39c has a specific and relatively narrow window of function and proper and highly regulated expression is required for myoblast commitment to differentiation.

Ttc39c associates with transport complexes and cytoskeletal elements of the primary cilium.

This study suggests proper Ttc39c expression is critical for myogenesis, as aberrant Ttc39c expression results in decreased Hh and MAPK signaling pathway activity (Fig. 21, 22, 27, and 28). This decrease in signaling results in a decrease in MRF expression, which then leads to a decrease in the expression of genes required for myogenesis (Fig. 19, 20, 25, and 26). While the exact functional mechanism of Ttc39c remains to be elucidated, previous studies suggest Ttc39c carries out its function within the primary cilium. A recent study by Xu et al. showed Ttc39c to be critical for proper cilia formation and function in zebrafish (Xu et al., 2015). While differentiated myotubes lack cilia, myoblasts possess primary cilia, which are structures that have been shown to be critical for proper myogenesis (Fu et al., 2014).

Xu et al. further observed via co-immunoprecipitation that Ttc39c weakly associated with IFT139 and IFT144, proteins belonging to the IFT-A complex in primary cilia (Xu et al., 2015). Interestingly, Xu et al. did not observe Ttc39c association with proteins from the IFT-B complex, suggesting it associates only with IFT-A complex proteins and may participate exclusively in retrograde transport within the primary cilium (Xu et al., 2015). Data presented in this study shows an increase in IFT144 protein levels but not IFT88 when Ttc39c is overexpressed (Fig. 23). This further implicates Ttc39c in primary cilia formation and function via its connection with the IFT-A complex, but not IFT-B. If the overexpression of Ttc39c is affecting proper transport of signaling components within the cilium, this could explain its significant impact on cell signaling and muscle cell differentiation. Whether Ttc39c acts as a scaffolding protein for the IFT-A complex via its TPR domains requires further investigation. The association of Ttc39c with transport complexes involved with microtubules is intriguing considering the data presented

in this study shows Ttc39c appears to localize with the cell cytoskeleton (Fig. 18). This apparent association of Ttc39c with the centrosome and microtubules is of interest, as the basal body of the primary cilium is derived from the mother centriole of the centrosome and is responsible for forming the axoneme of the cilium (Prevo, et al., 2017). This could explain the aberrant microtubule growth and improper primary cilium formation, but the exact mechanism remains unclear. While further investigation is required to confirm the associations with the centrosome and elucidate what is causing the aberrant protrusions, this is yet more evidence suggesting Ttc39c is associated with cytoskeletal elements that comprise primary cilia.

Ttc39c expression overlaps with the assembly and disassembly of primary cilia in muscle cells. A 2014 study by Fu et al. looking at primary cilia and Hh signaling in myoblasts suggests that primary cilia formation occurs within early differentiation of myoblasts and that the cilia are subsequently disassembled as differentiation progresses (Fu et al., 2014). This study found that cilia formation peaked at around 24 hours into the differentiation process but were then disassembled and greatly diminished by 48 hours into differentiation (Fu et al., 2014). The investigators also observed that disassembly of the primary cilia was a precursor to myoblast fusion, as most multi-nucleated muscle cells lacked primary cilia by 48 hours into differentiation, while the increase in MyHC expression was usually observed shortly thereafter (Fu et al., 2014). This temporally overlaps with data presented in this study showing Ttc39c mRNA and protein expression peaks in early differentiation but decreases as differentiation continues (Fig.7C and 9). Taken in context with previous findings showing that Ttc39c is critical for cilia formation and function, our data suggests that the temporal overlap in Ttc39c expression and primary cilia

formation is more than coincidental, and Ttc39c likely functions within the primary cilium of developing muscle cells (Fu et al., 2014; Xu et al., 2015).

Ttc39c may affect cell signaling during myogenesis via the primary cilium.

Ttc39c involvement with primary cilia formation and function is further supported by data presented in this study showing both the overexpression and repression of Ttc39c attenuates both myogenesis and cell signaling pathways (Fig. 19-22, 25-28). Hh and MAPK signaling is critical for proper myogenesis and both pathways require primary cilia for proper signal transduction (Bangs and Anderson, 2017; Christensen, et al., 2012). This study suggests aberrant Ttc39c expression results in attenuated Hh and MAPK signaling via improper primary cilia formation, which leads to a decrease in MRF expression. This decrease in MRF expression in turn leads to a decrease in the expression of genes required for myogenesis, thus resulting in the inhibition of skeletal muscle cell differentiation.

How Ttc39c and primary cilia function within skeletal muscle atrophy has yet to be studied. Based on data presented in this study, the induction of Ttc39c expression during neurogenic muscle atrophy requires the expression of MuRF1, a major regulator of skeletal muscle atrophy (Fig. 6). Considering proper myogenesis requires the formation and function of primary cilia, this suggests MuRF1 is necessary for the expression of genes that are involved in the assembly and function of primary cilia. The presence of primary cilia then facilitates the cell signaling required for proper myogenesis. These findings are intriguing and suggest that induction of Ttc39c is likely the result of increased primary cilia formation in differentiating myoblasts that

arise from activated satellite cell division in response to muscle wasting in an attempt to repair the muscle tissue.

References

1. Frontera WR, Ochala J. 2014. Skeletal Muscle: A Brief Review of Structure and Function. *Calcified Tissue International*. 96: 183-195.
2. Crist C. 2016. Emerging new tools to study and treat muscle pathologies: genetics and molecular mechanisms underlying skeletal muscle development, regeneration, and disease. *Journal of Pathology.* 241: 264-272.
3. McKinnell IW, Rudnicki MA. 2004. Molecular mechanisms of muscle atrophy. *Cell.* 119(7): 907-910.
4. Bodine SC, Baehr LM. 2014. Skeletal muscle atrophy and the E3 ubiquitin ligases MuRF1 and MAFbx/atrogin-1. *American Journal of Physiology - Endocrinology and Metabolism*. 307: LE469-E484.
5. Bodine SC, Latres E, Baumhueter S, et al. 2001. Identification of ubiquitin ligases required for skeletal muscle atrophy. *Science Signaling*. 294(5547):1704.
6. Bonaldo P, Sandri M. 2013. Cellular and molecular mechanisms of muscle atrophy. *Disease Models & Mechanisms.* 6:25-39.
7. Waddell DS, Baehr LM, van den Brant J, et al. 2008. The glucocorticoid receptor and FOXO1 synergistically activate the skeletal muscle atrophy-associated MuRF1 gene. *American Journal of Physiology - Endocrinology and Metabolism*. 295: 785-797.
8. McNaught KSP, Olanow CW, Halliwell B, Isacson O, Jenner P. 2001. Failure of the ubiquitin–proteasome system in parkinson's disease. *Nature Reviews Neuroscience.* 2(8):589-594.
9. Ardley HC, Robinson PA. 2005. E3 ubiquitin ligases. *Essays In Biochemistry.* 41:15-30.

10. Dodd, R. 2011. Ubiquitylation [open access image]. Attribution: By Rogerdodd at the English language Wikipedia, CC BY-SA 3.0, https://commons.wikimedia.org/w/index.php?curid=7677277
11. Furlow JD, Watson ML, Waddell DS, et al. 2013. Altered gene expression patterns in muscle ring finger 1 null mice during denervation and dexamethasone induced muscle atrophy. *Physiological genomics.* 45:1168-1185.
12. Mrosek M, Meier S, Ucurum-Fotiadis Z, et al. 2008. Structural analysis of B-box 2 from MuRF1: identification of a novel self-association pattern in a RING-like fold. *Biochemistry*. 47(40): 10722-10730.
13. McElhinny AS, Kakinuma K, Sorimachi H, et al. 2002. Muscle-specific RING finger-1 interacts with titin to regulate sarcomeric M-line and thick filament structure and may have nuclear functions via its interaction with glucocorticoid modulatory element binding protein-1. *The Journal of Cell Biology*. 157(1): 125-136.
14. Hohlfeld S, Pattis I, Püls J, et al. 2006. A C-terminal translocation signal is necessary, but not sufficient for type IV secretion of the *Helicobacter pylori* CagA protein. *Molecular Microbiology.* 59(5): 1624-1637.
15. D'Andrea LD, Regan L. 2003. TPR proteins: the versatile helix. *Trends in Biochemical Sciences*. 28(12): 655-662.
16. Blatch GL, Lassle M. 1999. The tetratricopeptide repeat: a structural motif mediating protein-protein interactions. *BioEssays.* 21(11):932-939.
17. Xu Y, Cao J, Huang S, et al. 2015. Characterization of Tetratricopeptide Repeat-Containing Proteins Critical for Cilia Formation and Function. *PLoS ONE*. 10(4): 1-17.

18. Fu W, Asp P, Canter B, Dynlacht BD. 2014. Primary cilia control hedgehog signaling during muscle differentiation and are deregulated in rhabdomyosarcoma. *Proceedings of the National Academy of Sciences.*

19. Prevo B, Scholey JM, Peterman EJG. 2017. Intraflagellar transport: mechanisms of motor action, cooperation, and cargo delivery. *The FEBS Journal*. 284: 2905-2931.

20. Satir P, Pedersen LB, Christensen ST. 2010. The primary cilium at a glance. *Journal of Cell Science*. 123: 499-503.

21. Bangs F, Anderson KV. 2017. Primary Cilia and Mammalian Hedgehog Signaling. *Cold Spring Harbor Perspectives in Biology*. 9:a028175.

22. Goetz SC, Anderson KV. 2010. The Primary Cilium: A Signaling Center During Vertebrate Development. *Nature Reviews Genetics.* 11(5): 331-344.

23. Yuan X, Yang S. 2015. Cilia/Ift protein and motor-related bone diseases and mouse models. *Frontiers in Bioscience*. 20: 515-555.

24. Ye F, Nager AR, Nachury MV. 2018. BBSome trains remove activated GPCRs from cilia by enabling passage through the transition zone. *Journal of Cell Biology.* DOI: 10.1083/jcb.201709041.

25. Liu P, Lechtrek KF. 2018. The Bardet-Biedl syndrome protein complex is an adapter expanding the cargo range of intraflagellar transport trains for ciliary export. *Proceedings of the National Academy of Sciences.* 115(5): E934-E943.

26. Bentzinger CF, Wang YX, Rudnicki MA. 2012. Building Muscle: Molecular Regulation of Myogenesis. *Cold Spring Harbor Perspectives in Biology.* 4:a008342.

27. Mok GF, Sweetman D. 2011. Many routes to the same destination: lessons from skeletal muscle development. *Reproduction*. 141: 301-312.

28. Bismuth K, Relaix F. 2010. Genetic regulation of skeletal muscle development. *Experimental Cell Research*. 316: 3081-3086.

29. Koleva M, Kappler R, Vogler M, et al. 2005. Pleiotropic effects of sonic hedgehog on muscle satellite cells. *Cellular and Molecular Life Sciences*. 62: 1863-1870.

30. Gerber AN, Wilson CW, Chuang PT. 2007. The hedgehog regulated oncogenes Gli1 and gli2 block myoblast differentiation by inhibiting MyoD-mediated transcriptional activation. *Oncogene*. 26:1122-1136.

31. Duprez D, Fournier-Thibault C, Le Douarin N. 1998. Sonic Hedgehog induces proliferation of committed skeletal muscle cells in chick limb. *Development*. 125: 495-505.

32. Li X, Blagden CS, Bildsoe H, et al. 2004. Hedgehog can drive terminal differentiation of amniote slow skeletal muscle. *BMC Developmental Biology*. 4:9.

33. Christensen ST, Clement CA, Satir P, Pedersen LB. 2012. Primary cilia and coordination of receptor tyrosine kinase (RTK) signaling. 226: 172-184.

34. Knight JDR, Kothary R. 2011. The myogenic kinome: protein kinases critical to mammalian skeletal myogenesis. *Skeletal Muscle*. 1:29.

35. Kook SH, Son YO, Choi KC, et al. 2007. Cyclic mechanical stress suppresses myogenic differentiation of adult bovine satellite cells through activation of extracellular signal-regulated kinase. *Molecular and Cellular Biochemistry*. 309: 133-141.

36. Sarbassov DD, Jones LG, Peterson CA. 1997. Extracellular Signal-Regulated Kinase-1 and -2 Respond Differently to Mitogenic and Differentiate Signaling Pathways in Myoblasts. *Molecular Endocrinology*. 11(13): 2038-2047.

37. Winter B, Arnold HH. 2000. Activated Raf kinase inhibits muscle cell differentiation through a MEF2-dependent mechanism. *Journal of Cell Science*. 113: 4211-4220.

38. Rodriguez J, Vernus B, Chelh I, et al. 2014. Myostatin and the skeletal muscle atrophy and hypertrophy signaling pathways. *Cellular and Molecular Life Sciences*. 71: 4361-4371.

39. Adi S, Bin-Abbas B, Wu NY, Rosenthal SM. 2002. Early Stimulation and Late Inhibition of Extracellular Signal-Regulated Kinase ½ Phosphorylation by IGF-I: A Potential Mechanism Mediating the Switch in IGF-I Action on Skeletal Muscle Cell Differentiation. *Endocrinology*. 143(2): 511-516.

40. Bennett AM, Tonks NK. 1997 Regulation of Distinct Stages of Skeletal Muscle Differentiation by Mitogen-Activated Protein Kinases. *Science*. 278(5341): 1288-1291.

41. Gredinger E, Gerber AN, Tamir Y, et al. 1998. Mitogen-activated Protein Kinase Pathway Is Involved in the Differentiation of Muscle Cells. *The Journal of Biological Chemistry*. 273(17): 10436-10444.

42. Zeytuni N, Zarivach R. 2012. Structural and Functional Discussion of the Tetra-Trico-Peptide Repeat, a Protein Interaction Module. *Structure*. 20(3): 397-405

43. Singh K, Dilworth FJ. 2013. Differential modulation of cell cycle progression distinguishes members of the myogenic regulatory factor family of transcription factors. *The FEBS Journal*. 280: 3991-4003.

44. Londhe, P., Davie, J. 2011. Sequential association of myogenic regulatory factors and E proteins at muscle-specific genes. *Skeletal Muscle*. 1:14.

45. Moresi V, Williams AH, Meadows E, et al. 2010. Myogenin and Class II HDACs control neurogenic muscle atrophy by inducing E3 ubiquitin ligases. *Cell*. 143(1): 35-45.

46. Cohen TJ, Waddell DS, Barrientos T, et al. 2007. The Histone Deacetylase HDAC4 Connects Neural Activity to Muscle Transcriptional Reprogramming. *The Journal of Biological Chemistry*. 282: 33752-33759.

47. William AH, Valdez G, Moresi V, et al. 2009. MicroRNA-206 Delays ALS Progression and Promotes Regeneration of Neuromuscular Synapses in Mice. *Science*. 326: 1549-1554.

48. Tang H, Macpherson P, Marvin M, et al. 2009. A Histone Deacetylase 4/Myogenin Positive Feedback Loop Coordinates Denervation-dependent Gene Induction and Suppresion. *Molecular Biology of the Cell.* 20: 1120-1131.

49. Cao Y, Yao Z, Sarkar D, et al. 2010. Genome-wide MyoD Binding in Skeletal Muscle Cells: A Potential for Broad Cellular Reprogramming. *Developmental Cell*.18(4): 662-674.

50. Dasarathy S, Dodig M, Muc SM, et al. 2004. Skeletal muscle atrophy is associated with an increased expression of myostatin and impaired satellite cell function in the portacaval anastomosis rat. Gastrointestinal and Liver Physiology-*American Journal of Physiology*. 287: G1124-G1130.